DEGRADATION OF PERCHLOROETHYLENE AND NITRATE BY HIGH-ACTIVITY MODIFIED GREEN RUSTS

A Dissertation

by

JEONG YUN CHOI

Submitted to the Office of Graduate Studies of
Texas A&M University
in partial fulfillment of the requirements for the degree of

DOCTOR OF PHILOSOPHY

August 2005

Major Subject: Civil Engineering

DEGRADATION OF PERCHLOROETHYLENE AND NITRATE BY HIGH-ACTIVITY MODIFIED GREEN RUSTS

A Dissertation

by

JEONG YUN CHOI

Submitted to the Office of Graduate Studies of
Texas A&M University
in partial fulfillment of the requirements for the degree of

DOCTOR OF PHILOSOPHY

Approved by:

Chair of Committee,	Bill Batchelor
Committee Members,	Robin Autenrieth
	Timothy A. Kramer
	Bruce Herbert
Head of Department,	David V. Rosowsky

August 2005

Major Subject: Civil Engineering

ABSTRACT

Degradation of Perchloroethylene and Nitrate by High-activity

Modified Green Rusts. (August 2005)

Jeong Yun Choi, B.S., Chonbuk National University;

M.S., Chonbuk National University

Chair of Advisory Committee: Dr. Bill Batchelor

Green rusts (GRs), a group of layered Fe(II)-Fe(III) hydroxide salts, have been observed to be effective reductants for degrading organic and inorganic contaminants under suboxic conditions. Furthermore, the addition of a transition metal to GRs can produce high-activity modified green rusts (HMGRs) that demonstrate higher degradation rates. Methods of modifying GRs to obtain high reactivity for degradation of PCE and nitrate were developed and reduction kinetics of PCE and nitrate by HMGRs were characterized in this study.

First, the most promising HMGRs were developed through screening tests. GRs modified with Pt, Cu, Ag, or Pb were found to be effective in improving degradation rates of PCE. GR-F(Pt) and GR-F(Cu) were chosen because they showed high reactivity and produced non-chlorinated by-products. Pt and Cu showed the capability of improving reduction kinetics of nitrate by GRs. GR-F(Pt) and GR-F(Cu) were selected for further study.

Second, degradation of PCE by GR-F(Cu) and GR-F(Pt) was characterized using a batch reactor system. The reaction kinetics of PCE degradation by GR-F(Cu) and GR-F(Pt) was strongly dependent on pH over the range of pH 7.5-11, with the fastest rate at pH 11. Increasing concentrations of Cu(II) over the range of 0 to 5 mM resulted in improving the reduction kinetics by a factor of more than 400, although the rate at 7.5 mM of Cu(II) was unexpectedly lower than that at 5 mM. Surface saturation behavior was observed in the rates of dechlorination of PCE by GR-F(Cu).

Finally, nitrate reduction by GR-F(Cu) and GR-F(Pt) was further studied to determine the effects on degradation rates of pH, Cu(II) addition, and initial nitrate concentration. A reaction model with four sequential steps was proposed to describe the process of nitrate being reduced to ammonium and GR being oxidized to magnetite. The reaction rates of nitrate reduction by GR-F(Cu) and GR-F(Pt) was highest at pH 9. The reaction rates of GR-NO_3 were improved by three orders of magnitude when Cu(II) was added in the range of 0 to 2.5 mM, while reaction rate decreased at concentrations above 2.5 mM. Saturation behavior was also observed in nitrate reduction by GR-F(Cu).

To my parents

ACKNOWLEDGMENTS

I am grateful to numerous people who have contributed to this study. First of all, I wish to express my sincere gratitude to my advisor, Dr. Bill Batchelor, for his academic guidance, support and encouragement. He not only guided me in research, but also enhanced my insight with his knowledge and experience as an environmental engineer. I would also like to acknowledge my appreciation to committee members, Dr. Timothy Kramer, Dr. Robin Autenrieth, and Dr. Bruce Herbert. I was very fortunate to have a chance to work with them during my Ph.D. work.

My special thanks go to Dr. Jinwook Kim, Seabom Ko and Bahngmi Jung for help and support in this study. Their wonderful assistance and invaluable advice directed this research to a successful way. I would like to thank all my colleagues Jinkun Song, Sihyun Do, Eunjung Kim, Chunwoo Lee, and Sanghyun Kim for their opinion in a research as well as friendships.

Finally, I was sincerely grateful to my family members: father, mother, sister and brother. They encouraged and supported me to reach my goal during my studies.

TABLE OF CONTENTS

Page

CHAPTER Page

CHAPTER Page

LIST OF FIGURES

Page

Page

LIST OF TABLES

Page

Page

CHAPTER I

INTRODUCTION

Since Love Canal, many hazardous-waste sites have been recognized as environmental tragedies and the USEPA has made an extensive effort to search for such contaminated sites and clean them up under authority of the Comprehensive Environmental Response, Compensation, and Liability Act (CERCLA, 1980), which is also known as the Superfund Act (1). There are 45,516 contaminated sites in the United States and 1238 sites have been included in National Priority List (NPL) as of May 2004 according to the US Comprehensive Environmental Response, Compensation, and Liability Information System (CERCLIS) (2). These sites have been accidentally contaminated by toxic chemical spills or chronically polluted by abandoned chemical manufacturing plants, hazardous material storage, treatment, or disposal facilities, agricultural activities, or mining activities (1, 3).

Human exposure to contaminated soil and groundwater at these sites has occurred through ingestion of water or food, inhalation of air, and dermal contact and has resulted in short- and long-term health risks. Contaminated groundwater could pose a direct risk for people when it is used as the source of water for drinking, bathing, and other household uses (4, 5). In addition, the flow of polluted groundwater could act as a transport media spreading contaminants to water streams or lakes (3).

This dissertation follows the style of *Environmental Science and Technology*.

Perchloroethylene (PCE) is one of the most common toxic organic contaminants found in groundwater in the United State. PCE was detected in 43% of large groundwater systems which were serving more than 50,000 people in 1999 (6). It has been widely used in the dry cleaning industry and metal-degreasing processes during the past half century (7, 8). It has been reported that human exposure to PCE could depress the central nervous system and damage the kidney and liver. It has been classified as a probable human carcinogenic by USEPA's Science Advisory Board (9). PCE is known to be resistant to biodegradation under aerobic conditions. In addition, its degradation by reductive dechlorination is often kinetically limited, even in suboxic conditions where it is thermodynamically favorable (10). Therefore, substantial amounts of research have been conducted to understand the transformation mechanisms for PCE and to enhance their reaction rates.

Increasing nitrate concentrations in rivers, lakes, and groundwater is another considerable environmental problem. Nitrate in drinking water has been regulated because excessive levels of nitrate can cause the illness, methemoglobinemia, known as "blue baby syndrome" by interfering with the oxygen-carrying capacity of the child's blood (11). Ion exchange, reverse osmosis, biological denitrification and chemical reduction have been normally used to reduce nitrate concentration in water. However, ion exchange and reverse osmosis have the disadvantages of high operating costs and of producing secondary brine wastes. Biological methods are unfavorable because they are difficult to operate and their reaction rates are slower than those for chemical degradation. (12).

One of the effective methods to chemically remove both PCE and nitrate is to degrade them using a redox reaction with an iron-bearing solid such as green rust. Green rusts (GRs) are layered Fe(II)-Fe(III) hydroxide solid phases with an anion in the interlayer. A general formula for GR is $\left[Fe^{II}_{(6-x)}Fe^{III}_{x}(OH)_{12}\right]^{x+}\left[(A)_{x/n}\, yH_2O\right]^{x-}$ (where x = 0.9-4.2; A is an n-valent anion (Cl^-, SO_4^{2-}, CO_3^{2-} and etc); and y denotes the varying amounts of interlayer water). GRs have been found as intermediate corrosion products of iron in suboxic soils and sediments and have been observed to be strong reductants (13-15). In addition, GRs have been detected in zero-valent iron reactive barriers, and it is believed that they could play an important role in degrading contaminants in such systems (16, 17). Much research has been conducted in the last decade and they showed that GRs could reductively degrade a number of organic and inorganic contaminants, including uranate (18), nitrate and nitrite (19-22), selenate (23), chromate (24, 25) and halogenated hydrocarbons (13, 26-29). However, even though degradation of contaminants by GRs is thermodynamically favorable in suboxic conditions, slow degradation kinetics have limited the application of GR in water treatment systems.

Recently, it was reported that the addition of a transition metal to GRs could enhance the degradation rate of chlorinated compounds (13, 29, 30). This combination of GRs with a transition metal produces compounds called high-activity modified green rusts (HMGRs). The rate of dechlorination of chlorinated hydrocarbons by GR-SO_4, was enhanced by two or three orders of magnitude by modifying it with Ag(I), Au(III) or Cu(II) (13, 29). Furthermore, the byproducts of these dechlorination reactions were non-chlorinated compounds (13). Another study observed that the PCE dechlorination rate by

GR-Cl modified by Cu(II), Pt(IV) or Portland cement extract (PCX) was also dramatically increased. The degradation rate was observed to depend on pH and the concentration of the activating agent (30).

Therefore, development of methods to produce and characterize HMGRs would be a very attractive research topic and the results of such a study would be very useful in developing cost-effective treatment technologies for contaminated groundwater.

The goal of this research is to develop and characterize HMGR as reductants to degrade PCE and nitrate in contaminated groundwater. This goal will be accomplished through the following three objectives: 1) develop modification methods to produce HMGRs; 2) characterize reduction kinetics of PCE by HMGRs; and 3) characterize reduction kinetics of nitrate by HMGRs. The most promising HMGRs will be determined through screening tests with five types of GRs (GR-Cl, GR-SO_4, GR-CO_3, GR-F and GR-Br) and 10 trace metals. The ability of selected HGMR to reduce PCE and nitrate will be examined in objectives 2 and 3, respectively.

CHAPTER II

BACKGROUND

2.1 Iron-bearing Solids as Reductants

2.1.1 Green Rust

Green rust (GR) is a layered Fe(II)-Fe(III) hydroxide solid phase with an anion in the interlayer. Different types of GR have been reported as intermediate corrosion products of iron under natural to alkaline conditions in suboxic soil and sediments (15). GRs consists of two layers: 1) the positively charged Fe(II)-Fe(III) hydroxide layers which are often produced by oxidation of Fe(II) to Fe(III) in the trioctahedral sheet of $Fe(OH)_2$, and 2) the negatively charged hydrated anions which exist between the iron hydroxide layers to balance the positive charge (13-15, 31). The general formula for GR is, $\left[Fe^{II}_{(6-x)}Fe^{III}_{x}(OH)_{12}\right]^{x+}\left[(A)_{x/n}\cdot yH_2O\right]^{x-}$ where x is 0.9-4.2; A is an n-valent anion (Cl^-, F^-, SO_4^{2-}, CO_3^{2-}, etc); and y denotes the varying amounts of interlayer water.

In general, the type of GR is determined by the anion in the interlayer. For example, GR with chloride is called "chloride green rust" and written as "GR-Cl". The chemical formula of GR-Cl is $\left[Fe^{II}_{4.5}Fe^{III}_{1.5}(OH)_{12}\right]^{1.5+}\cdot\left[Cl_{1.5}\cdot yH_2O\right]^{1.5-}$. Figure 2-1 shows the schematic structure of GR-Cl and GR-CO_3 (32). GRs containing different anions can be categorized into two types based on the structure of anion in interlay, which results in different X-ray diffraction patterns. GR1 represents GRs that have a planar anion,

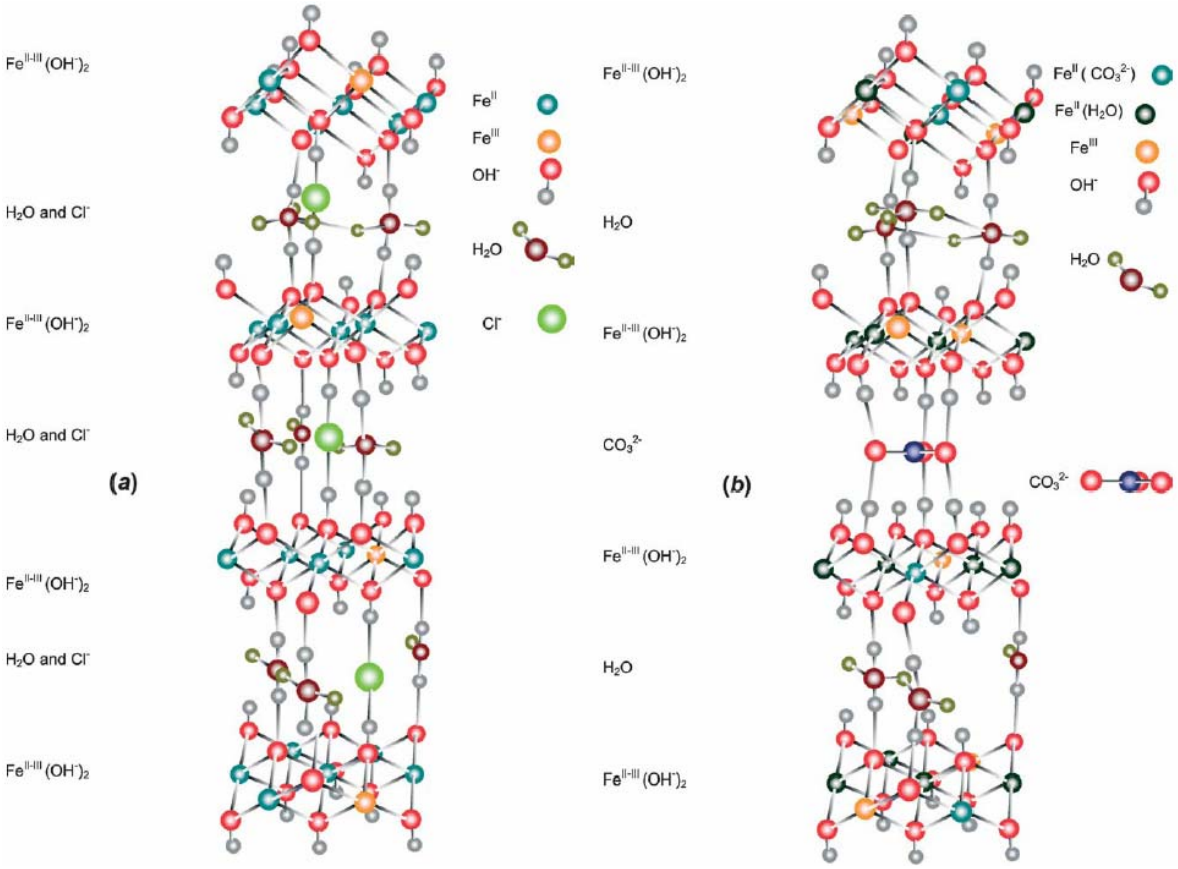

$[Fe^{III}_3Fe^{II}(OH)_8]^+ \cdot [Cl^- \cdot \sim 3H_2O]^-$ $[Fe^{III}_4Fe^{II}_2(OH)_{12}]^+ \cdot [CO_3^{2-} \cdot \sim 3H_2O]^{2-}$

Figure 2.1 Representation of a unit cell for (a) GR-Cl and (b) GR-CO_3. (32).

such as Cl^-, CO_3^{2-} and F^-. GR2 has an anion with a three dimensional structure, such as SO_4^{2-} and SeO_4^{2-} (33). Figure 2-2 is an example of X-ray diffraction patterns of GR-SO_4, GR-Cl and GR-CO_3. In X-ray diffraction patterns, GR1 is characterized as having two strong peaks before 25 º2θ and GR2 has three strong peaks before 30º 2θ. The d-spacing values of several GRs are presented in Figure 2.2. The image of SEM (scanning electron microscope) is also used to identify GRs. The shape of GRs has been known to be hexagonal platy particles as shown in Figure 2.3.

One of the important characteristic of GRs in environmental engineering is their high reactivity as a reductant. Because GRs are highly reduced, the reductive reactions with organic and inorganic contaminants are known to be thermodynamically favorable in suboxic conditions (13). In addition, their double layered structures provide relatively high external and internal surface area, resulting in sufficient reactive sites for chemical reduction (31).

Hansen and coworkers studied nitrate reduction by GR-SO_4 and GR-Cl. In their study, nitrate was totally reduced to ammonium by a GR while magnetite and Fe(II) were observed as byproducts of GR oxidation. The reduction rate by GR-Cl was faster than that by GR-SO_4 (19-22). GR also appeared to be able to reduce metal contaminants. GR-SO_4 showed the capability to reduce U(VI) to UO_2 (18) and Se(VI) to Se(0) (23). GR-CO_3 successfully reduced Cr(VI) to Cr(III) (24, 25). Furthermore, GR was observed to be able to reduce chlorinated organics. Carbon tetrachloride (CT) was reductively dechlorinated by GR-SO_4 (14) and perchloroethylene (PCE), trichloroethylene (TCE),

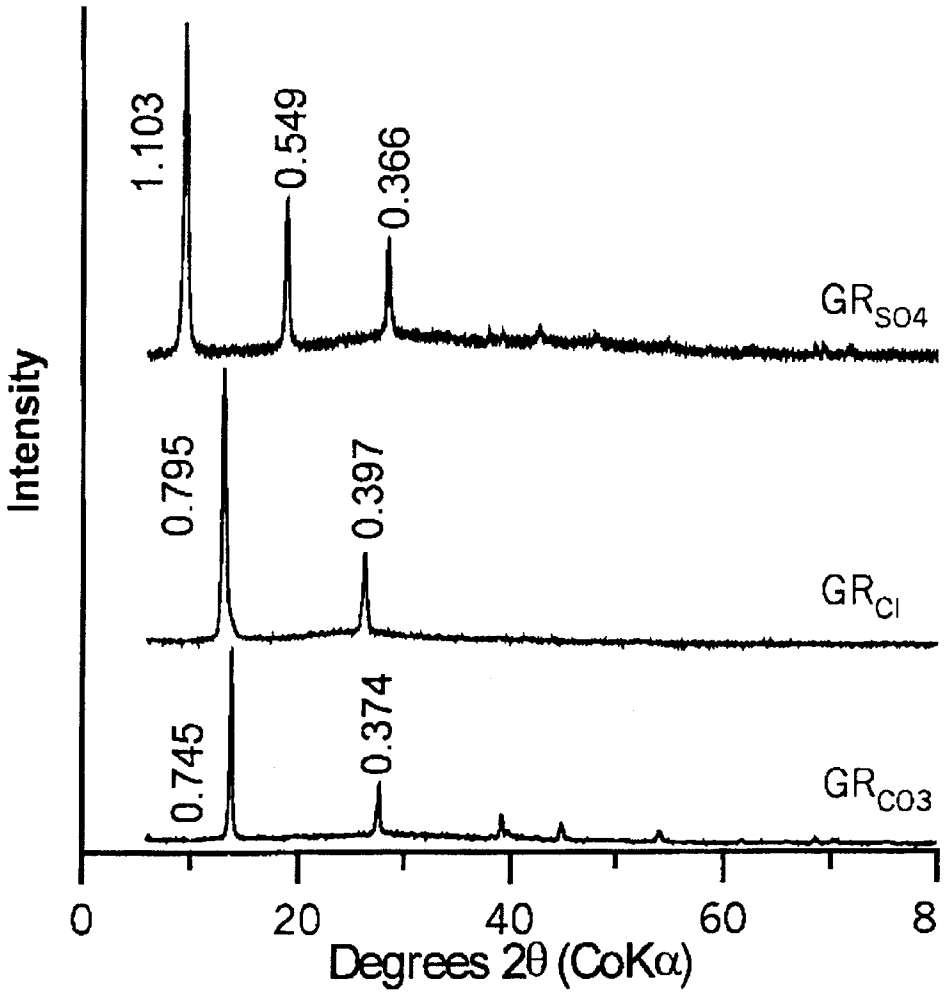

Figure 2.2 Typical X-ray diffraction traces of GR-SO_4, GR-Cl, and GR-CO_3 scanned as glycerol smears. Only d-spacings for basal reflections are shown (nm) (31).

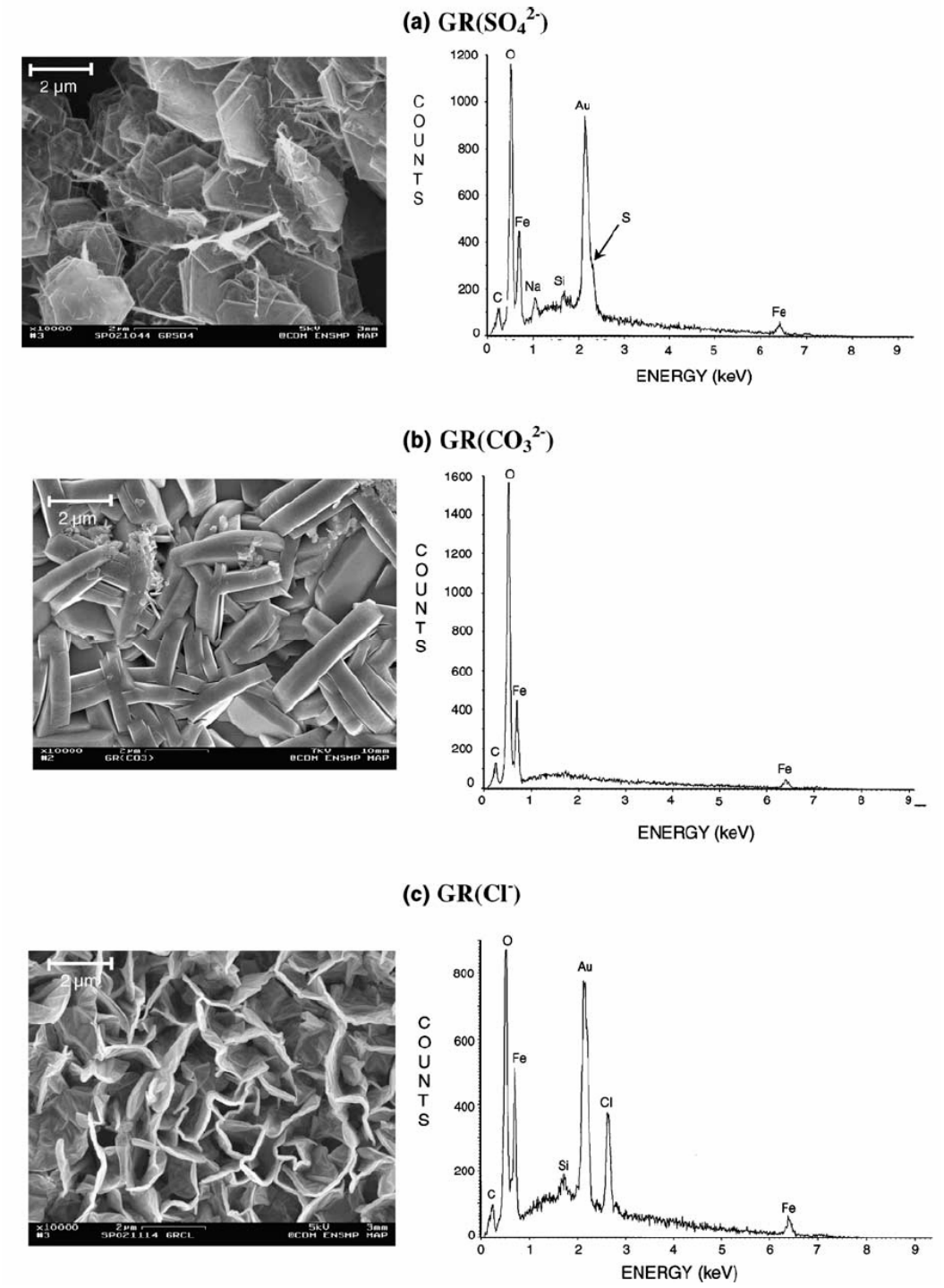

Figure 2.3 SEM (scanning electron microscope) image and EDS (energy dispersive spectrometry) spectra of electrodeposited GR-SO_4, GR-CO_3 and GR-Cl layers on gold substrate (34).

cis-dichloroethylene (cis-DCE), and vinyl chloride (VC) was successively transformed by GR-SO_4 (26-28). Lee observed that the ability of GR-SO_4 to reductively dechlorinate PCE was less than that predicted by the content of the Fe(II) in GR. Therefore, he measured the reductive capacity of GR, which was defined as the maximum amount of a particular oxidant that could be reduced when sufficient time was given. He measured the reductive capacity of GR-SO_4 with PCE as the oxidant (27).

Even though GRs have been reported to reduce inorganic and organic contaminants, the kinetically slow reactions of GRs have been an obstacle to apply them in groundwater treatment systems.

2.1.2 Modification of Green Rusts

Recently, it was reported that the addition of a transition metal to GRs could enhance the degradation rate of chlorinated compounds. These compounds can be described as high-activity modified green rusts (HMGRs). In this study, HMGRs will be named based on the type of GR and the type of an activating agent. For example, GR-SO_4(Ag) represents sulfate green rust that was modified by Ag. O'Loughlin (13) observed that the addition of Ag(I), Au(III) or Cu(II) to GR-SO_4 resulted in nearly two or three orders of magnitude faster reaction in the reductive dechlorination of carbon tetrachloride (CT) than GR-SO_4 itself. Additionally, the terminal products of the reaction were primarily nonchlorinated hydrocarbons, such as methane, ethane, ethene and acetylene (13). The reduction of chlorinated ethanes by GR-SO_4 amended with Cu(II) or Ag(I) was examined. Hexachloroethane (HCA), pentachloroethane (PCA), tetrachlorethane (TeCA) and trichloroethane (TCA) were reduced within times ranging

from several minutes through 24 hr. It took more time to reduce the less chlorinated ethanes, so that the time of reaction increased in the order: HCA< PCA< TeCA< TCA. In general, the reaction rate of GR-SO_4(Ag) was faster than that of GR-SO_4(Cu). The added Ag(I), Au(III) and Cu(II) were observed to be reduced rapidly by GR-SO_4 to the zero-valent state (Ag(0), Au(0) and Cu(0)), which were present as nanometer-sized particles. These particles were believed to act as a catalyst for the reaction between the chlorinated organics and GR-SO_4 (13, 35).

Son also observed an enhancement in the reactivity of GR-Cl for reductive dechlorination of PCE by the addition Cu(II), Pt(IV), Portland cement (PC) or Portland cement extract (PCX). The addition of Cu(II) to GR-Cl induced five hundred times faster reaction than GR-Cl itself and the reactivity of GR-Cl with Pt was increased by a factor of a hundred. The degradation rate was observed to depend on pH in the solution and the concentration of activating agent (30). This behavior may be analogous to the enhancement of reactivity of zero valent iron (ZVI) by a catalytic metal such as Pd, Ni or Pt. The combination of ZVI and the catalytic metal has been called a bimetallic reductant (13).

2.1.3 Modification of Zero Valent Iron

Zero valent iron (ZVI) has been intensively studied as a reductant for organic and inorganic pollutants such as nitrate (12), Cr(VI) (36), U (37) and chlorinated organics (38, 39). It is not only relatively reactive but also readily available, inexpensive and environmentally acceptable so that it has been commonly used as a reactive media in permeable reactive barriers (PRB) to remediate contaminated groundwater (40). The

methods to enhance the reactivity of ZVI have been developed to achieve much faster reaction rate, which can minimize the size of equipment for above ground application. Because the modification mechanism of ZVI is comparable to that for modification of GRs, this section summarizes research on modified ZVI, to give a better understanding of the modification of GRs.

In general, bimetallic reductants consist of two metals, an electron donor and a transition metal. The electron donor is a primary metal such as Fe(0) or Zn(0) and is the source of electrons that are transferred to oxidized compounds during redox reactions. A transition metal plated on the surface of a primary metal acts as a catalyst to improve the reactivity of the primary metal (41).

Pd, Pt, Ni, Cu, Ru and Au have been studied as catalysts in bimetallic reductants used for dehalogenation reactions (41-47). Pd was the most commonly used catalyst to improve the reactivity of ZVI (43). Pd/Fe bimetallic reductant has been investigated to dechlorinate pentachlorophenol (PCP) (43), tetrachloroethylene (PCE) (41, 44), trichloroethylene (TCE) (41, 44, 46) and carbon tetrachloride (CT) (45, 47). In the reductive dechlorination of TCE, the addition of Pd to ZVI with the ratio of 1 to 400 (w/w) produced three orders of magnitude faster reaction compared to untreated ZVI (46). In addition, TCE and PCE were transformed to ethane and no substantial amount of chlorinated byproduct was detected (44). Wan reported that CT was successively dechlorinated by Pd/Fe (500 mg Fe with 0.25 mg Pd) in the sequence of $CHCl_3$ and CH_2Cl_2 and then the final product was CH_4 (45). Pt was also examined as a catalyst in

reductive dechlorination of TCE and the reaction rate of Pt/Fe was more than three times as fast as that of untreated Fe (46).

Fennelly and Roberts (42) examined the catalytic effect of Cu or Ni on the dechlorination of 1,1,1-trichloroethane (1,1,1-TCA) in laboratory-scale batch experiments. 1,1,1-TCA (0.2 mM) was transformed to 1,1-dechloroethane (1,1-DCA) by Ni/Fe and Cu/Fe in 3 hrs reaction time and the reaction rates in both cases were improved by a factor of about three compared to ZVI itself. Ethane and ethylene was observed as byproducts.

2.1.4 Mechanism of Modification of ZVI

Bimetallic reductants were generated by reductive deposition of a transition metal on a primary metal (ZVI) resulting in a thin layer on the surface on ZVI. This reaction is shown in equation 2-1.

$$2Fe^{0} + Pd^{4+} \rightarrow 2Fe^{2+} + Pd^{0} \downarrow \qquad (2\text{-}1)$$

There are two hypothetical mechanisms which have been suggested to explain the enhancement of the reactivity of bimetallic reductants. The first one is that a transition metal on the surface of ZVI might act as a catalyst by reducing the activation energy of the reaction and thereby improving rates of dehalogenation (41). Another opinion is that the modification of the bimetallic system might involve the hydrogen production from water by corrosion of ZVI with a catalyst. The accumulated atomic hydrogen or hydride

on the surface of bimetals, especially on the surface of transition metals, might contribute to rapid reduction of halogenated compounds in the presence of a catalyst (48).

Three steps in dehalogenation by bimetallic reductant like Pd/Fe had been proposed by Cheng and co-worker to explain the mechanism of dehalogenation on modified ZVI (49). The first step is the production of hydrogen gas through the reduction of water by elemental iron. The second step is the formation of strong reducing species, $Pd{\cdot}H_2$ by adsorption of produced hydrogen gas onto the surface of the trace metal. The final step is the reduction of the chlorinated hydrocarbon that is adsorbed onto the surface of the bimetallic reductant (49). The overall reaction is shown in equation 2-2 and the schematic mechanism of the dehalogenation reaction on the surface of bimetallic reductant is illustrated in Figure 2-4.

$$Fe^0 + RX + H^+ \rightarrow Fe^{2+} + RH + X^- \qquad (2\text{-}2)$$

The surface area of the bimetallic system and the content of a catalyst are the important factors (41, 46). The reactivity of ZVI was increased with decreasing particle sizes of ZVI. Zhang *et al.* observed that the reactivity for degrading PCE of nano-sized ZVI (1-100 nm, average BET surface area was 33.5 m^2/g) was significantly increased compared to that of micro-scale ZVI (< 10 μm, average BET surface area was 0.9 m^2/g) (41). The increase of reactivity of a bimetallic reductant (Ru/Fe) was observed with increasing catalyst content. The observed rate constant of TCE dechlorination by Ru/Fe

was increased from 0.245 (hr^{-1}) to 2.4 (hr^{-1}) with increasing Ru content from 0.25 %(w/w) to 1.5 %(w/w) (46).

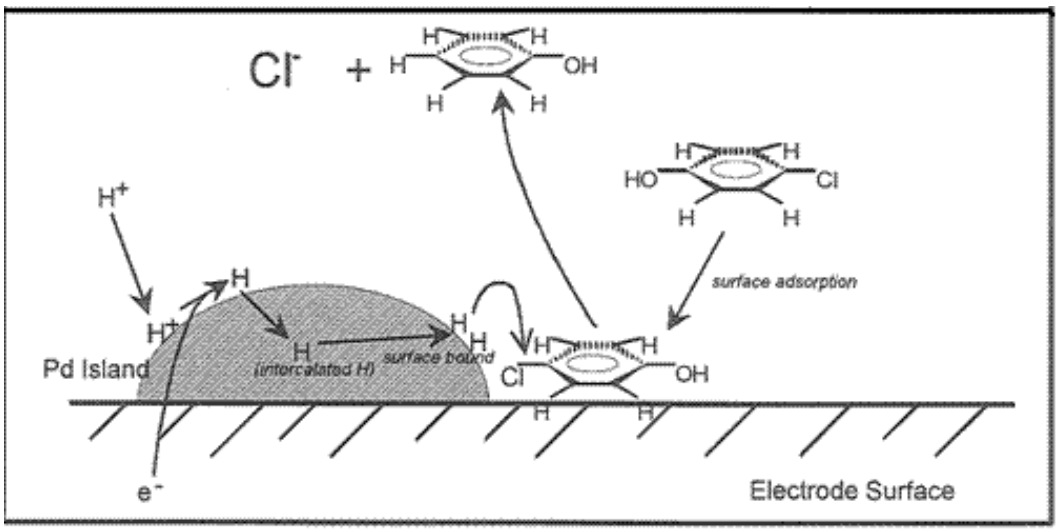

Figure 2.4 Schematic of reductive dehalogenation reaction on the surface of bimetallic reductant (Pd/Fe) proposed by Cheng *et al.* (49).

2.2 Transformation of Chlorinated Organics

There are two transformation mechanisms for chlorinated alkenes that differ in the extent of electron transfer. In a reductive transformation, electrons are transferred to an external electron acceptor, which results in a change in the oxidation number of carbon in the hydrocarbon compound. The other mechanism is a non-reductive transformation

which does not involve electron transfer (50). In this section, the transformation mechanisms of alkenes will be summarized with the focus on the reductive transformation reaction.

2.2.1 Non-reductive Transformation of Chlorinated Organics

Substitution and dehydrochlorination are two types of non-reductive transformation of chlorinated organics (50). Substitution occurs when a chlorine atom is replaced by a nucleophile, which has unshared electrons that are used to form a covalent bond with carbon as shown in equation 2-3. The alkoxide ion (RO^-), hydrogen sulfide ion (HS^-), cyanide ion ($N\equiv C^-$) and alkynide ion ($RC\equiv C^-$) are known to be nucleophiles that can substitute for chlorine on alkyl chlorides (51). The particular reaction in which a water molecule or hydroxide ion (OH^-) substitutes for chlorine is called a hydrolysis reaction and this reaction is described by equation 2-4. Many nucleophilic substitution reactions are known to be very slow in the absence of an inorganic or biochemical catalyst (50).

$$RCl + Nu^- \rightarrow RNu + Cl^- \quad (2\text{-}3)$$

$$RCl + H_2O \rightarrow ROH + HCl \quad (2\text{-}4)$$

Dehydrochlorination occurs when a proton from one carbon and the chloride from the adjacent carbon are eliminated at the same time (51). This converts a chlorinated

alkane or alkene into an alkene or alkyne, respectively. Equation 2-5 illustrates the dehydrochlorination of PCA to PCE, which is catalyzed by semectite (52).

$$CCl_3\text{-}CHCl_2 \rightarrow CCl_2=CCl_2 + H^+ + Cl^- \quad (2\text{-}5)$$

2.2.2 Reductive Transformation of Chlorinated Organics

Abiotic reductive dechlorination by metal particles has been recognized as one of the main processes to determine the fate of chlorinated organics in reducing environments. Because chlorinated organics are relatively oxidized, reductive dechlorination tends to be thermodynamically favorable in the presence of appropriate reductants, such as ZVI and GRs (13, 14, 27-29, 38, 39, 50, 52, 53). There are two major pathways in abiotic reductive dechlorination of chlorinated ethylenes: hydrogenolysis and reductive β-elimination (38). These pathways and their intermediates for reductive dechlorination of PCE are shown in Figure 2-5

2.2.2.1 Hydrogenolysis

Hydrogenolysis is the reaction in which chlorine is replaced with hydrogen due to a two-electron transfer from a reductant to the chlorinated hydrocarbon. This pathway corresponds to reactions 1, 3, 4, 5, 7, 9, 14, 17 and 18 in Figure 2-5 (53) and the electron transfer reaction is carried out through several steps as shown in Figure 2-6. The alkyl radical or alkyl carbanion is as an intermediate of these reactions (38).

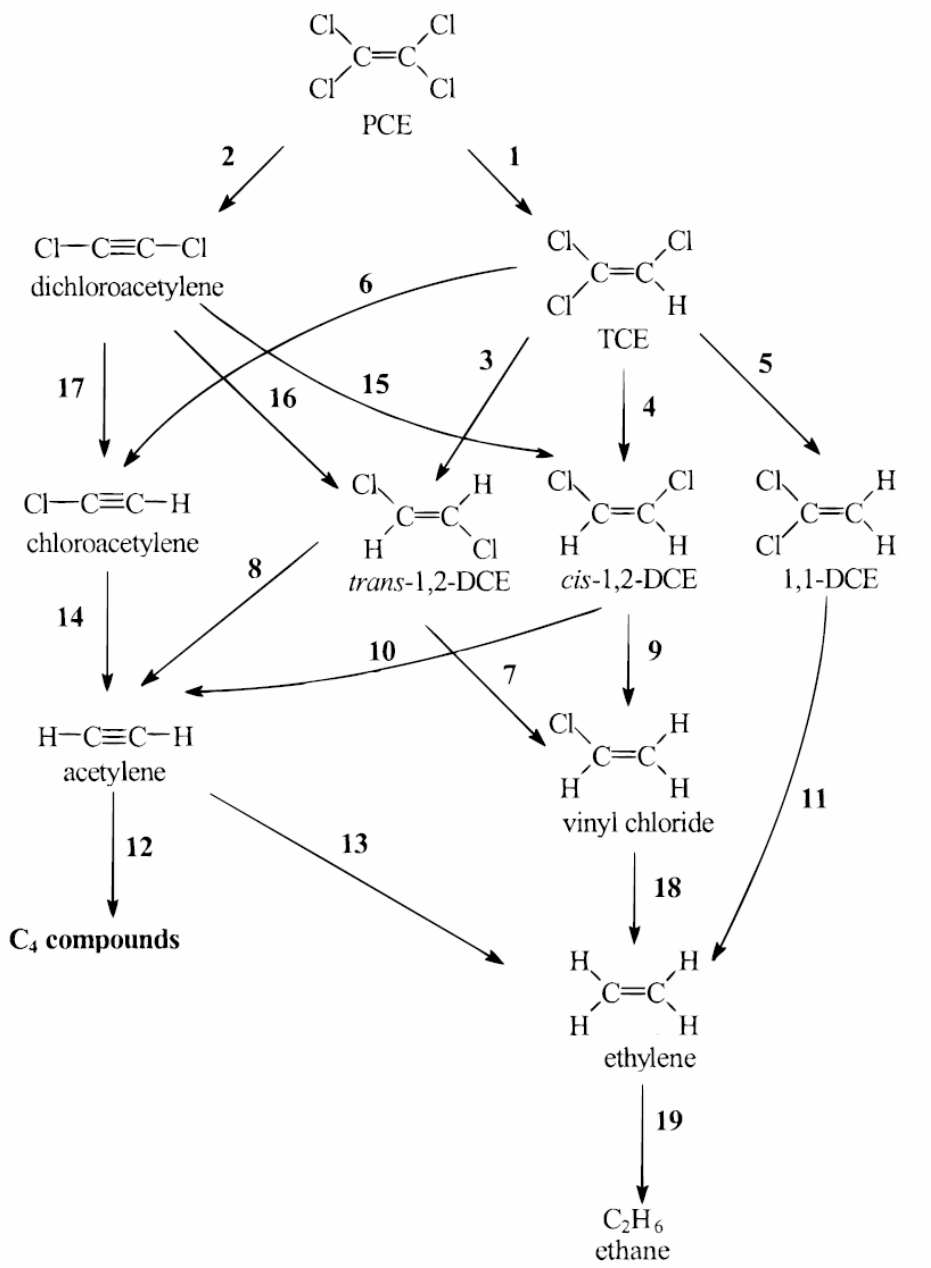

Figure 2.5 Hypothesized reaction pathways for chlorinated ethylenes and other intermediates during reaction with ZVI. Reactions 1, 3, 4, 5, 7, 9, 14, 17 and 18 correspond to the hydrogenolysis pathway; reactions 2, 6, 8 and 10 correspond to the reductive β-elimination pathway; reaction 11 proceeds via reductive α-elimination; and reactions 13, 15, 16 and 19 are hydrogenation reactions (53).

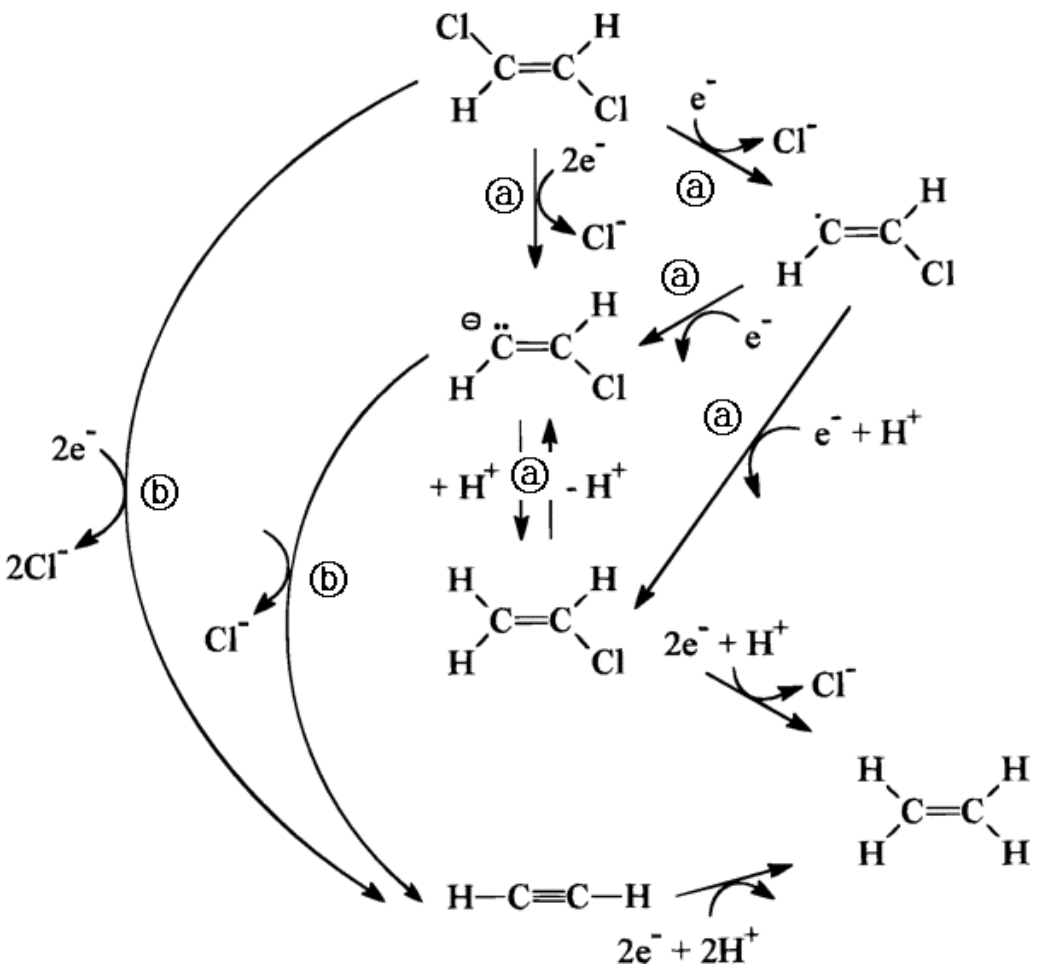

Figure 2.6. Proposed pathways for reduction of trans-dichloroethylene by zero-valent metals. Reaction ⓐ corresponds to the hydrogenolysis pathway and reaction ⓑ corresponds to the reductive β-elimination pathway (38).

O'Hannesin and Gillham observed that TCE was reductively transformed by granular iron in a permeable wall to form cis-DCE, trans-DCE, and 1,1-DCE, meaning that the dechlorination reaction occurred through the hydrogenolysis pathway (39). This reaction pathway was also observed in PCE degradation by ZVI (38). Reductive dechlorination of pentachloroethane (PCA) by commercial Fe(0) has been reported to occur by an initial transformation to PCE and then by hydrogenolysis of PCE to TCE (52). Carbon tetrachloride (CT) was transformed via stepwise hydrogenolysis to chloroform (CF), methylene chloride (MC), chloromethane (CM) and methane in the Fe(II)-based DS/S system and the kinetics of this degradation was strongly dependent on pH (54).

2.2.2.2 Reductive β-Elimination

Reductive β-elimination of chlorinated organic compounds occurs with the elimination of two chlorine atoms from adjacent carbons. Two electrons are transferred and double or triple bonds are formed between the carbons. This reaction is denoted with ⓑ in Figure 2-6 and corresponds to reactions 2, 6, 8 and 10 in Figure 2-5.

Many researchers have identified the reductive β-elimination pathway as an important mechanism of dechlorination. Roberts reported that the concentration of trans-DCE decreased in the presence of ZVI and that the concentrations of acetylene and ethylene increased, which means that reaction 8 (β-elimination) and reaction 13 (hydrogenation) in Figure 2-5 occurred in that order (38). PCE degradation by GR-SO_4 (28), pyrite (55) and iron-bearing phyllosilicates (biotite, vermiculite and montmorillonite) (56) has also been reported to occur via reductive β-elimination.

Chlorinated ethanes such as HCA, PCA, TeCA and TCA have been reported to be reduced by GR-SO_4(Ag) and GR-SO_4(Cu) to PCE, TCE, DCE and VC, respectively, via reductive β-elimination (29).

The β-elimination pathway for reduction of chlorinated ethylenes has the environmental advantage of producing chlorinated acetylene instead of the less chlorinated ethylenes such as DCE and VC (Figure 2-5). This is an advantage, because chlorinated ethylenes are known to be much more stable than chlorinated acetylenes. In particular, the accumulation of vinyl chloride via hydrogenolysis is recognized to be an environmental problem because of the toxic and recalcitrant characteristics of VC (27, 53).

2.3 Reduction of Nitrate

The removal of nitrate from water using physical, biological and chemical methods has been widely studied. Physico-chemical methods including ion exchange, reverse osmosis and electrodialysis have been shown to be stable, fast and easily automated processes. However, they have been considered not to be applicable to a large scale systems, because of high operational costs and the generation of concentrated brine wastes (12, 57).

Biological methods for nitrate removal from water are known as biological denitrification and have been used primarily for wastewater treatment. In biological denitrification, microorganisms called as denitrifiers use nitrate as an electron acceptor in the absence of oxygen. Nitrate (NO_3^-) is sequentially reduced to nitrite (NO_2^-), nitric oxide (NO), nitrous oxide (N_2O) and nitrogen gas (N_2) as shown by equation 2-6 (58).

This process has been observed to occur naturally in suboxic conditions such as can occur in sediments and soils.

$$\begin{aligned}
&2NO_3^- + 4e^- + 4H^+ \rightarrow 2NO_2^- + 2H_2O && \text{; Nitrate reduction}\\
&2NO_2^- + 2e^- + 4H^+ \rightarrow 2NO + 2H_2O && \text{; Nitrite reduction}\\
&2NO + 2e^- + 2H^+ \rightarrow N_2O + H_2O && \text{; Nitric oxide reduction}\\
&N_2O + 2e^- + 2H^+ \rightarrow N_2(g) + H_2O && \text{; Nitrous oxide reduction}
\end{aligned} \qquad (2\text{-}6)$$

Biological denitrification has the environmental advantage of producing nitrogen gas as a final product, which is easily dispersed into the air phase. However, excessive production of biomass, the need to provide a continual supply of electron donor for the growth of the microorganisms, and difficulty of operating the treatment system have been obstacles in the application of biological methods in water treatment. Moreover, reaction rates for biological denitrification are slower than those for chemical reduction (12, 57).

Many research studies have been conducted during the last decade on nitrate reduction by chemical reductants as an alternative to biological denitrification. Zero valent iron (ZVI) has been shown to be a promising reductant for nitrate, which is generally reduced to the ammonium ion (12, 59-63). It has been observed that 400 mg/L of NO_3^- can be completely removed by 0.5 g of nano-scale ZVI in an anaerobic batch system in 30 minutes (12). In general, pH and dissolved oxygen (DO) concentration appear to be important operational factors in nitrate reduction by ZVI. Most of the

research shows that the reaction rate increases at low pH in the range of pH 2-5 and at low concentrations of DO (59-63).

Yang and Lee proposed two pathways for nitrate reduction by ZVI that are based on the observation of increasing ferrous and decreasing hydrogen ion concentrations during the reaction as shown in equations 2-7 and 2-8. They found that the reaction producing ammonium (equation 2-7) was dominant, while both reactions might be thermodynamically favorable under when pH $\leq$ 4 (62). GR was identified as a byproduct of ZVI oxidation when the system pH was initially adjusted to pH 2-3 with the addition of HCl and H_2SO_4 (61).

$$NO_3^- + 4Fe^0 + 10H^+ \rightarrow 4Fe^{2+} + NH_4^+ + 3H_2O \quad (2\text{-}7)$$

$$2NO_3^- + 5Fe^0 + 12H^+ \rightarrow 5Fe^{2+} + N_{2(g)} + 6H_2O \quad (2\text{-}8)$$

Hansen and coworkers (20, 21) evaluated the reactivity of GRs for nitrate reduction at neutral pH. Nitrate was reduced to ammonium with transformation of GR-Cl to magnetite as shown in equation 2-9 and the ratio of ammonium formed to GR-Cl consumed was the same as that predicted by the ideal stoichiometry ($\Delta NH_4^+/\Delta$ Fe(II) in solid = 5/72) (21).

$$Fe^{II}_{4.5}Fe^{III}_{1.5}(OH)_{12}Cl_{1.5} + \frac{5}{16}NO_3^- \rightarrow 2Fe_3O_4 + \frac{5}{16}NH_4^+ + \frac{14}{16}H^+ + \frac{3}{2}Cl^- + \frac{79}{16}H_2O \quad (2\text{-}9)$$

Solids that contain Fe(II) have been observed to be good reductants for nitrate when combined with metallic catalysts. Ottley *et al.* combined Cu(II) with Fe(II)-containing solids and observed that the time required to achieve 15% reduction of nitrate with was three orders of magnitude smaller than that achieved by Fe(II)-containing solids alone. The efficiency of nitrate reduction with Cu/Fe(II) was improved by increasing the concentration of Cu(II) and by increasing pH in the range of 7 to 9. It was proposed that Cu(II) was reduced to the zero-valent state and present as solid phases on the surface of iron oxide or as a saturated solid (64). The results of this study sufficiently provided the evidence that the addition of a transition metal to GRs could enhance the reactivity of GR for nitrate reduction as well as dechlorination.

CHAPTER III

METHODOLOGY

3.1 Experimental Systems

GRs were modified and characterized under anaerobic conditions in this study, because they are known to react with oxygen. Anaerobic conditions were obtained by using an anaerobic chamber (Coy Laboratory Products Inc.) in which the atmosphere was filled with a mixed gas containing 5% hydrogen and 95% nitrogen. Palladium catalysts were used to remove any oxygen that entered the chamber. Oxygen could accidentally enter when chemicals and laboratory equipment were introduced into the chamber or it could continuously diffuse through the chamber wall. Palladium acted as a catalyst to initiate the reaction between hydrogen and oxygen to produce water in the chamber. The anaerobic conditions of chamber were monitored using a colorimetric redox indicator solution (resazurin, 89%, Aldrich). The color of the indicator solution turned from colorless to pink when the redox state of chamber became higher than - 218 mV at pH 9 (65).

Deaerated deionized water (DDIW) was used in this study to maintain deoxygenated conditions during all experimental procedures. DDIW was prepared from DIW (deionized water) purified by a Barnstead Nanopure system by purging it with 99.99% nitrogen for 2 hours and then by purging it in an anaerobic chamber for more than 12 hours.

Two types of completely mixed batch reactor systems were used in this research. The first one was a clear borosilicate glass vial (normally 20 mL, Kimble) with an open-top screw cap lined with PTFE film (Norton Performance Plastics Co.), lead foil (3M), and a rubber septum (Kimble). Because this reactor was carefully designed to be placed under aerobic conditions during the reaction period, it effectively minimized the intrusion of oxygen and the volatilization losses of organic compounds. This reactor was used in both screening tasks for developing HMGRs and reductive dechlorination of perchloroethylene (PCE) by HMGRs. The other reactor was a 250-mL polypropylene bottle (Nalgene) which was used for nitrate reduction experiment by HMGRs.

3.2 Chemicals

Tetrachloroethylene (99.9+%, HPLC grade, Aldrich) and sodium nitrate (A.C.S. certified, Fisher) were used in this research as target compounds. Ferrous chloride (tetrahydrate, 99%, Aldrich), ferrous sulfate (septahydrate, 99+%, Aldrich), sodium hydroxide (97.0% min. EM), sodium carbonate (99.5+%, Sigma), sodium fluoride (99.8%, J.T. Baker), and sodium bromide (99+%, Aldrich) were used in the procedure for synthesizing five types of GRs (GR-Cl, GR-SO_4, GR-CO_3, GR-F and GR-Br). Ten trace metals were used as activating agents to modify GRs: silver chloride (99%, Aldrich), barium chloride (dihydrate, 99+%, Fisher), cobalt chloride (hexahydrate, 98%, Aldrich), copper chloride (dihydrate, 99+%, Aldrich), manganese chloride (tetrahydrate, 98+%, Aldrich), nickel chloride (hexahydrate, Aldrich), lead chloride (99.999%, Aldrich), platinum chloride (98%, Aldrich), titanium oxide (99.9+%, Aldrich), and zinc chloride (98% min, EM).

Two biological buffers were used in the experiment for determining the effect of pH on the reduction of PCE and nitrate by HMGRs. CAPS (3-[cyclohexylamion]-1-propanesulfonic acid, pKa = 10.4, Sigma) and CHES (2-[N-cyclohexylamino]ethanesulphonic acid, pKa = 9.3, Sigma) were used at pH 11 and pH 9, respectively.

PCE was extracted from the aqueous solution prior to analysis by gas chromatography (GC) with hexane (98.5+%, ACS grade, EM) that contained 1,2-dibromopropane (1,2-DBP, 97%, Aldrich) as an internal standard. Stock solutions were prepared by diluting concentrated PCE solutions in methanol (99.8%, HPLC grade, EM). The following chemicals were used as standards to analyze the chlorinated by-products of PCE degradation: trichloroethylene (TCE, 99.6%, Sigma), cis-dichloroethylene (c-DCE, 97%, Aldrich), trans-dichloroehtylene (t-DCE, 98%, Aldrich), 1.1-dichloroethylene (1,1-DCE, 99%, Aldrich), and vinyl chloride (VC, 200 μg/mL in methanol, Sigma-Aldrich). A mixed gas (1% CO, CO2, methane, ethane, ethylene, and acetylene in nitrogen, Alltech) was used as the standard for analysis of the non-chlorinated byproducts.

Concentrations of ammonia formed as the final product of nitrate reduction were measured by the phenate method (66) using the following chemicals: phenol (liquefied, min. 88%, EM), ethanol (99.5%, Aldrich), sodium nitroferricyanide (III) (dehydrate, 99%, Sigma-Aldrich), sodium citrate (dehydrate, 99.9%, Sigma), and sodium hydrochlorite (6%, VWR).

3.3 Synthesis and Characterization of Green Rusts

3.3.1 Synthetic Method of Green Rusts

Five types of GRs were synthesized by the partial air oxidation method, which was developed by Genin and co-workers (15, 67-69) and modified by Son (30). $Fe(OH)_2$ was prepared by mixing Fe(II) and NaOH solution in an anaerobic chamber and allowing it to be partially oxidized by oxygen in the air in the presence of an appropriate anion. Equation 3-1 describes the reaction of GR synthesis, where A^{-n} is an n-valent anion; x is 1.5 when n=1 and is 2 when n=2; and y denotes the varying amounts of interlayer water. The chemical recipes for synthesizing five types of GRs and the theoretical ratios of Fe(II) to Fe(III) in synthesized GRs are summarized in Table 3.1.

$$6Fe(OH)_2 + \frac{x}{4}O_2 + \frac{x}{n}A^{-n} + (\frac{x}{2} + y)H_2O \leftrightarrow Fe^{II}_{(6-x)}Fe^{III}_{x}(OH)_{12}A_{x/n}yH_2O + xOH^- \quad (3\text{-}1)$$

The synthesis reaction was monitored by recording pH in the solution. The pH increased while Fe(II) in the structure of $Fe(OH)_2$ was being oxidized to Fe(III) and GR was being formed as shown in equation 3-1. The pH started to decrease when the ratio of Fe(II) to Fe(III) in GR became less than the ideal ratio of GR. Figure 3.1 clearly shows the relationship of pH and the ratio of Fe(II) to Fe(III) during the synthesis of GR-F. The synthesized GRs were introduced into an anaerobic chamber when the pH in the solution began to drop and were kept in an anaerobic chamber to prevent further oxidation. GRs were washed by DDIW twice to reduce excess ion concentrations before using them.

The iron concentration was measured using the ferrozine method (70). The iron in the solid phase was determined by subtracting iron content in the liquid from iron content in the suspension (solid + liquid).

Table 3.1 Chemical recipes of GR synthesis and ideal ratios of Fe(II) to Fe(III) in synthesized solids.

Green rust type	Chemical recipes of green rust synthesis			Ideal ratio of Fe(II) to Fe(III)
	Iron	Hydroxide	Anion	
GR-Cl	0.115 M $FeCl_2 \cdot 4H_2O$	0.2 M NaOH	-	3
GR-SO_4	0.12 M $FeSO_4 \cdot 7H_2O$	0.2 M NaOH	-	2
GR-CO_3 [a]	0.12 M $FeSO_4 \cdot 7H_2O$	0.2 M NaOH	0.12 M Na_2CO_3	2
GR-F [a]	0.12 M $FeCl_2 \cdot 4H_2O$	0.2 M NaOH	0.12 M NaF	3
GR-Br [b]	0.115 M $FeCl_2 \cdot 4H_2O$	0.2 M NaOH	0.23 M NaBr	3

[a] In the synthesis of GR-CO_3 and GR-F, an anion was mixed into $Fe(OH)_2$ solution, right after $Fe(OH)_2$ solids were synthesized.

[b] In the synthesis of GR-Br, the concentration of Cl^- in $Fe(OH)_2$ solution was initially reduced before mixing Br^- into $Fe(OH)_2$ solution by separating liquid and solid of $Fe(OH)_2$, removing liquid phase, and refilling the same amount of DDIW into $Fe(OH)_2$ solid as that of liquid removed. After that, Br^- was added into washed $Fe(OH)_2$.

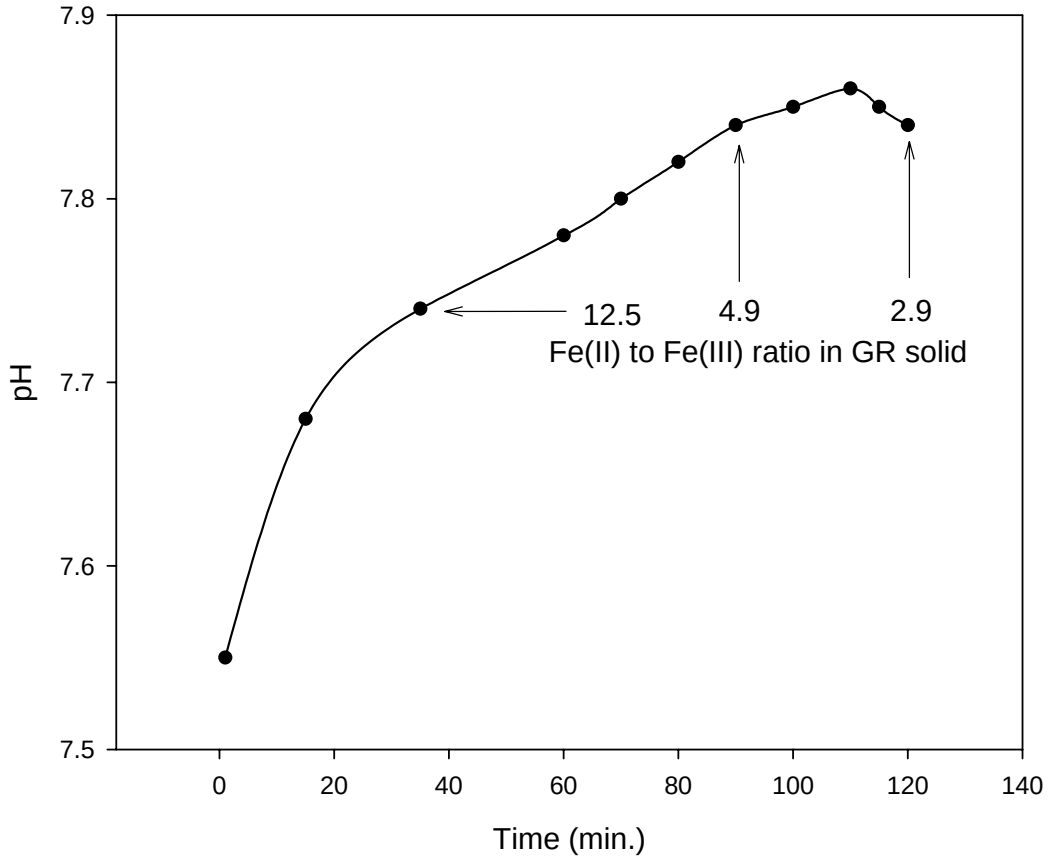

Figure 3.1 Change of pH in solution and ratios of Fe(II) to Fe(III) in solid during the oxidation of $Fe(OH)_2$ in the synthesis of GR-F. The ideal ratio of Fe(II) to Fe(III) in GR-F is 3.

3.3.2 Characterization of Green Rusts

The characterization of synthesized GRs was determined through the measurement of iron and anion content and the analysis of X-ray diffraction (XRD) and scanning

electron microcopy (SEM). The iron content in GRs was mainly used to evaluate the synthesized solid. Fe(II) and Fe(III) concentrations in solids were measured at each synthesis and compared with the ideal ratios. Table 3-2 shows the average concentrations of Fe(II) and Fe(III) in GR solids and the average ratio of Fe(II) to Fe(III).

Table 3.2 Iron contents and ratios of Fe(II) to Fe(III) in synthesized GR solids.

Green rust	Fe(II)[a] (mM)	Fe(III)[a] (mM)	Fe(II)+Fe(III)[a] (mM)	Fe(II)/Fe(III)
GR-Cl	84.4(±6.0%)	25.9(±5.7%)	110.3(±4.7%)	3.3(±8.1%)
GR-SO_4	78.5(±2.4%)	39.1(±7.0%)	117.6(±2.5%)	2.0(±8.8%)
GR-CO_3	79.1(±7.4%)	38.2(±14.9%)	117.3(±9.5%)	2.1(±8.9%)
GR-F	90.0(±2.6%)	29.8(±4.2%)	119.8(±2.3%)	3.0(±4.5%)
GR-Br	88.0(±6.2%)	28.0(±4.9%)	115.9(±5.7%)	3.1(±3.7%)

[a] Fe(II) and Fe(III) concentration in solid phase obtained by Ferrozine method.

Anion content in the interlayer of the solids was measured at the synthesis of GR-CO_3, GR-F and GR-Br, because there were two anions in solution during their production. For example, since $FeCl_2$ and NaF were added as the source of iron and anion, respectively, in GR-F synthesis, both Cl^- and F^- could compete for the position in the interlayer. The type of GR produced was determined by calculating the differences of both anion concentrations between synthesis steps. Anions removed from solution

were assumed to be placed in the interlayer of GR. These analyses showed that GR-CO_3 and GR-F were produced at 98% purity and that GR-Br was produced at 86% purity. The reason for the low yield of GR-Br was due to the relative affinity of GR for different anions. Refait and coworkers (69) observed that GR-CO_3 was preferentially formed during the competition between CO_3^{2-} and SO_4^{2-} and the sequence of anion selectivities for GR was $CO_3^{2-} > SO_4^{2-} > Cl^-$. Rives (31) also reported the sequence of selectivities in layered double hydroxide (LDH) other than GR. The sequence for monovalent anions was $OH^- > F^- > Cl^- > Br^- > I^-$ and the selectivity for divalent anion was $CO_3^{2-} > SO_4^{2-}$.

Figure 3.2 shows the X-ray diffraction (XRD) patterns of five GRs and their d-space values of three intensive peaks. The XRD patterns of GR-Cl, GR-CO_3, and GR-SO_4 synthesized in this study were analogous to the references shown in Figure 2.2 (31). There were no appropriate references for GR-F and GR-Br. However, it was expected that the XRD patterns of GR-F and GR-Br might be comparable with those of GR-Cl and GR-CO_3 based on the similarity of anion structures and it was confirmed in the results of XRD analysis as shown in Figure 3.2.

Figure 3.3 shows the image of scanning electron microscopy (SEM) of GR-F. Hexagonal shape of the solids was observed and their particle sizes were less than 1μm.

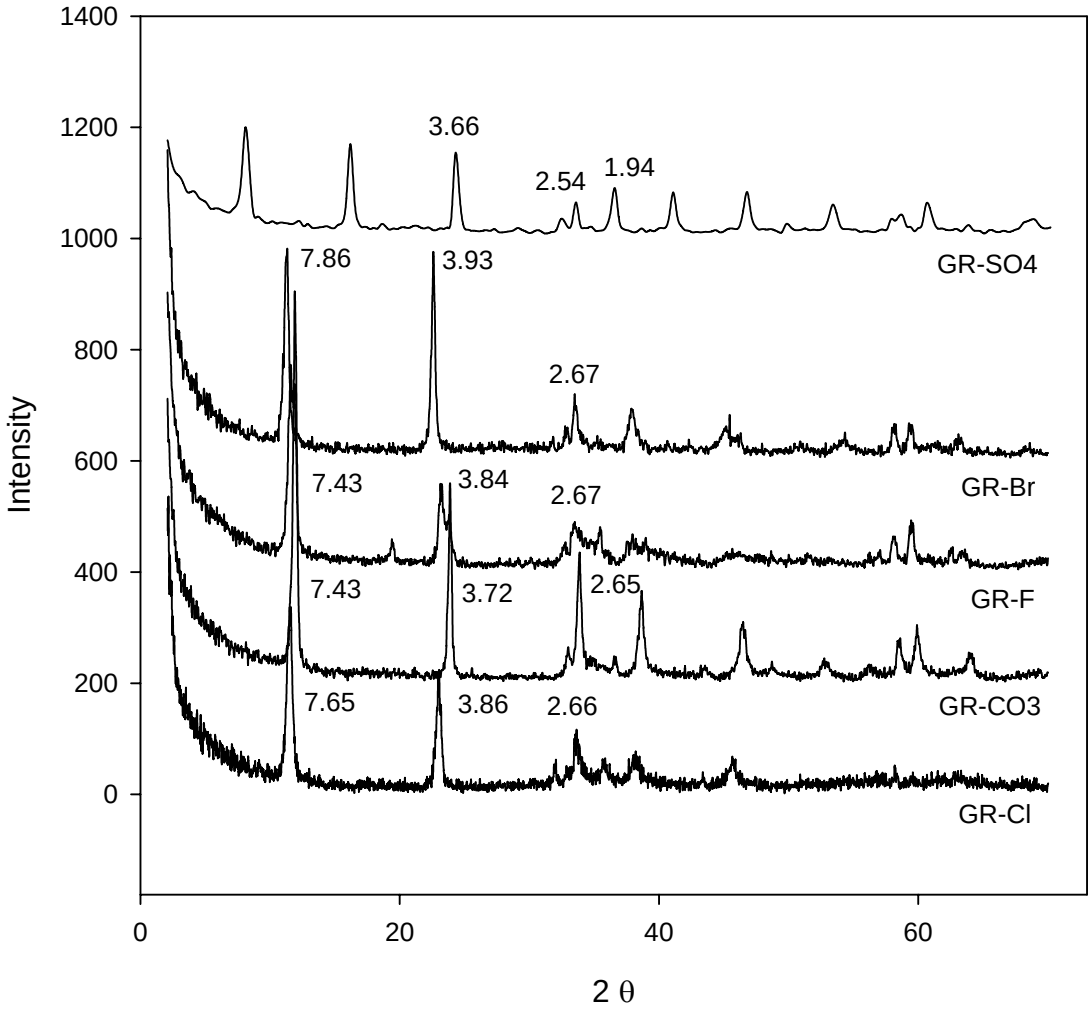

Figure 3.2 X-ray diffraction patterns for synthesized GRs. The numbers in graph are d-space values of each GRs. GR-Cl, GR-CO_3, GR-F and GR-Br were classified as GR 1 and GR-SO_4 was classified as GR 2.

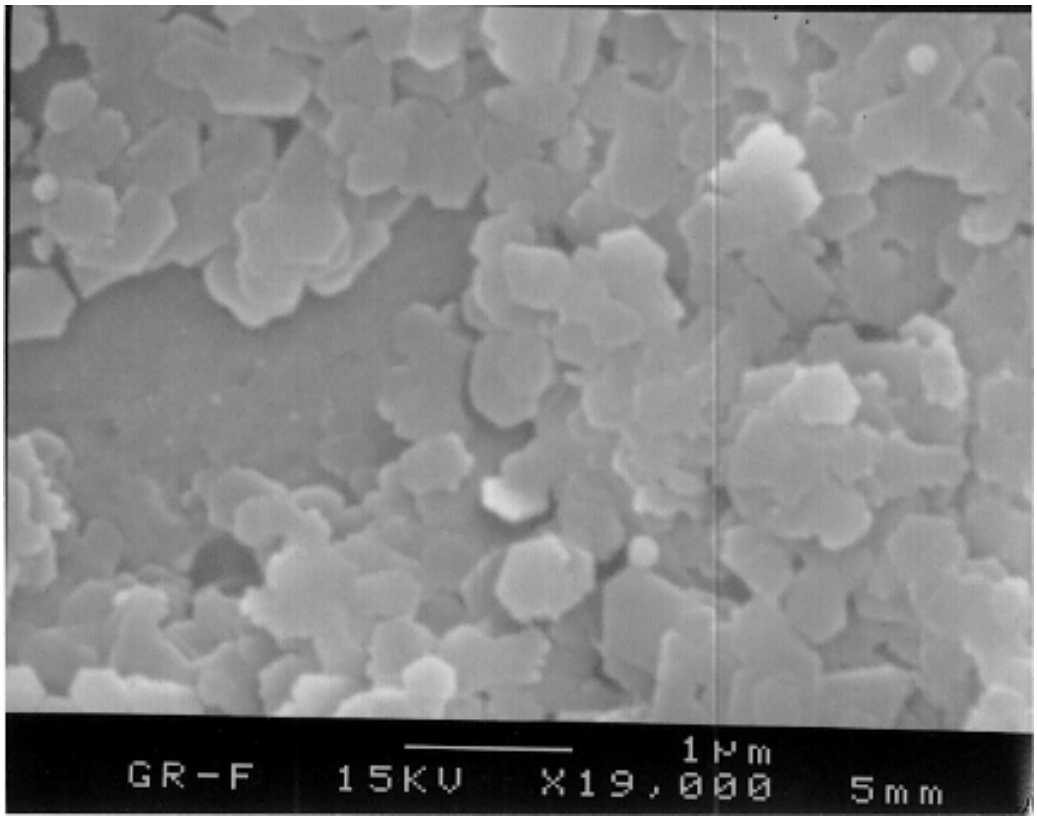

Figure 3.3 SEM image of GR-F.

3.4 Analytical Procedures

3.4.1 Measurement of PCE and Its Daughter Products

PCE and its chlorinated daughter products (TCE, trans-DCE, cis-DCE, 1,1-DCE and VC) were analyzed using gas chromatography. PCE and TCE were measured through the following steps. The retrieved vials were centrifuged at 2960 g for 20 minutes (Beckman, model J-6M centrifuge, JS-7.5 rotor). A 50-μL volume of supernatant was transferred to 2-mL target vials (National Scientific Co.) containing 1 mL extractant (hexane with 0.025 mM of 1,2-DBP). They were extracted for about 1 hr on an orbital shaker and were then placed on an auto-sampler installed on a gas chromatograph (Hewlett-Packard 6890 GC) equipped with DB-VRX column (60 m × 0.25 mm i.d. ×1.8 μm film thickness, J&W Scientific) and electron capture detector (ECD). The operational conditions for GC were: injector temperature = 220 ºC; detector temperature = 240 ºC; oven temperature started 80 ºC for 2 minutes and increased to 120 ºC at the rate of 5 ºC min and then held for 1 minute; injection volume = 1 μL; split ratio = 20:1; carrier gas = nitrogen; make up gas flow rate = 4 mL/min.

1,1-DCE, t-DCE, c-DCE and VC were measured using a Trace GC 2000 (Thermo Finnigan) with HP-5MS column (30 m × 0.25 mm i.d. ×0.25 μm film thickness, J&W Scientific) and flame ionization detector (FID). A 10-mL sample of the liquid phase produced by centrifugation was transferred into a 20-mL vial and then rapidly capped with three layered closures. The vials were shaken for 1 hr using orbital shaker to equilibrate gas and liquid phase and then stood for 1 hr at the room temperature. A 100-μL sample of the gas phase was taken with a 100-μL gas-tight syringe (Hamilton) and

manually injected into the injection port of GC. The temperature of the injection port and detector were 200 ºC and oven temperature was isothermally maintained at 50 ºC for 5 minutes. Injection volume was 100 μL with a split ratio of 10:1. Helium was used as the carrier gas and makeup gas at a constant flow rate of 1.5 mL/min. Hydrogen and zero-grade air were used as ignition gas. The aqueous phase concentrations of t-DCE, c-DCE, 1,1-DCE and VC in the samples were calculated using dimensionless Henry's law constants, which were 0.14, 0.359, 0.975 and 0.891 at room temperature, respectively (71, 72). Equation 3-2 was used to calculate the liquid phase concentration using the measured gas phase concentration. It was developed based on a mass balance and Henry's law.

$$C_{1(aq)} = \frac{C_{2(g)}}{V_{1(aq)}} \times \left(\frac{V_{2(aq)}}{H} + V_{2(g)} \right) \qquad (3\text{-}2)$$

Where $C_{1(aq)}$ is the concentration of chlorinated byproduct in the aqueous phase before equilibrium; $C_{2(g)}$ is the concentration of chlorinated byproduct in gas phase after equilibrium; $V_{1(aq)}$ is the volume of liquid before equilibrium and $V_{2\,(aq)}$ is the volume of liquid phase after equilibrium; $V_{2(g)}$ is the volume of gas phase after equilibrium; and H is dimensionless Henry's law constant.

Non chlorinated byproducts, ethane, ethylene and acetylene, were analyzed by HP 6890 GC equipped with GC-Alumina column (30 m × 0.53 mm i.d., J&W Scientific) and FID detector. The temperature of injection port and detector were 150 ºC and the

temperature of the oven was programmed to be isothermal at 80 ºC for 5 minutes. Injection volume was 100 μL with a split ratio of 2:1. Nitrogen was used as carrier gas and makeup gas at a constant flow rate of 6.3 mL/min and hydrogen and zero air were used as ignition gases. The procedure of sample preparation and analysis and the calculation method for aqueous phase concentration were the same as those of chlorinated byproducts. The dimensionless Henry's law constants used for ethane, ethylene and acetylene were 20.4, 8.7 and 1.1, respectively (55).

3.4.2 Measurement of Ammonium

The phenate method was used to measure the concentration of ammonium produced by nitrate reduction (66). An appropriate amount of sample was taken and filtrated by 0.45 μm cellulose nitrate membrane filters (Whatman). Diluted samples of 10 mL were transferred into 50-mL plastic bottles (BD Falcon) and phenol, sodium nitroprusside and alkaline citrate were added in that order. A blue compound, indophenol, was produced by the reaction of ammonia, hypochlorite, and phenol and its intensity was measured by a UV-VIS spectrophotometer (Hewlett Packard G1103A) at 640 nm with a light path of 1 cm.

3.4.3 Measurement of Iron Concentration in Solid and Liquid

Iron content in the solid and liquid phases was analyzed by the ferrozine method in which Fe(II) reacts with ferrozine and produces a purple color. The intensity of the color was measured using a UV-VIS spectrophotometer (Hewlett Packard G1103A) at 562 nm (70). Two sets of samples were prepared in this method. One sample was used to

determine the Fe(II) concentration. The other sample was used to determine the total iron (Fe(II) + Fe(III)) concentration. The sample for the total iron was prepared by adding 10% hydroxylamine in order to reduce all Fe(III) to Fe(II) before analysis. Fe(III) concentration was determined by subtracting Fe(II) concentration from total iron concentration. The iron content in solid phase was determined by the difference between iron in suspension (solid + liquid) and iron in the liquid phase. A solution of 1.2 N HCl was used to dissolve all solid particles and to prevent further oxidation of Fe(II), even in aerobic conditions.

3.4.4 Measurement of Anion Concentration

Anion concentrations (F^-, Cl^-, Br^-, NO_2^-, NO_3^-, and SO_4^{2-}) were measured by an ion chromatograph (Dionex DX-80) equipped with AS14A column and DS5 detection stabilizer. The samples were taken and filtrated with 0.2-μm cellulose nitrate membrane filters in an anaerobic chamber. Sample volumes of 1 mL were manually injected into the column, right after they were diluted with DDIW.

3.4.5 X-ray Diffraction (XRD) Spectroscopy

X-ray diffraction analysis for five types of GRs and HMGRs was performed using a Riga automated diffractometer using Cu Kα radiation. GRs were separated by centrifugation at 2960 g for 5 minutes (Beckman, model J-6M centrifuge, JS-7.5 rotor) and carefully dried in an anaerobic chamber. Dry GR was ground and transferred into 20-mL glass vials with three layered closures which were used to transport the GR and

were found to successfully prevent the oxidation of GRs. The samples were scanned between 2.1° to 70° 2θ with a scan speed of 1° 2θ/min.

CHAPTER IV

DEVELOPMENT OF HIGH-ACTIVITY MODIFIED GREEN RUSTS (HMGRs)

4.1 Introduction

Green Rust (GR) is a layered Fe(II)-Fe(III) hydroxide solid phase with an appropriate anion in the interlayer. The general formula for GR is $\left[Fe^{II}_{(6-x)}Fe^{III}_{x}(OH)_{12}\right]^{x+}\left[(A)_{x/n}\, yH_2O\right]^{x-}$, where x = 0.9-4.2; A is an n-valent anion(Cl^-, SO_4^{2-}, CO_3^{2-}, etc); and y denotes the varying amounts of interlayer water (31). GR was discovered as the transient corrosion product of iron pipe in early 1900 (31) and its chemical formula and crystal structure have been extensively studied by Genin and his coworkers (15, 32, 68, 69, 73). GRs have been classified into two groups, GR1 and GR2, based on the structure of the interlayer anion, which induces different X-ray diffraction patterns. GR1 has a planar anion, such as Cl^- or CO_3^{2-} and GR2 has a three-dimensional anion, such as SO_4^{2-} (15, 31, 32, 68, 69, 73).

Early researchers reported that GRs have the capability of reducing organic and inorganic contaminants in suboxic conditions. Hansen and coworkers have researched the reduction of nitrate by GR-SO_4 and GR-Cl. They observed that nitrate was reduced to ammonium, while GRs were transformed to magnetite, and the reaction kinetics were first order with respect to Fe(II) in GR (19-21). Chromate and selenate were reported to be reduced by GRs (23-25, 74, 75). Cr(VI) was reduced by GR-CO_3 to Cr(III) which produced a poorly crystalline Cr(III)-Fe(III) oxide at the reaction surface (24, 25, 74) and Se(VI) was reduced by GR-SO_4 to Se(IV) (23, 75). Furthermore, GR was observed

to be able to reduce chlorinated organics. Carbon tetrachloride (CT) and chlorinated ethylenes were successively transformed by GR-SO_4 (14, 26, 28). It means that GRs might play an important role in the degradation of contaminants in suboxic soils and sediments. However, even though the reductive degradation of contaminants by GRs can occur under suboxic conditions, the kinetics are not necessarily fast enough to apply GRs in water treatment systems.

Recently, it was reported that the addition of a transition metal to GRs enhanced the dechlorination reaction rate of chlorinated compounds. Ag(I), Au(III), Cu(II) and Portland cement extract (PCX) have been observed to be able to improve the reactivity of GRs by factors of up to three orders of magnitude (13, 29, 30). These compounds can be described as high-activity modified green rusts (HMGRs).

The goal of the research reported in this chapter is to develop HMGRs for degradation of PCE and nitrate. Five types of GRs (GR-Cl, GR-SO_4, GR-CO_3, GR-F, and GR-Br) were used and each GR was contacted with 10 activating agents (Ba, Mn, Co, Ni, Pt, Cu, Ag, Zn, Ti and Pb). The most promising HMGR was chosen based on the rate coefficient, byproducts of the reaction, cost, and ease of application.

4.2 Experimental Procedure

Screening experiments were conducted to examine the capability of trace metals to improve the reductive activity of GRs for degrading two target compounds (PCE and nitrate). Five types of GRs (GR-Cl, GR-SO_4, GR-CO_3, GR-F, and GR-Br) were used and each GR was contacted by 10 metals (Ba, Mn, Co, Ni, Pt, Cu, Ag, Zn, Ti and Pb). Each set of screening tests consisted of one type of GR with 10 trace metals. Therefore, five

sets of screening tests were conducted for each target compound. Three sample vials (PCE with GR suspensions) and two blank vials (PCE in DDIW) were prepared for each sampling time for PCE degradation experiments, whereas one sample was prepared for the nitrate reduction experiments.

Each GR was prepared by washing twice with deaerated deionized water (DDIW) in an anaerobic chamber. Trace metal stock solutions (0.4 M) were prepared for each screening test. The modification of GR was initiated by adding 0.625 mL of the trace metal stock into 250 mL of GR suspensions contained in polypropylene bottles, resulting in 1 mM concentration of trace metal. The GR suspensions containing the trace metals were kept in an anaerobic chamber during the 3-day reaction period and regularly shaken by a hand. After the reaction period, the pH in solution was adjusted to pH 9 (± 0.1) by adding appropriate amounts of acid or base. The modified GR was transferred to the clear borosilicate glass vials (24.3±0.1 mL) with three layered closures while it was mixed by a magnetic stirrer to maintain homogeneous conditions.

A PCE stock solution in methanol (0.596(±0.002) mM) was freshly prepared for each test. The reaction was initiated by spiking 10 μL of PCE stock into 24.3 mL of modified GR suspension using a gas-tight syringe in an anaerobic chamber. It was rapidly capped with the closure and then placed on a tumbler which provided end-over-end rotation at 7 rpm at room temperature. Three samples were taken at the estimated times to achieve 10% and 90% degradation of PCE. The PCE concentrations in solution were analyzed using gas chromatograph.

Nitrate stock solution (0.4 M) was prepared by dissolving an exact amount of sodium nitrate in DDIW. A volume (20 mL) of modified GR suspension was added into clear borosilicate glass vials (24.2 mL) in an anaerobic chamber and 0.1 mL of the nitrate stock was spiked to initiate the reaction. The vials were mounted on a shaker that provided orbital shaking at 250 rpm at room temperature. After about 4 and 20 hrs of reaction, 5 mL of suspension was taken and filtrated in the anaerobic chamber. The filtrate was diluted with DDIW to measure the ammonium concentration in solution.

4.3 Results and Discussion

4.3.1 Treatment of Kinetic Data

4.3.1.1 PCE Degradation

The kinetics of PCE dechlorination by modified GRs was generally described using a pseudo second-order rate law which reduces to a pseudo first-order rate law for a constant concentration of GR (30). When partitioning of PCE into solid and gas phases was considered, the disappearance of PCE in solution was described by the following equation.

$$\frac{dC_{L,PCE}}{dt} = -\frac{k_{PCE}\cdot C_{Fe(II)\text{-}GR}}{\left(1+H_{PCE}(V_g/V_L)+K_{S,PCE}\right)}C_{L,PCE} = \frac{k_{PCE}\cdot C_{Fe(II)\text{-}GR}\cdot C_{L,PCE}}{P_{PCE}} = -k_{app\_PCE}\cdot C_{L,PCE} \quad (4\text{-}1)$$

where $C_{L,PCE}$ is the concentration of PCE in solution; k_{PCE} is the second-order rate constant; $C_{Fe(II)\text{-}GR}$ is the concentration of solid-phase Fe(II) in the suspension of GR;

H_{PCE} is the dimensionless Henry's law constant for PCE; V_g and V_l are volumes of the gas and liquid phase, respectively; $K_{S,PCE}$ is the solid phase partition coefficient of PCE (ratio of mass of PCE in solid phase to mass of PCE in liquid phase); P_{PCE} is the partitioning factor; and k_{app_PCE} is the apparent pseudo-first order rate constant. The value of partitioning factor (P_{PCE}) used in this study was 1.10, which was calculated using 0.533 for H_{PCE} (71), 0.1 mL for V_g, and 24.2 mL for V_l, and 0.099 for $K_{S,PCE}$ (value calculated by Lee (28) for GR-SO_4).

The use of a first-order rate model was based on the assumption that the concentration of solid-phase Fe(II) was high enough to remain approximately constant during the reaction with PCE. The concentration of solid-phase Fe(II) in the suspension was used as a measurement of the concentration of GR. Value of k_{app_PCE}, was obtained by conducting nonlinear regression of PCE concentration using a Gauss-Newton algorithm coded in the function 'nlinfit" of MATLAB® (MathWorks Inc.). The MATLAB function 'nlparci' was used to calculate 95% confidential confidence intervals for the rate constants.

Three data points, initial PCE and two points of PCE observation were used for the regression in this screening test. Because it was observed that the PCE concentration in blanks was rapidly decreased and remained constant at approximately 90% of calculated initial PCE concentration, the measured PCE concentrations in the blanks were used as initial PCE concentration instead of the theoretical PCE concentration calculated from the amount of PCE added. This loss of PCE in DDIW was due to adsorption of PCE on the triple-layered septum and the reactor wall (76).

The second order rate constant (k_{PCE}) was obtained by the following equation.

$$k_{PCE} = \frac{k_{app\_PCE}}{C_{Fe(II)\text{-}GR}} \cdot P_{PCE} \quad (4\text{-}2)$$

Hereafter, k_{PCE} will be termed the solid-phase Fe(II)-normalized pseudo first-order rate constant.

4.3.1.2 Nitrate Reduction

The initial nitrate concentration was set to 2 mM and the concentration of NH_4^+ produced by the degradation of nitrate was measured after 4 and 20 hours. The kinetics of nitrate reduction by modified GRs were expressed by a pseudo second-order rate model that depends on the concentration of nitrate as shown in equation 4-3. The assumption of constant GR concentration was made to allow for the use of a pseudo first-order rate model.

$$\frac{dC_{NO_3}}{dt} = k_{NO_3} \cdot C_{Fe(II)\text{-}GR} \cdot C_{NO_3,} = k_{app\_NO_3} \cdot C_{NO_3} \quad (4\text{-}3)$$

where C_{NO3} is concentration of nitrate ion; k_{NO3} is second-order rate constant; $C_{Fe(II)\text{-}GR}$ is concentration of solid-phase Fe(II) in the suspension; and k_{app_NO3} is apparent pseudo-first order rate constant. Because the concentration of ammonium was measured, the concentration of nitrate was calculated by equation 4-4 which was developed by assuming theoretical stoichiometry (21).

$$C_{NO_3} = C_{NO_3\_init} - C_{NH_4} + C_{NH_4\_init} \quad (4\text{-}4)$$

where C_{NH4} is concentration of ammonium ion; C_{NH4_init} is initial concentration of ammonium ion which was zero in this experiment; C_{NO3_init} is initial concentration of nitrate ion. All of these concentrations were expressed in millimolar units. A MATLAB program was used to calculate values of k_{app_NO3} using three data points (initial nitrate concentration and nitrate concentrations at the two sampling times). The second-order rate constant, k_{NO3}, is termed the ferrous iron-normalized pseudo first-order rate constant with the assumption that solid-phase Fe(II) remained constant during the reduction period. It was calculated with the following equation.

$$k_{NO_3} = \frac{k_{app\_NO_3}}{C_{Fe(II)\text{-}GR}} \quad (4\text{-}5)$$

4.3.2 Iron Measurement of GRs

Table 4-1 shows the solid-phase Fe(II) contents of five types of GRs that were used for normalizing the pseudo-first order rate constants. These iron contents were measured before the modification procedure, which means that the iron content in the GRs could change due to reaction with a trace metal. However, because the trace metal concentration was much less than solid phase Fe(II), the differences of sold-phase Fe(II) concentration between each modified GRs were ignored. The Fe(II) to Fe(III) ratios

measured in GR solids were almost the same as the ideal ratio of each GRs based on the typical formulas. The purity of a GR was determined by anion measurement after each GR was synthesized. Purity greater than 98% was obtained in the synthesis of GR-Cl, GR-SO_4, GR-CO_3, and GR-F, while GR-Br was composed of 76 % GR-Br and 24% GR-Cl. Low purity of GR-Br was due to selectivity of GR for different anions. The anion affinity of LDH (layered double hydroxide) for monovalent anions is $OH^- > F^- > Cl^- > Br^- > I^-$. Therefore, the lower affinity of LDH for Br^- compared to Cl^- caused the lower purity of GR-Br, even though the concentration of Br^- was much higher than of Cl^-.

Table 4.1 Iron contents in GR solids

Type of GR	GR-Cl	GR-SO_4	GR-CO_3[a]	GR-F[b]	GR-Br[c]
Solid-phase Fe(II) [mM]	87.7 (±1.2)	84.6 (±2.3)	82.6 (±3.1)	84.9 (±1.3)	87.2 (±0.14)
Ratio of Fe(II) to Fe(III)	3.2	2.2	2.2	2.9	3.1
Purities of GRs	100%	100%	98%	98%	76%

[a] GR-CO_3 was synthesized in the mixture of CO_3^{2-} and SO_4^{2-} and the purity of GR was calculated by analyzing CO_3^{2-} and SO_4^{2-} concentration after synthesis procedure was accomplished.

[b] GR-F was synthesized in the mixture of Cl^- and F^- and the purity of GR was calculated by measuring the difference of Cl^- and F^- concentration after synthesis procedure was accomplished.

[c] GR-Br was synthesized in the mixture of Cl^- and Br^- and the purity of GR was calculated by measuring the difference of Cl^- and Br^- concentration after synthesis procedure was accomplished. 76 % of GR-Br and 24 % of GR-Cl were obtained.

4.3.3 Screening Experiments for Reductive Dechlorination of PCE

The effect of adding a trace metal into GRs on the enhancement of reductive activity of GRs for the dechlorination of PCE was determined in these screening tests. Figure 4.1 shows Fe(II) normalized pseudo-first order rate constants for the five sets of screening tests. Four metals (Pt, Cu, Ag and Pb) were shown to be capable of increasing the reaction rate of PCE degradation by GRs. Pt appeared to be the most effective activating agent for all types of GRs. The reductive activity for PCE degradation by GRs with Pt was improved up to three orders of magnitude. In particular, all PCE added was completely removed by GR-Cl(Pt) and GR-F(Pt) within 10 days, which means the real rate constant might be much faster than those reported in Table 4.2. This result was well expected because Pt has been reported to be effective in enhancing reductive dechlorination by bimetallic reductants (41, 46). Cu was an effect trace metal for GR-F. The solid-phase Fe(II)-normalized first-order rate constant for PCE degradation by GR-F(Cu) was 3.43 $M^{-1}day^{-1}$, which was two orders of magnitude larger than that for GR-F. In addition, the reaction rate of GR-CO_3(Cu) was increased by a factor of 18 compared with GR-CO_3. Ag was an effective agent for GR-CO_3 and GR-SO_4 and Pb was effective for GR-CO_3, GR-Cl and GR-Br. The rate constant of GR-SO_4(Ag), GR-CO_3(Ag), GR-CO_3(Pb) were observed to be in the range from 1.2 to more than 3.86 $M^{-1}day^{-1}$, which were more than two orders of magnitude faster reaction than the unmodified GRs. The comparison of reaction kinetic among five types of unmodified GR indicated that the reaction rate by GR-CO_3 and GR-Cl was relatively faster than that by the others.

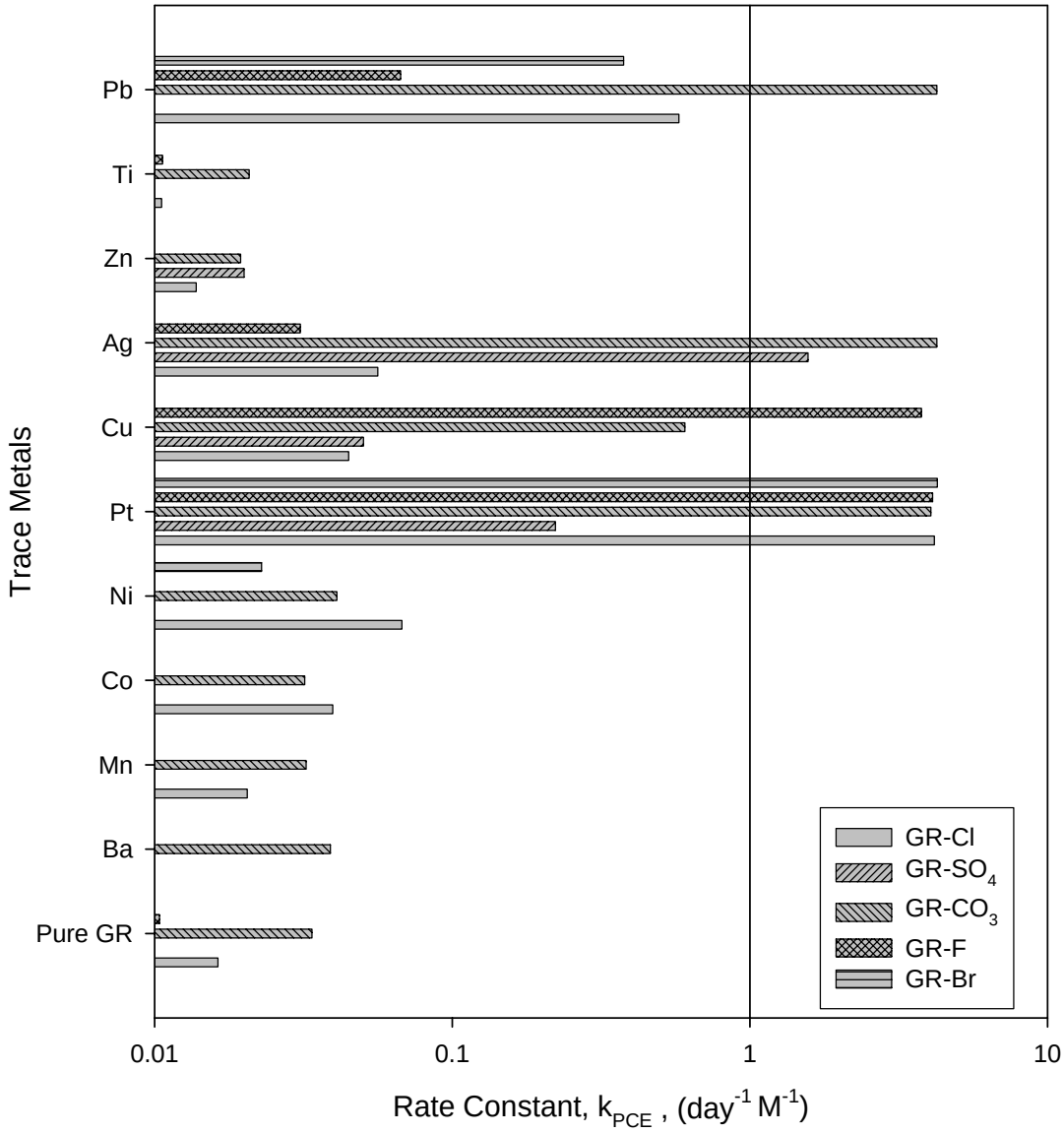

Figure 4.1 Effects of trace metals on reduction kinetic of reductive dechlorination reaction of PCE by HMGRs

Table 4.2 Pseudo first-order rate constants and Fe(II) ion normalized rate constants for PCE degradation by five types of GRs with 10 trace metals[a]

Exp.	Green Rust	Trace Metal	k_{app_PCE}[c] (day^{-1})	k_{PCE}[d] ($M^{-1}day^{-1}$)	Ratio of k_{PCE}[e]
1	GR-Cl	Control[b]	0.0013 (±55.6%)	0.016	1.0
		Ba	0.00064 (±98.9%)	0.008	0.5
		Mn	0.0016 (±51.4%)	0.020	1.3
		Co	0.0032 (±128%)	0.040	2.4
		Ni	0.0054 (±133%)	0.068	4.2
		Pt	> 0.333[f]	> 4.17	255
		Cu	0.0036 (±20.2%)	0.045	2.8
		Ag	0.0045 (±35.0%)	0.056	3.4
		Zn	0.0011 (±101%)	0.014	0.8
		Ti	0.00084 (±107%)	0.011	0.6
		Pb	0.0461 (±15.1%)	0.578	35.4
2	GR-SO_4	control	-0.00076 (±66.7%)	-0.010	1.0
		Ba	-0.00063 (±142.1%)	-0.008	0.8
		Mn	-0.0009 (±81.2%)	-0.012	1.2
		Co	-0.00035±176.1%)	-0.005	0.5
		Ni	-0.00076 (±83.3%)	-0.010	1.0
		Pt	0.0171 (±12.6%)	0.222	22.6
		Cu	0.0039 (±21.5%)	0.050	5.1
		Ag	0.121 (±24.8%)	1.57	159
		Zn	0.0015 (±100%)	0.020	2.0
		Ti	-0.00018 (±507%)	-0.002	0.2
		Pb	0.00067 (±101%)	0.009	0.9
3	GR-CO_3	control	0.0025 (±37.7%)	0.034	1.0
		Ba	0.0029 (±135%)	0.039	1.2
		Mn	0.0024 (±42.3%)	0.032	1.0
		Co	0.0024 (±90.8%)	0.032	0.9
		Ni	0.003 (±34.3%)	0.041	1.2
		Pt	0.305 (±20.7%)	4.06	120
		Cu	0.0455 (±64.7%)	0.605	17.9
		Ag	> 0.319[f]	> 4.25	125
		Zn	0.0015 (±45.1%)	0.019	0.6
		Ti	0.0016 (±72.2%)	0.021	0.6
		Pb	> 0.319[f]	> 4.25	125

Table 4.2 (Cont'd)

Exp.	Green Rust	Trace Metal	k_{app_PCE}[c] (day^{-1})	k_{PCE}[d] ($M^{-1}day^{-1}$)	Ratio of k_{PCE}[e]
4	GR-F	control	0.00080 (±102%)	0.010	1.0
		Ba	-0.00087 (±692%)	-0.001	-0.1
		Mn	0.00067 (±151%)	0.009	0.8
		Co	0.00059(±97.4%)	0.008	0.7
		Ni	0.00057 (±99.8%)	0.007	0.7
		Pt	> 0.318[f]	> 4.12	396
		Cu	0.291 (±31.1%)	3.77	363
		Ag	0.0024 (±24.4%)	0.031	3.0
		Zn	0.00046 (±236%)	0.006	0.6
		Ti	0.00082 (±86.4%)	0.011	1.0
		Pb	0.0052 (±71.3%)	0.067	6.5
5	GR-Br	control	-0.00024 (±6.4%)	-0.003	1.0
		Ba	0.00018 (±102%)	0.002	0.8
		Mn	0.00043 (±437%)	0.005	1.8
		Co	0.00012 (±189%)	0.002	0.5
		Ni	0.0018 (±208%)	0.023	7.6
		Pt	0.338 (±13.7%)	4.27	1420
		Cu	0.00029 (±745%)	0.004	1.2
		Ag	0.00049 (±363%)	0.006	2.0
		Zn	-0.00051 (±395%)	-0.006	2.1
		Ti	-0.0015 (±109%)	-0.019	6.5
		Pb	0.0299 (±11.2%)	0.377	125

[a] Initial PCE concentration was 0.248 mM in exp. 1, 0.246 mM in exp. 2, 0.246 mM in exp. 3, 0.248 mM in exp. 4 and 0.247 mM in exp. 5. pH was initially adjusted at 9±0.1 after modification was completed. The trace metal concentration was fixed to 1 mM in all cases.

[b] Control for each test was prepared with GR itself without adding a trace metal.

[c] Uncertainties represent 95 % confidence limits expressed in % relative to estimate for k_{app_PCE}[c].

[d] k_{PCE} was calculated by using the equation 4.2.

[e] Ratio of k_{PCE} = k_{PCE} of GR with a trace metal / k_{PCE} of control in using same type of GR.

[f] 100% removal was accomplished before the first observation. The values were calculated using the following equation, $k_{app\_PCE} = -\ln(C_{PCE}/C_{PCE\_init})/t$, where t is the first observation time.

The enhancement of the reactivity of GR by adding a trace metal is partially explained as a catalyst effect in which a trace metal deposited on the iron surface facilitated the electron transfer from reductant to target compound (13). However, the reason for observing different reaction rates among modified GRs is not clear. It is assumed that the difference is due to the surface atomic structure and electronic properties of trace metals and the stability and reactivity of GRs.

The reduction pathway in dechlorination of PCE by modified GRs was investigated. As shown in Figure 2.5, two pathways have been reported for reductive dechlorination of PCE (53). PCE can be converted sequentially to TCE (trichloroethylene), DCE (dichloroethylene), VC (vinyl chloride), and ethylene through the hydrogenolysis pathway. The accumulation of VC could be a particular problem in the hydrogenolysis pathway, because VC is more toxic and persistent than PCE (27, 53). In the reductive β-elimination pathway, chlorinated ethylenes are transformed to chlorinated acetylenes, which usually are degraded rapidly to completely dechlorinated products such as acetylene and ethylene (53). Therefore, the β-elimination pathway is advantageous, because it does not produce stable chlorinated intermediates.

In this study, both reduction pathways were observed. Results presented in Table 4.3 show that when GRs were modified by Ag or Pb, PCE was converted to TCE with the conversion ratio of 62 - 112 %. It means that almost all PCE removed by GR with Ag or Pb was transformed to TCE through the hydrogenolysis pathway. However, in the case of GR modification by Cu or Pt, TCE was not detected in the solution and

Table 4.3 PCE removal by HMGRs in 10 days and their by-product

Green Rust	Trace Metal	$C_{PCE\_removed}$ (mM)[a]	$C_{TCE\_Produced}$ (mM)[b]	$C_{TCE\_Produced}$ / $C_{PCE\_removed}$[c]	k_{PCE} ($day^{-1}M^{-1}$)[d]
GR-Cl	Pt	0.205 (±0.0001)	-	-	> 3.79
	Pb	0.083 (±0.0083)	0.052 (±0.022)	62.7%	0.525
GR-SO_4	Ag	0.135 (±0.012)	0.154 (±0.011)	114%	1.42
GR-CO_3	Pt	0.205 (±0.0019)	-	-	3.69
	Ag	0.206 (±0.023)	0.182 (±0.001)	88.3%	> 3.86
	Pb	0.206 (±0.023)	0.208 (±0.003)	109%	> 3.86
GR-F	Pt	0.201 (±0.003)	-	-	> 3.74
	Cu	0.199 (±0.0035)	-	-	3.43
GR-Br	Pt	0.199 (±0.0011)	-	-	3.88

[a] $C_{PCE\_removed} = C_{PCE\_init} - C_{PCE}$, C_{PCE} was the PCE concentration in liquid phase observed in 10 day reaction time

[b] TCE concentration observed in 10 days reaction time

[c] $C_{TCE\_Produced}$ was divided by $C_{PCE\_removed}$

[d] Fe(II)-normalized pseudo first order rate constant presented in Table 4.2

more than 80 % of PCE was removed. Two possibilities were suggested to explain the pathway of GR with Cu or Pt. The first possibility was that PCE removed was generally transformed through a reductive β-elimination pathway to dichloroacetylene which is known to be rapidly converted in sequence to chloroacetylene, acetylene, and then ethylene (7, 28, 76). The other possibility was that PCE was initially reduced to TCE through the hydrogenolysis pathway and then TCE was promptly transformed to DCE or chloroacetylene which were not detected in the analytical procedure for measuring PCE (7). Unfortunately, there is no experimental data to differentiate between these possibilities. However, it was generally reported that the reduction rates of TCE by GR-SO_4 or ZVI were slower than those of PCE (28, 53), meaning that TCE conversion might be the rate limiting step in the sequential reactions (equation 4-5) that explain the second possibility.

$$\text{PCE} \xrightarrow{k_{PCE}} \text{TCE} \xrightarrow{k_{TCE}} \text{DCE or chloroactylene} \qquad (4\text{-}5)$$

Therefore, if PCE was transformed by GR with Cu or Pt to TCE, TCE should be observed as an intermediate of reaction. So, the first possibility was presumed to be more reasonable than the second as the main pathway for transformation of PCE by GR with Cu or Pt.

GR-F(Pt) and GR-F(Cu) were selected as reductants for further study based on reaction kinetics of PCE degradation and extent of the production of intermediates. First, Pt and Cu were chosen because they could effectively enhance the reactivity of GR-Cl,

GR-CO_3, GR-F and GR-Br and they appeared to produce non-chlorinated by-products through a reductive β-elimination pathway. In the next step, GR-F was selected among five types of GRs because only GR-F showed the enhancement of its reactivity by both Pt and Cu. Pt could positively modify GR-Cl, GR-SO_4, GR-Br, while Cu could not.

4.3.4 Screening Experiment for Nitrate Reduction

Figure 4.2 and Table 4.4 show the effect of trace metals on nitrate reduction by GRs. In the nitrate reduction experiments, only Pt and Cu showed the capability of improving reduction kinetics. Pt was an effective activating agent for all GRs. GR-Br(Pt) showed the fastest reaction rate followed by GR-SO_4, GR-Cl, GR-F and GR-CO_3. The Fe(II) normalized pseudo-first order rate constant of GR-Br(Pt) was 522 $M^{-1}day^{-1}$ which was one order of magnitude larger than that of GR-CO_3(Pt). In addition, nitrate reduction by GR-Br was faster than that by GR-SO_4, by factor of 28. However, because GR-Br was observed to be much less pure than the others, GR-Br was not considered for further study during the characterization phase. Cu was observed to have the ability of enhancing the reactivity of GR-Cl and GR-F. The Fe(II) normalized rate constants of GR-F(Cu) and GR-Cl(Cu) were 131 $M^{-1}day^{-1}$ and 13.8 $M^{-1}day^{-1}$, respectively. The reaction rate of GR-Cl with Cu was much less than that of GR-Cl with Pt, while the reaction rate of GR-F(Cu) was almost the same as that for GR-F(Pt). Therefore, it was concluded that the most effective HMGRs for nitrate reduction were GR-F(Cu) and GR-F(Pt) based on treatment efficiency and availability of GR.

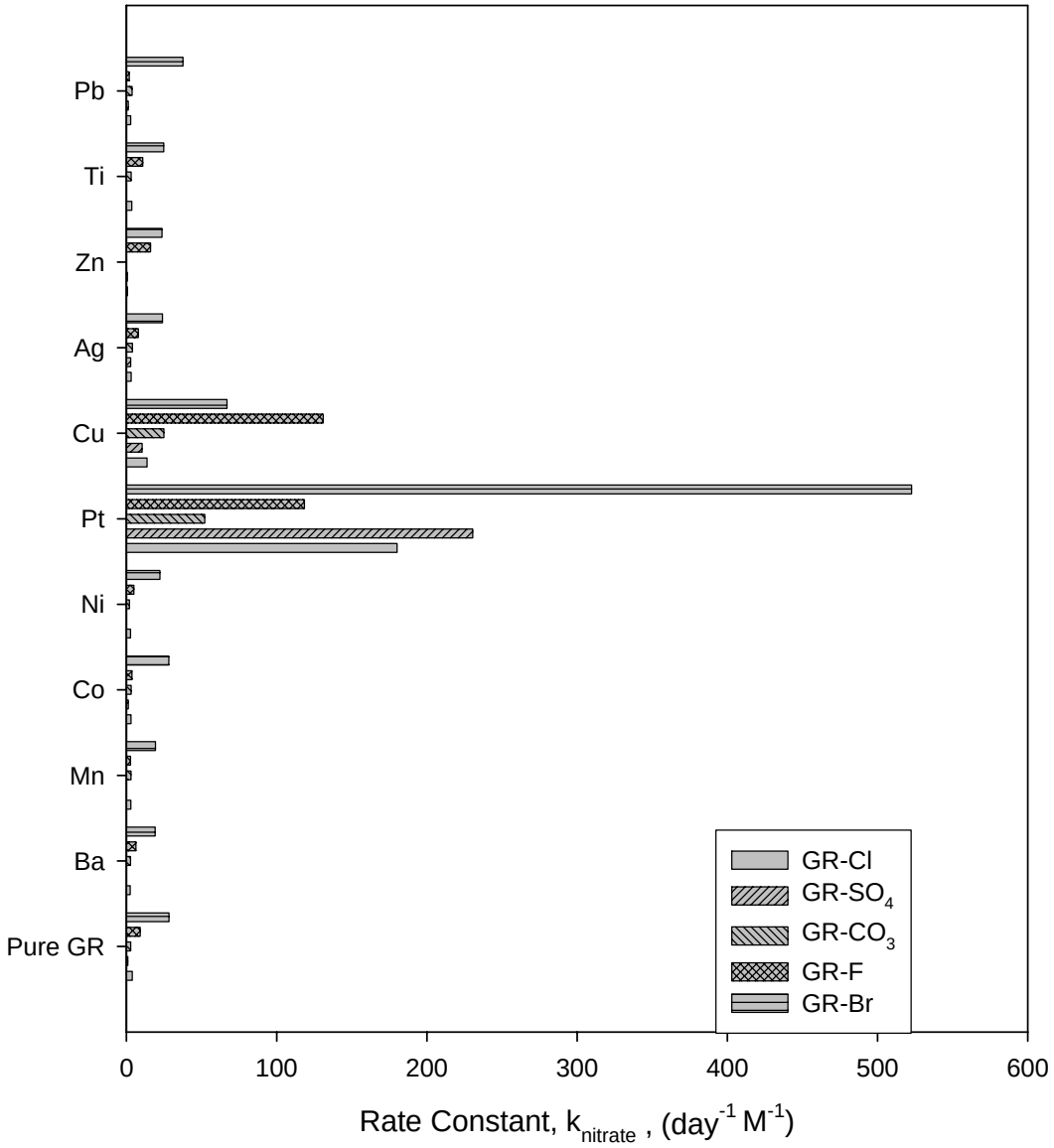

Figure 4.2 Effects of trace metals on reaction kinetic of nitrate reduction to ammonium by HMGRs

Table 4.4 Pseudo first-order rate constants and Fe(II) ion normalized rate constants for nitrate reduction by five types of GRs with 10 trace metals[a]

Exp.	Green Rust	Trace Metal	k_{app_NO3} (day^{-1})[c]	k_{NO3} ($M^{-1}day^{-1}$)[d]	Ratio of k_{NO3}[e]
6	GR-Cl	control[b]	0.350 (±21.1%)	4.00	1
		Ba	0.224 (±17.0%)	2.55	0.638
		Mn	0.266 (±93.8%)	3.03	0.758
		Co	0.273 (±152%)	3.11	0.779
		Ni	0.247 (±159%)	2.82	0.705
		Pt	15.8 (±259%)	180	45.1
		Cu	1.21 (±78.9%)	13.8	3.443
		Ag	0.280 (±151%)	3.20	0.800
		Zn	0.069 (±743%)	0.79	0.197
		Ti	0.323 (±2.62%)	3.68	0.921
		Pb	0.257 (±103%)	2.93	0.733
7	GR-SO_4	control	0.087 (±44.5%)	1.03	1
		Ba	0.030 (±327%)	0.36	0.35
		Mn	0.011 (±1108%)	0.13	0.13
		Co	0.110 (±112%)	1.30	1.26
		Ni	0.019 (±372%)	0.22	0.21
		Pt	19.5 (±116%)	231	224
		Cu	0.882 (±583%)	10.43	10.1
		Ag	0.249 (±148%)	2.94	2.86
		Zn	0.058 (±49.2%)	0.68	0.66
		Ti	0.027 (±1063%)	0.32	0.31
		Pb	0.111 (±197%)	1.31	1.27
8	GR-CO_3	control	0.24 (±162%)	2.94	1
		Ba	0.23 (±241%)	2.82	0.96
		Mn	0.25 (±228%)	3.07	1.04
		Co	0.26 (±133%)	3.17	1.08
		Ni	0.17 (±267%)	2.07	0.70
		Pt	4.31 (±26%)	52.1	17.7
		Cu	2.07 (±142%)	25.0	8.51
		Ag	0.34 (±144%)	4.07	1.38
		Zn	0.04 (±250%)	0.51	0.17
		Ti	0.27 (±176%)	3.22	1.10
		Pb	0.32 (±55%)	3.84	1.31

Table 4.4 (Cont'd)

Exp.	Green Rust	Trace Metal	k_{app_NO3} (day^{-1})[c]	k_{NO3} ($M^{-1}day^{-1}$)[d]	Ratio of k_{NO3}[e]
9	GR-F	control[b]	0.78 (±149%)	9.21	1
		Ba	0.54 (±26%)	6.33	0.69
		Mn	0.24 (±29%)	2.80	0.30
		Co	0.31 (±16%)	3.71	0.40
		Ni	0.43 (±159%)	5.05	0.55
		Pt	10.1 (±196%)	118	12.9
		Cu	11.1 (±188%)	131	14.2
		Ag	0.68 (±77%)	7.98	0.87
		Zn	1.36 (±142%)	16.0	1.74
		Ti	0.92 (±38%)	10.8	1.18
		Pb	0.17 (±177%)	1.99	0.22
10	GR-Br	control	2.47 (±134%)	28.4	1
		Ba	1.68 (±81%)	19.2	0.68
		Mn	1.69 (±358%)	19.4	0.68
		Co	2.46 (±104%)	28.2	1.00
		Ni	1.95 (±127%)	22.4	0.79
		Pt	45.6 (±681%)	522	18.4
		Cu	5.84 (±118%)	67.0	2.36
		Ag	2.10 (±312%)	24.1	0.85
		Zn	2.07 (±764%)	23.7	0.84
		Ti	2.17 (±164%)	24.9	0.88
		Pb	3.28 (±25%)	37.6	1.32

[a] Initial nitrate concentration was 2 mM. pH was initially adjusted at 9±0.1 after modification was completed. The trace metal concentration was fixed to 1 mM in all cases.

[b] Control for each test was prepared with GR itself without adding a trace metal.

[c] Uncertainties represent 95 % confidence limits expressed in % relative to estimate for k_{app_NO3}.

[d] k_{NO3} was calculated using equation 4-5.

[e] Ratio of k_{NO3} = (k_{NO3} of GR with a trace metal) / (k_{NO3} of control that used the same type of GR).

CHAPTER V

REDUCTIVE DECHLORINATION OF TETRACHLOROETHYLENE BY FLUORIDE GREEN RUST MODIFIED WITH COPPER OR PLATINUM

5.1 Introduction

Perchloroethylene (PCE) is one of the most common toxic organic contaminants found in the soil and groundwater of the United States. It has been widely used in industrial processes such as dry cleaning and metal-degreasing processes during the past half century (7, 8). It has been reported that human exposure to PCE can depress the central nervous system and damage the kidney and liver. PCE has been also classified as a probable human carcinogenic by USEPA's Science Advisory Board (9) and the maximum contamination level (MCL) was set at 5 μg/L under the Safe Drinking Water Act (SDWA) (68).

There are several treatment methods that have been applied to remove PCE from soil and groundwater. Air sparging and soil vapor extraction (SVE) have been conventionally used as an extraction method based on the volatile characteristics of PCE (77). However, the treatment efficiency of SVE is significantly dependent on the air permeability and heterogeneity of the soil (78). Moreover, additional treatment is required for the extracted gas that contains PCE. Biodegradation and chemical reduction methods have been intensively studied as destructive treatments. However, it has been reported that the biodegradation of PCE is restricted under aerobic conditions (79) and that the rate of degradation is slow even under anaerobic conditions (10).

Recently, chemical reduction of PCE by Fe(II)-containing reductants such as iron sulfide (7), pyrite, magnetite (55), and green rust (GR) (28) has been found to be able to degrade PCE. Iron sulfide transformed PCE to trichloroethylene (TCE) and acetylene via hydrogenolysis and β-elimination pathways, respectively. Reaction rates could be expressed with a pseudo-first order rate law (7). Lee and Batchelor observed that pyrite and magnetite have the capability of reducing PCE and they measured the reductive capacities of these compounds to be 1.01 and 0.33 μM/g, respectively (55). The reductive capacity was defined as the maximum amount of a particular oxidant that could be reduced when sufficient time was given (27).

Green Rust (GR) is another compound that contains Fe(II) and can act as a reductant. It is a layered Fe(II)-Fe(III) hydroxide solid phase with an appropriate anion in the interlayer. The general formula for GR is $\left[Fe^{II}_{(6-x)}Fe^{III}_{x}(OH)_{12}\right]^{x+}\left[(A)_{x/n}\, yH_2O\right]^{x-}$, where x = 0.9-4.2; A is an n-valent anion(Cl^-, SO_4^{2-}, CO_3^{2-}, etc); and y denotes the varying amounts of interlayer water (31). GR was discovered as a transient corrosion product of iron pipe in early 1900 (31) and more recently it has been found to be an effective chemical reductant for chlorinated methanes and chlorinated ethylenes in suboxic soils and sediments (14, 26, 28). Furthermore, it was reported that the addition of a transition metal to GRs could enhance the degradation rate of chlorinated compounds. Ag(I), Au(III), Cu(II) and Portland cement extract (PCX) have been observed to be able to improve the reactivity of GRs by factor of up to three orders of magnitude (13, 29, 30). These compounds with enhanced reactivity can be described as high-activity modified green rusts (HMGRs). The objective of this study is to characterize the reductive

dechlorination of PCE by GR-F modified with Cu or Pt. Development of these HGMR was described in Chapter IV. The effect of pH, activating agent concentration, initial PCE concentration on reductive chlorination of PCE, as well as products and pathways of degradation will be described in this chapter.

5.2 Experimental Procedure

Fluoride green rust (GR-F) was freshly synthesized by partial air oxidation of $Fe(OH)_2$ solid in the presence of F^-. Equal volumes of solutions of $FeCl_2$ (0.12 M) and NaOH (0.2 M) were mixed in an anaerobic chamber to precipitate $Fe(OH)_2$ and then 0.12 mM of NaF was added. After about 5 minutes of mixing, the suspension was taken out of the chamber and allowed to contact the air in order to oxidize Fe(II). This process was monitored by observing the pH of the solution. After the synthesis, the GR-F was taken into the anaerobic chamber and was stored to prevent further oxidation.

GR-F solids were separated by centrifugation and washed twice with deaerated deionized water (DDIW). The pH in washed GR-F suspension was around 7.5 and was fairly constant, because GR-F itself acted as a buffer. In the experiment for determining pH effect, 0.1 M of biological pH buffer (CHES for pH 9 and CAPS for pH 11) was used to wash the solids instead of DDIW during the second washing. The pH in the solution containing biological pH buffers remained constant throughout the experiment.

The process of modification was initiated by addition of Cu or Pt into the GR-F suspension. The trace metals were usually added to achieve a concentration of 1 mM. In the experiment that investigated the effect of Cu(II) concentration on PCE degradation, a Cu(II) concentration of 0.5 to 7.5 mM was achieved by adding appropriate amounts of

0.4 M Cu(II) stock solution into the GR-F suspensions. During the 1-hr modification period, the mixture of GR-F and a trace metal was continuously mixed by a magnetic stirrer. GR-F modified by Cu or Pt were called GR-F(Cu) and GR-F(Pt), respectively.

Kinetic experiments for PCE degradation were conducted using clear borosilicate glass vials (24.3±0.1 mL) with a three-layered septum system (PTFE film, lead foil and PTFE film lined rubber septum). An aliquot (24.2 mL) of modified GR-F was removed from the suspension while it was being mixed by a magnetic stirrer and transferred into the glass vials. PCE stock solutions in methanol (242, 596 (±2), 1125 and 1711 mM) were freshly prepared at each test and they were used to prepare initial PCE concentrations of 0.1001, 0.245, 0.465 and 0.707 mM, respectively. The reaction was initiated by spiking 10 μL of PCE stock solution into 24.2 mL of modified GR suspension using a 10-μL gas-tight syringe. The vials were rapidly capped with the closure, taken out of the chamber, and placed on a tumbler that provided end-over-end rotation at 7 rpm at room temperature. The degradation kinetics of PCE were determined by monitoring the PCE concentration at each sampling point. GR-F(Cu) samples were prepared in triplicate. GR-F(Pt) samples were prepared in duplicate to save a time in the process of spiking PCE, because reaction rates were very fast.

5.3 Results and Discussion

5.3.1 Modification of GR-F

The modifications of GR-F were achieved by contacting GR-F with Cu(II) or Pt(IV) for about 1 hr. To understand the modification process, XRD analyses were conducted for GR-F modified with 1 mM of Cu(II) and Pt(IV) and iron measurements were made for GR-F with Cu(II). Figure 5.1 shows the results of XRD analyses in which GR-F and magnetite were mainly observed. This result indicates that GR-F reduced a trace metal ion to the metallic form (zero valent metal) and GR-F itself was oxidized to magnetite. This idea was supported by the results of the studies by O'Loughlin (35) and Zhang (41). O'Loughlin *et al.* reported that almost all Ag(I), Au(III), Cu(II), and Hg(II) were reduced to Ag^0, Au^0, Cu^0, and Hg^0 by GR-SO_4 within 30 minutes. Furthermore, the XRD pattern of GR with Cu provided in his paper is comparable to that in Figure 5.1 (35). Zhang and his coworkers used bimetallic reductants such as Pd/Fe and Pt/Fe in dechlorination reactions. They mentioned that a bimetallic reductant was produced by reductive deposition of Pd on the surface of Fe^0 through the following reaction:

$$Pd^{2+} + Fe^0 \rightarrow Pd^0 \downarrow + Fe^{2+} \qquad (5\text{-}1)$$

They also proposed that Fe^0 served predominantly as electron donor while Pd^0 acted as catalyst in dechlorination reaction (41).

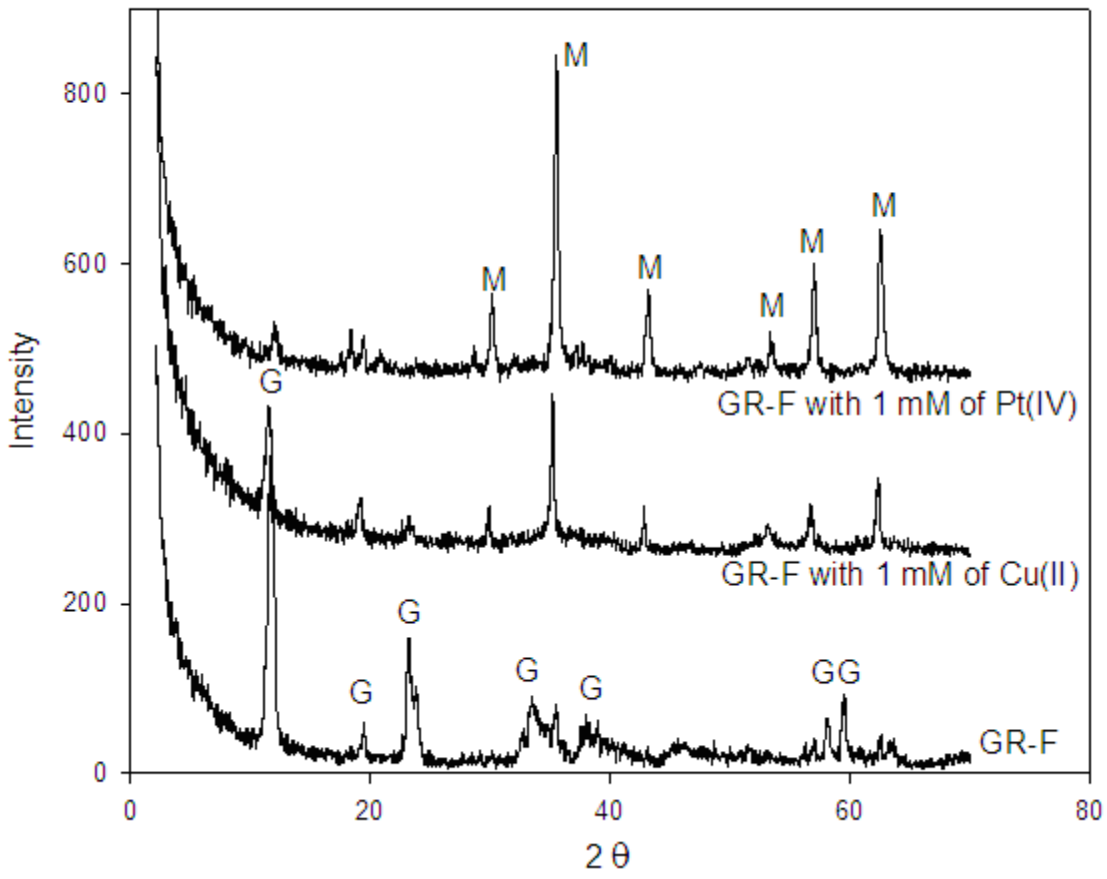

Figure 5.1 Results of XRD analysis for GR-F and GR-F modified with 1 mM of Cu(II) and 1 mM of Pt(IV). G represents GR-F and M represents magnetite.

Therefore, the following redox reaction between GR-F and Cu(II) is proposed.

$$\text{Oxidation} \quad : \quad 3Fe^{II}_{3}Fe^{III}_{1}(OH)_8 \cdot F \rightarrow 4Fe^{II}_{1}Fe^{III}_{2}O_4 + 5e^- + 3F^- + 8H^+ + 8H_2O \quad (5\text{-}2)$$

$$\text{Reduction} \quad : \quad Cu^{2+} + 2e^- \rightarrow Cu^0 \quad (5\text{-}3)$$

$$\text{Redox reaction:} \quad 6Fe^{II}_{3}Fe^{III}_{1}(OH)_8 \cdot F + 5Cu^{2+} \rightarrow 8Fe^{II}_{1}Fe^{III}_{2}O_4 + 5Cu^0 + 6F^- + 16H^+ + 16H_2O \quad (5\text{-}4)$$

In addition, Fe(II) concentration in solution increased and pH slightly decreased during the modification of GR-F with Cu. The extents to which these reactions occurred were dependent on the concentration of Cu(II), which means that Fe(II) was also a byproduct of modification of GR-F. This could be explained by using the dissolution reaction of GR. Hansen reported that when GR-SO_4 was titrated with acid, magnetite and Fe(II) was produced as described by the following reaction (31).

$$Fe^{II}_{4}Fe^{III}_{2}(OH)_{12} \cdot SO_4 + 4H^+ \rightarrow Fe^{II}_{1}Fe^{III}_{2}O_4 + 3Fe^{2+} + SO^{2-}_{4} + 8H_2O \quad (5\text{-}5)$$

Thus, it was assumed that the hydrogen ion produced by the redox reaction dissolved GR, which produced Fe(II). However, the equation proposed by Hansen does not fit the experimental results of this study. Therefore, the following generalized equation is proposed to describe the dissolution reaction.

$$2Fe_3^{II}Fe_1^{III}(OH)_8 \cdot F + 8H^+ \rightarrow 1Fe_1^{II}Fe_2^{III}O_4 + 2F^- + 5Fe^{2+} + 12H_2O \quad (5\text{-}6)$$

Since the redox reaction and the dissolution reaction occurred simultaneously, the redox reaction (equation 5-4) was combined with the dissolution reaction (equation 5-6) multiplied by a factor of *x*, resulting in equation 5-7.

$$\begin{aligned}&(6+2x)\,Fe_3^{II}Fe_1^{III}(OH)_8 \cdot F + 5Cu^{2+} \rightarrow \\ &\quad (8+x)\,Fe_1^{II}Fe_2^{III}O_4 + 5Cu^0 + (6+2x)\,F^- + 5x\,Fe^{2+} + (16-8x)\,H^+ + (16+12x)\,H_2O\end{aligned} \quad (5\text{-}7)$$

The coefficient, *x*, was empirically determined through the following steps: 1) changing *x* over the range of 1 to 2, 2) calculating the Fe(II) concentration produced at each *x* if 1 mM of Cu(II) were reduced, 3) comparing the calculated change of Fe(II) concentration with that measured by experiment. This method was used with the assumptions that Fe(II) was produced only by dissolution of GR and all Cu(II) was reduced to Cu^0. When *x* was 1, 1.4, and 2, the Fe(II) concentration estimated to be produced with reduction of 1 mM of Cu^{2+} was 1, 1.4, and 2 mM, respectively. The measured change in Fe(II) concentration was 1.4 mM , so a value of 1.4 was chosen for *x*. Equation 5-7 was re-expressed as follows:

$$\begin{aligned}&1.76Fe_3^{II}Fe_1^{III}(OH)_8 \cdot F + Cu^{2+} \rightarrow \\ &\qquad 1.88Fe_1^{II}Fe_2^{III}O_4 + 1.4Fe^{2+} + Cu^0 + 0.96H^+ + 6.56H_2O + 1.76F^-\end{aligned} \quad (5\text{-}8)$$

Equation 5-8 is supported by the results of measuring the Fe(II) concentration in solution at other doses of Cu(II) as shown in Table 5.1. The increase in the concentration of Fe(II) measured in the experiments was almost the same as that calculated for doses of Cu(II) that ranged from 1 to 7.5 mM.

Table 5.1 Comparisons of the change of Fe(II) concentration estimated with that measured in experiment[a].

Reductant	Cu(II) (mM)[b]	Fe(II) measured (mM)[c]	Fe(II) increased (mM)[d]	Fe(II) estimated (mM)[e]
GR-F	0	0.5	0	0
GR-F	1	1.9	1.4	1.4
GR-F	2.5	0.4	3.5	3.5
GR-F	5	7.3	6.8	7.0
GR-F	7.5	10.5	10	10.5

[a] Solid phase Fe(II) and Fe(III) of GR-F was 84.2 and 30.2 mM, respectively, and its ratio of Fe(II) to Fe(III) in GR-F was 2.8.

[b] The addition of Cu(II) to modify GR-F.

[c] The measured Fe(II) concentration in liquid phase. It was measured by filtering GR-F suspension with 0.45 μM cellulose nitrate membrane filters

[d] The increased Fe(II) was calculated by subtracting Fe(II) in unmodified GR-F from Fe(II) in modified GR-F.

[e] The calculated Fe(II) concentration using the equation 5-5, when all of Cu(II) was reduced to elemental Cu.

The overall reaction for the modification of GR-F with Pt is presented in equation 5-9, which was obtained using the coefficients used in equation 5-8.

$$1.76Fe_3^{II}Fe_1^{III}(OH)_8 \cdot F + \frac{1}{2}Pt^{4+} \rightarrow 1.88Fe_1^{II}Fe_2^{III}O_4 + 1.4Fe^{2+} + \frac{1}{2}Pt^0 + 0.96H^+ + 6.56H_2O + 1.76F^- \quad (5\text{-}9)$$

Equation 5-8 and 5-9 were used to calculate the solid-phase Fe(II) concentration after modification based on the measured solid-phase Fe(II) concentration before modification.

5.3.2 Treatment of Kinetic Data

A pseudo first-order rate law was used to describe PCE degradation kinetics at any specific concentration of GR-F. Combining this rate law with the material balance for a batch reactor provides equation 5-10 (30).

$$\frac{dC_{T,PCE}}{dt} = -k_{PCE}' \cdot C_{L,PCE} = -k_{PCE} \cdot C_{Fe(II)\text{-}GR} \cdot C_{L,PCE} \quad (5\text{-}10)$$

where $C_{T,PCE}$ represents total PCE concentration in all phases of the system, k_{PCE}' is the pseudo-first order rate constant, $C_{L,PCE}$ is the concentration of PCE in liquid phase, $C_{Fe(II)\text{-}GR}$ is the concentration of Fe(II) in the solid-phase of GR, and k_{PCE} is the second-order rate constant.

Because the aqueous phase PCE concentrations were used to describe the reaction rate in a system containing soil and gas, the effects of partitioning of PCE among those phases was considered with assuming instantaneous equilibrium among the gas, liquid, and solid phase using the following equation (54, 76).

$$C_{T,PCE} = \left(1 + H_{PCE}\frac{V_g}{V_l} + K_{S,PCE}\right) \cdot C_{L,PCE} = P_{PCE} \cdot C_{L,PCE} \quad (5\text{-}11)$$

where H_{PCE} is the dimensionless Henry's law constant for PCE, V_g and V_l are volumes of the gas and liquid phase, respectively, $K_{S,PCE}$ is the solid phase partition coefficient of PCE (ratio of mass of PCE in solid phase to mass of PCE in liquid phase), and P_{PCE} is the partitioning factor. The value of the partitioning factor used in this study was 1.10. It was calculated using 0.533 for H_{PCE} (71), 0.1 mL for V_g, and 24.2 mL for V_l, and 0.099 for $K_{S,PCE}$ from $K_{S,PCE}$ of GR-SO_4 which was calculated by Lee (28). In addition, the sorption of PCE on the Teflon lining material of the closure and the reactor wall was observed, which was considered as the main cause for the approximately 90% of PCE recovery observed in blanks (76).

Combining equations 5-10 and 5-11, the reaction kinetics of PCE degradation in aqueous phase was expressed as follows:

$$\frac{dC_{L,PCE}}{dt} = -\frac{k_{PCE} \cdot C_{Fe(II)\text{-}GR} \cdot C_{L,PCE}}{P_{PCE}} = -\frac{k_{PCE}' \cdot C_{L,PCE}}{P_{PCE}} = -k_{app,PCE} \cdot C_{L,PCE} \quad (5\text{-}12)$$

where $k_{app,PCE}$ was the apparent pseudo first-order rate constant.

The value of the apparent pseudo-first order rate constant ($k_{app,PCE}$) was obtained by conducting nonlinear regression of aqueous-phase PCE concentrations using a Gauss-Newton algorithm incorporated in the MATLAB® function 'nlinfit' (MathWorks Inc.). The 95% confidential levels for the rate constants were calculated by the 'nlparci' function. The second-order rate constant, k_{PCE}, was obtained by the following equation.

$$k_{PCE} = \frac{k_{app,PCE}}{C_{Fe(II)\text{-}GR}} \cdot P_{PCE} \quad (5\text{-}13)$$

Hereafter, k_{PCE} is called the solid-phase Fe(II) normalized pseudo first-order rate constant based on the assumption that the concentration of solid-phase Fe(II) was high enough to remain approximately constant during the reaction with PCE.

Some experimental data showed a better fit to the second-order or the half-order kinetic model. The second-order or half-order rate constants were obtained by nonlinear regression using the following equations and were compared with first-order rate constants,

$$\frac{dC_{L,PCE}}{dt} = -k_{app,PCE,second} \cdot C_{L,PCE}^{2} \quad (5\text{-}14)$$

$$\frac{dC_{L,PCE}}{dt} = -k_{app,PCE,half} \cdot C_{L,PCE}^{1/2} \quad (5\text{-}15)$$

where $k_{app,PCE,second}$ is the apparent second-order rate constant and $k_{app,PCE,half}$ is the apparent half-order rate constant.

5.3.3 Effect of pH

The effect of pH on reductive dechlorination of PCE by GR-F(Cu) and GR-F(Pt) was studied over the range of pH from 7.5 to 11. Figure 5.2 shows the results of PCE degradation by GR-F(Cu) at pH 7.5, 9 and 11. The lines in Figure 5.2 are calculated using the pseudo first-order kinetic model, which reasonably describes the removal of PCE in these experiments. The results show that PCE reduction by GR-F(Cu) was clearly dependent on pH. The reaction kinetics increased as pH increased. The value of $k_{app,PCE}$ obtained at pH 11 was 10.3 (day^{-1}), which was two orders of magnitude larger than that obtained at pH 7.5 (Table 5.2). These results are similar to those obtained in other studies. Lee (28) and Marchal (26) reported that the reaction rates of TCE and PCE degradation by GR-SO_4 increased as pH increased in the range of pH 7 to 11. In addition, Son observed that PCE degradation by GR-Cl modified with Cu(II) showed a maximum reaction rate at pH 11.4 (30) .

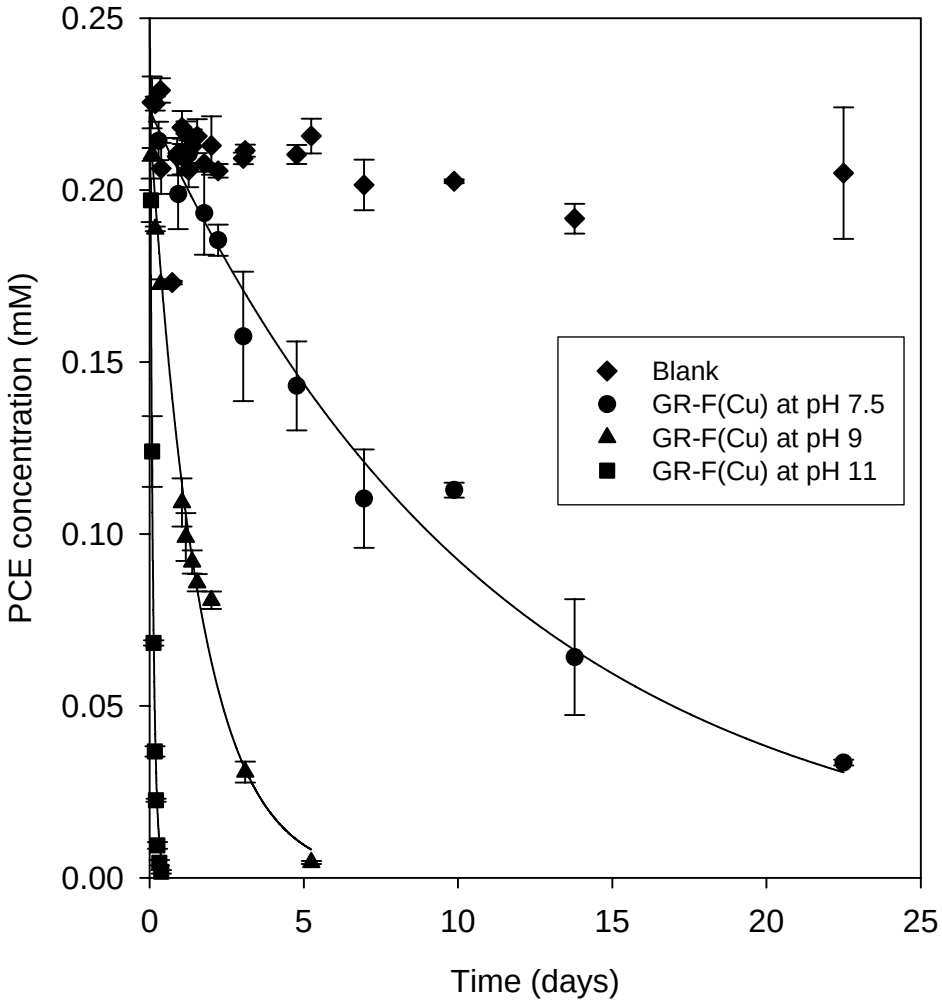

Figure 5.2 Results of kinetic experiments on PCE degradation by GR-F(Cu) at various pH. Error bars are the standard deviations of measured PCE concentrations. Some error bars are smaller than the symbols. The solid lines represent fits by first-order kinetic models. $[PCE]_0 = 0.247$ mM, Solid-phase Fe(II) = 83.3 mM, [Cu(II)] = 1 mM.

Table 5.2 Apparent pseudo first-order rate constants and solid phase Fe(II)-normalized rate constants for PCE degradation by GR-F(Cu) and GR-F(Pt) at various pH[a]

Exp	Reductant	pH[b]	$k_{app,PCE}$ (day^{-1})[c]	k_{PCE} ($M^{-1}day^{-1}$)[d]
11	GR-F(Cu)	7.5-7.4	0.088 (±25.1%)	1.17
12	GR-F(Cu)	8.95-8.7	0.628 (±9.5%)	8.29
13	GR-F(Cu)	11.0-10.6	10.3 (±13.8%)	136
21	GR-F(Pt)	7.5-7.3	8.91 (±6.5%)	126
22	GR-F(Pt)	9.0-8.8	2.12 (±14.4%)	29.9
23	GR-F(Pt)	11-10.7	10.3 (±15.9%)	145

[a] Initial PCE concentration was 0.247(±0.001) mM. The trace metal concentration was fixed to 1 mM in all cases. Solid-phase Fe(II) was 83.3 M in exp. 11-13 and 78 mM in exp. 21-23.

[b] The pH range which were measured during the reaction period.

[c] Uncertainties represent 95 % confidence limits expressed in % relative to estimate for k_{app_PCE}.

[d] k_{PCE} was calculated by using equation 5-13.

Figure 5.3 shows the reductive dechlorination of PCE by GR-F(Pt) at pH 7.5, 9 and 11. PCE degradation by GR-F(Pt) was dependent on pH. The PCE degradation reaction was the fastest at pH 11 and the slowest at pH 9. Values of $k_{app,PCE}$ at pH 7.5, 9, and 11 were 8.91, 2.12, and 10.3 (day^{-1}), respectively.

Lee (28) observed that the dechlorination of PCE rate by GR-SO_4 increased as pH increased and Butler (7) was also reported that increasing pH induced a faster degradation rate of hexachloroethane by iron sulfide. Both mentioned that deprotonated surface groups on the iron solid would increase the rate of dechlorination.

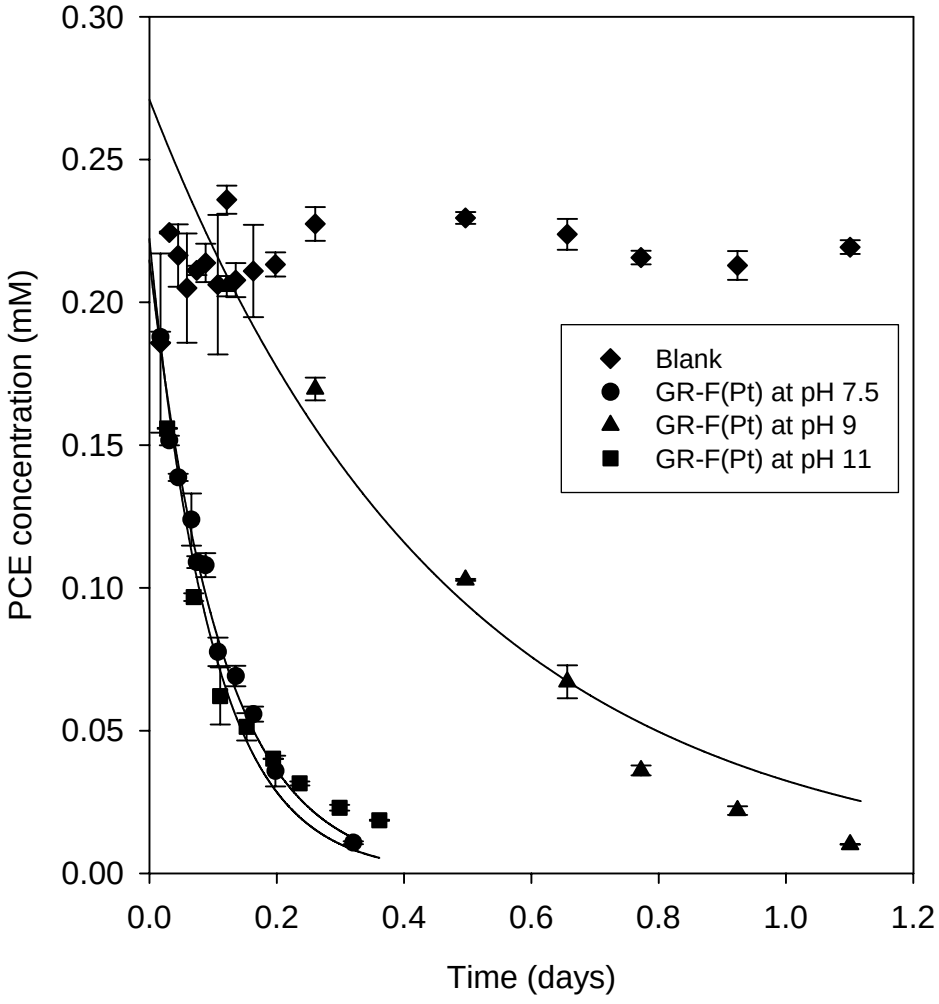

Figure 5.3 Results of kinetic experiments on PCE degradation by GR-F(Pt) at various pH. Error bars are the standard deviations of measured PCE concentrations. Some error bars are smaller than the symbols. Solid lines represent fits by first-order kinetic models. $[PCE]_0$ = 0.247 mM, Solid-phase Fe(II) = 78 mM, [Pt(IV)] = 1 mM.

Iron hydroxide minerals have a pH-dependent surface charge caused by surface hydroxides donating or accepting a proton. GR is a mixture of Fe(III) and Fe(II) hydroxide. Therefore, they could have deprotonated surface groups at high pH that could cause the high rates of reaction observed in this study.

The first-order kinetic model effectively described PCE reduction kinetics by GR-F(Pt) at pH 7.5, while it was not applicable at pH 9 and pH 11. Therefore, second-order and half-order kinetic models were used and are shown in Figure 5.4. Figure 5.4 clearly demonstrates that a half-order kinetic model provides a better fit to the data at pH 9 and a second-order model provides a better fit at pH 11. The superiority of these models is also seen in their lower uncertainties of rate constants and sum of square (SS) values as shown in Table 5.3. The better fit by the second-order kinetic model at pH 11 means that PCE degradation was faster at the beginning of reaction and then slower at the end of reaction compared to what would be observed with a first-order model (Figure 5.3). Moreover, it was observed at the end of the reaction that all of GR-F(Pt) was transformed to a black solid that was assumed to be magnetite, the volume of solution was noticeably decreased, and gas bubbles were produced, that were assumed to be hydrogen. Therefore, based on the model fitting and the observation in the experiment, it appears that GR-F(Pt) reduced water as well as PCE (44, 49, 80), resulting in a lower amount of reductant at the later reaction times.

In contrast, the half-order model was good for describing PCE reduction at pH 9. Figure 5.3 and 5.4 clearly show that the reaction at pH 9 became faster than what it would be by a first-order reaction model. However, the reason for this is not clear.

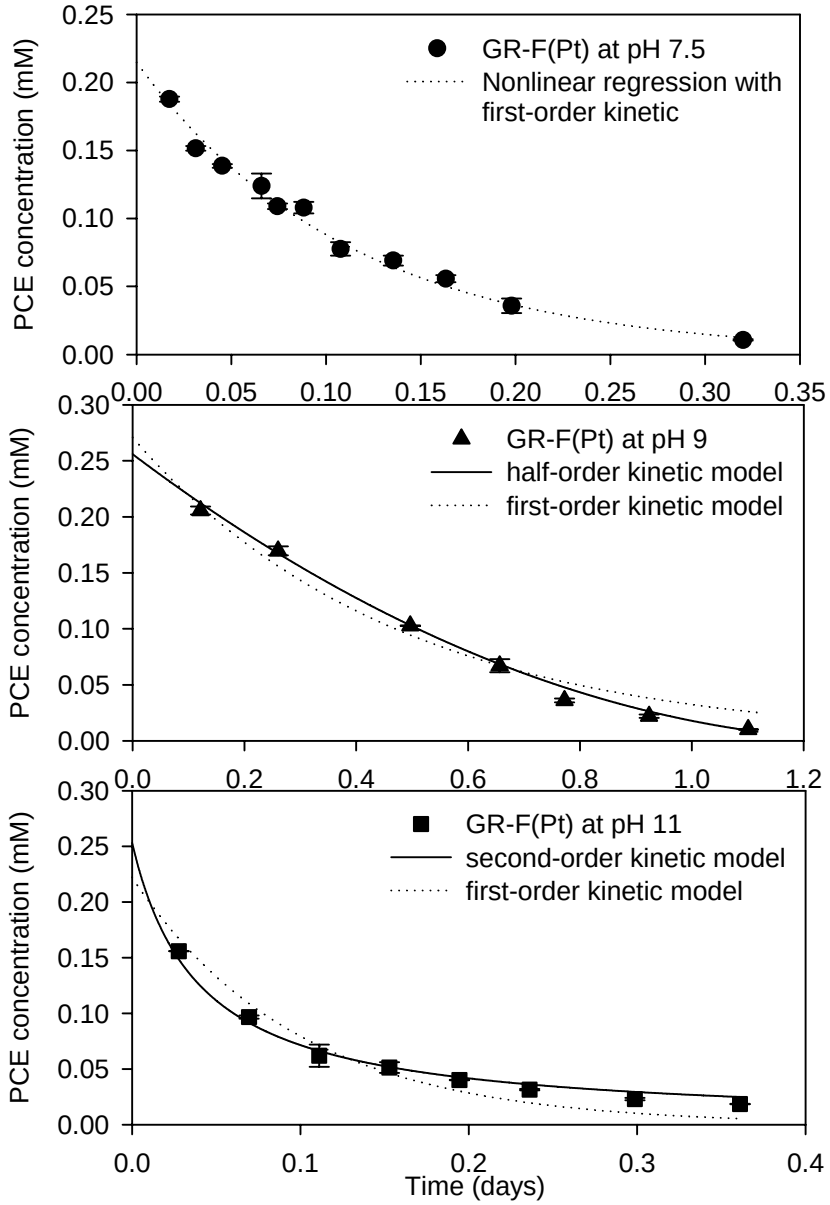

Figure 5.4 Comparison of kinetic models for PCE degradation by GR-F(Pt) at various pH. Error bars are the standard deviations of measured PCE concentrations. Some error bars are smaller than the symbols. Lines represent fits of different kinetic models. $[PCE]_0$ = 0.247 mM, Solid-phase Fe(II) = 78 mM, [Pt(IV)] = 1 mM.

Table 5.3 Comparisons of apparent pseudo first-order rate constants with apparent second-order rate constant and apparent half-order rate constant for PCE degradation by GR-F(Pt) at various pH[a]

		First-order		Second-order[d]		Half-order[e]	
Exp.	pH	$k_{app,PCE}$ (day^{-1})[b]	SS [c]	$k_{app,PCE,second}$ ($M^{-1}day^{-1}$)[b]	SS [c]	$k_{app,PCE,half}$ ($M^{1/2}day^{-1}$)[b]	SS[c]
21	7.5	8.91 (±12.2%)	0.0026	37.4 (±14.2%)	0.0033	2.85 (±14.6%)	0.0038
22	9	2.12 (±14.4%)	0.0031	7.32 (±37.2%)	0.0135	0.744 (±5.11%)	0.000456
23	11	10.3 (±15.9%)	0.0027	50.2 (±8.26%)	0.00057	3.24 (±17.5%)	0.0067

[a] Initial PCE concentration was 0.247(±0.001) mM. The trace metal concentration was fixed to 1 mM in all cases. Solid-phase Fe(II) was 78 mM.

[b] Uncertainties represent 95 % confidence limits expressed in % relative to estimate for $k_{app,PCE}$, $k_{app,PCE,second}$, and $k_{app,PCE,half}$.

[c] SS = ∑ (residuals of PCE concentration between observed and predicted)^2.

[d] Second-order rate constant $k_{app,PCE,second}$ was calculated using the following equation, $C_{L,PCE} = \frac{C_{L,PCE,init}}{1 + 2k \cdot C_{L,PCE,init} \cdot t}$, which was derived from equation 5-14.

[e] Half-order rate constant $k_{app,PCE,half}$ was calculated using the following equation, $C_{L,PCE} = \left(\sqrt{C_{L,PCE,init}} - \frac{k \cdot t}{2} \right)^2$, which was derived from equation 5-15.

5.3.4 Effect of Cu Concentration

The effect of the initial concentration of Cu(II) on the reductive dechlorination of PCE by GR-F was investigated over the range of 0 to 7.5 mM of Cu(II) at pH 7.5. The results of PCE reduction by GR-F(Cu) and the results of nonlinear regression for the data using first-order reaction model are shown in Figure 5.5. Table 5.4 presents the apparent pseudo first-order rate constant, $k_{app,PCE}$, and the solid-phase Fe(II) normalized pseudo first-order rate constant, k_{PCE}, for these experiments (exp. 11 and 14-17) and Figure 5.6 illustrates k_{PCE} as function of the amount of Cu(II) added. The PCE reduction rate increased with increasing initial concentration of Cu(II) over the range of 0.5 to 5 mM, whereas the rate of PCE dechlorination at 7.5 mM of Cu(II) was less than that at 5 mM of Cu(II). Because it was believed that Cu acted as a catalyst in these experiments, it was expected that faster reactions would always be observed with higher Cu(II) concentration. However, the reaction rate was decreased at high Cu(II) addition.

Lin and coworkers (46) also reported similar results in the dechlorination of trichloroethylene (TCE) by iron with Ru (Ru/Fe). They observed that the reduction rate was increased in the range of 0.25 to 1.5 % Ru (w/w) and then decreased above 1.5 % Ru. As a reason for this trend, they mentioned the aggregation of Ru particles on iron. The higher addition of Ru resulted in larger Ru particles and less surface area of Ru by aggregation than lower addition of Ru. If a similar mechanism occurred on modification of GR, aggregated Cu particles at high Cu addition rates could explain the low reactivity of GR-F(Cu) at higher Cu(II) doses that was observed in this study.

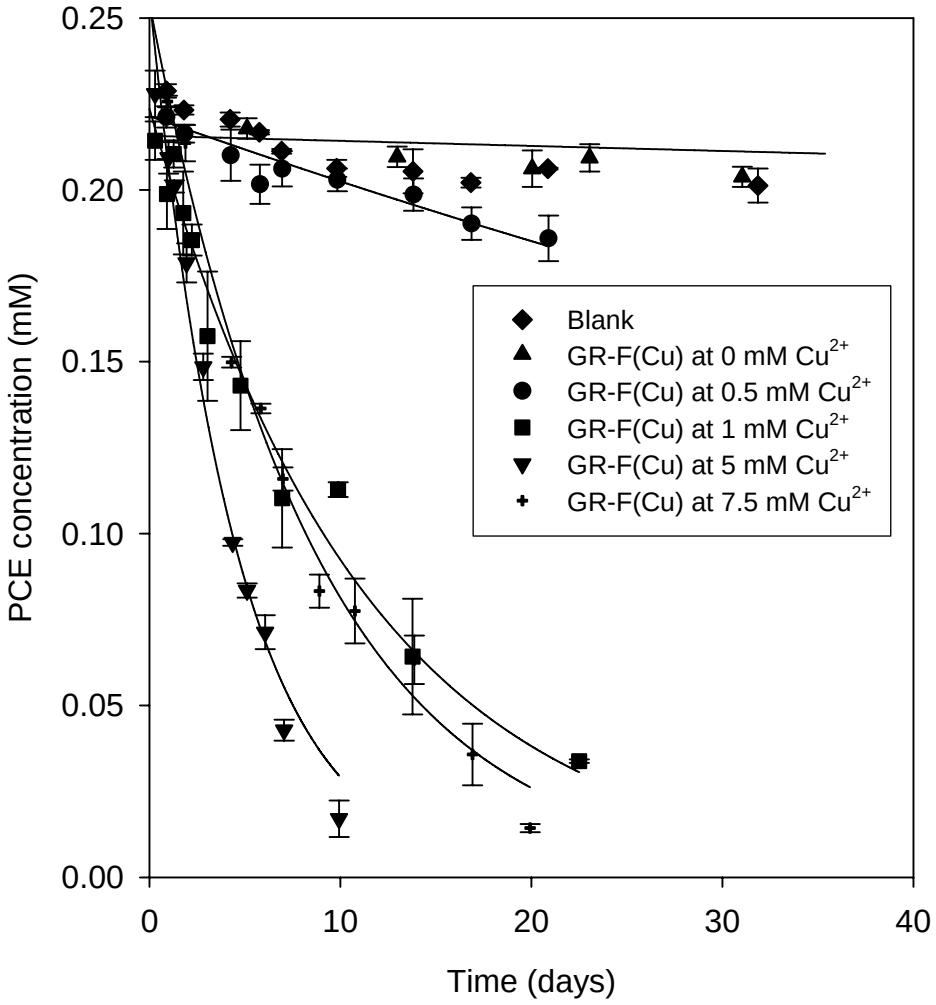

Figure 5.5 Results of kinetic experiments on PCE degradation by GR-F(Cu) at various Cu(II) concentrations. Error bars are the standard deviations of measured PCE concentrations. Some error bars are smaller than the symbols. Solid line represents first-order fits. $[PCE]_0 = 0.247$ mM, pH=7.5.

Table 5.4 Apparent pseudo first-order rate constants and solid phase Fe(II)-normalized rate constants for PCE degradation by GR-F(Cu) with various C(II) addition and initial PCE concentration[a]

exp.	Reductant	Solid-phase Fe(II) (mM)[b]	Cu(II) (mM)[c]	PCE (mM)[d]	$k_{app,PCE}$ (day^{-1})[e]	k_{PCE} ($M^{-1}day^{-1}$)[f]
14	GR-F(Cu)	88.6	0	0.247	0.00069 (±128%)	0.00856
15	GR-F(Cu)	85.9	0.5	0.247	0.009 (±24.4%)	0.114
11	GR-F(Cu)	83.3	1	0.248	0.0884 (±25.1%)	1.17
16	GR-F(Cu)	62.1	5	0.247	0.218 (±6.74%)	3.85
17	GR-F(Cu)	48.9	7.5	0.247	0.114 (±5.91%)	2.56
18	GR-F(Cu)	85.3	1	0.1	0.154 (±17.7%)	1.99
19	GR-F(Cu)	85.3	1	0.465	0.0458 (±13.0%)	0.59
20	GR-F(Cu)	85.3	1	0.707	0.03 (±10.4%)	0.389

[a] The pH in solution was 7.5.

[b] Solid phase Fe(II) concentration after modification which was calculated using the equation 5-5. Solid-phase Fe(II) before modification was 88.6 mM in exp. 11, 14-17 and 90.6 mM in exp. 18-20.

[c] The concentration of Cu(II) which was added to modify GR-F.

[d] Initial PCE concentration.

[e] Uncertainties represent 95 % confidence limits expressed in % relative to estimate for k_{app_PCE}.

[f] k_{PCE} was calculated by using equation 5-13.

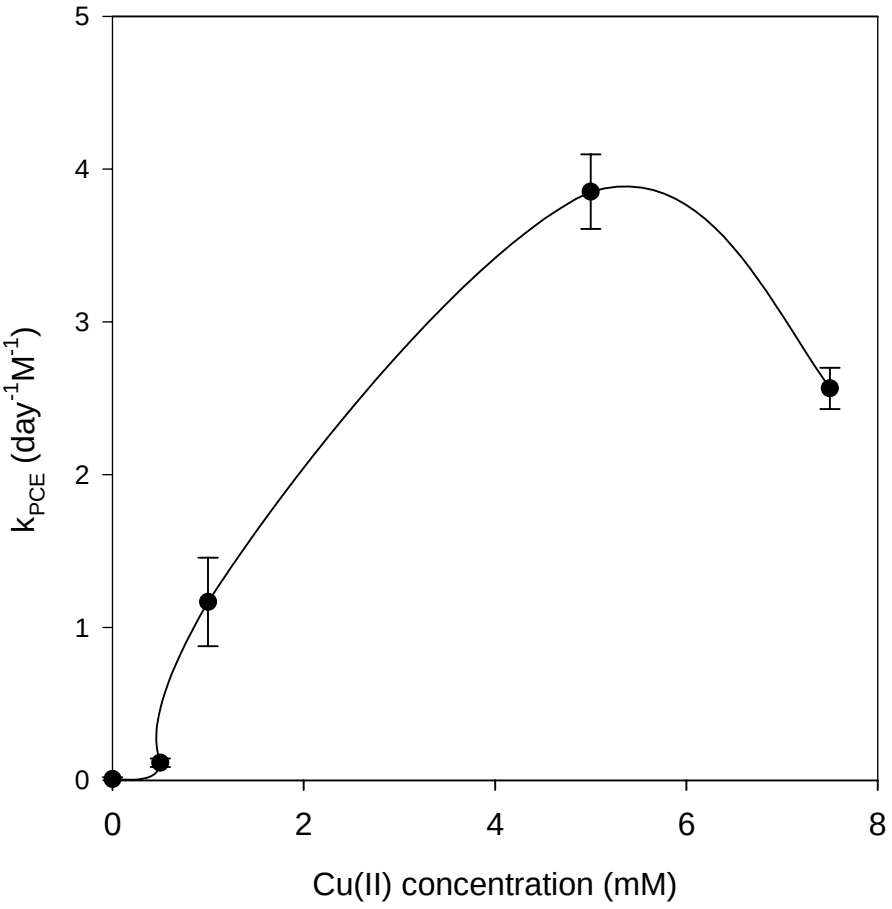

Figure 5.6 Dependence of solid phase Fe(II) normalized pseudo first-order rate constant of PCE degradation rate on Cu(II) concentration. Error bars for k_{PCE} represent 95% confidential intervals.

5.3.5 Effect of Initial PCE Concentration

Figure 5.7 shows PCE degradation by GR-F(Cu) with various initial PCE concentrations ranging from 0.100 to 0.707 mM and the results of fitting these data using a pseudo first-order kinetic model. The ratio of PCE to initial PCE was used on the y-axis instead PCE concentration in order to have all the data displayed on the same scale. Table 5.4 presents the apparent pseudo first-order rate constants ($k_{app,PCE}$) obtained through nonlinear regression using MATLAB and solid-phase Fe(II) normalized first-order rate constants (exp. 18-20). The values of $k_{app,PCE}$ decreased from 0.154 to 0.03 day^{-1} as initial PCE concentration increased from 0.1 to 0.707 mM. However, the initial reaction rates seem to approach a limiting value at high PCE concentration as shown in Figure 5.8. Unfortunately, this behavior was not consistent with a pseudo first-order kinetic model. In a first-order kinetic model, the reaction rate is only a function of the PCE in solution so that there should be a linear relationship between reaction rates and initial PCE concentrations. Hence, the following saturation model was applied to describe the nonlinear relationship of initial reaction rate and initial PCE concentration (54, 81) and the results are presented in Figure 5.8.

$$r_{0,PCE} = \frac{r_{max,PCE} C_{PCE,0}}{\left(K_{m,PCE} + C_{PCE,0}\right)} \tag{5-16}$$

where, $r_{0,PCE}$ is the initial degradation rate, $r_{max,PCE}$ is the maximum degradation rate, $K_{m,PCE}$ is the PCE concentration at its half maximal degradation rate, and $C_{PCE,0}$ is the

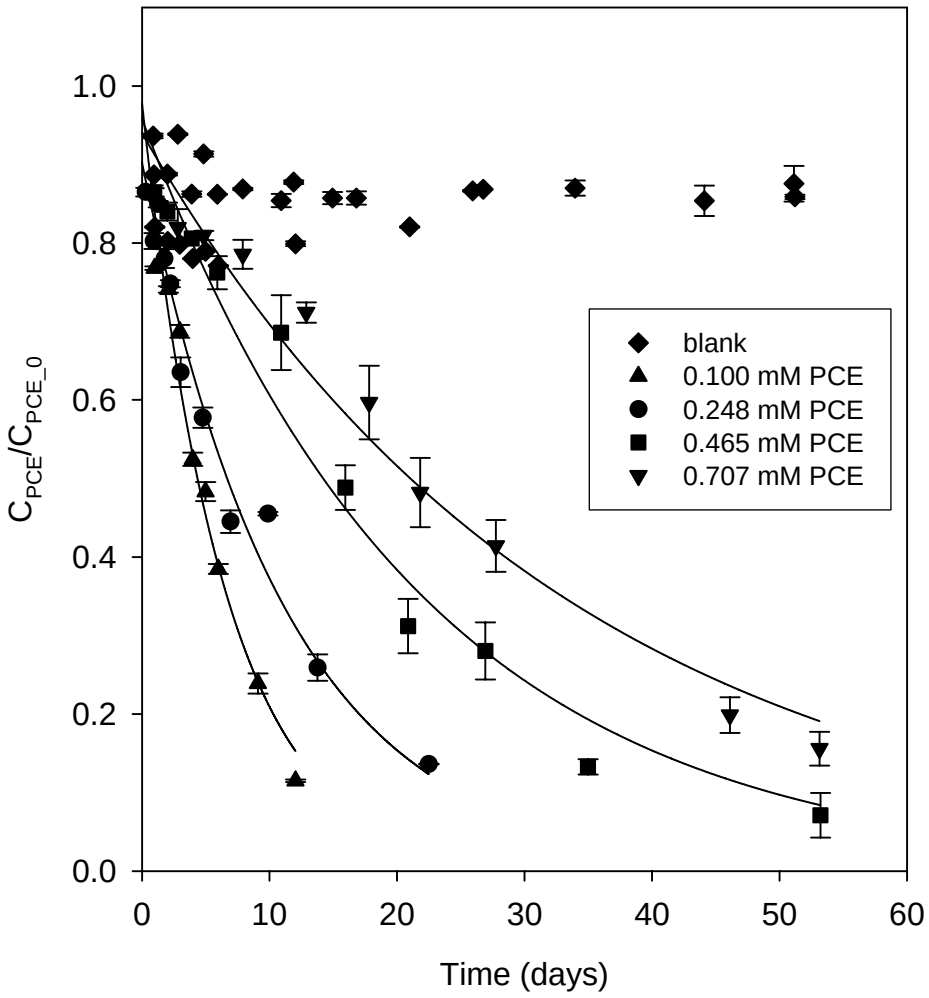

Figure 5.7 Results of kinetic experiments on PCE degradation by GR-F(Cu) at various initial PCE concentrations. Error bars are the standard deviations of measured PCE concentrations. Some error bars are smaller than the symbols. Solid lines represent fits of a first-order kinetic model. [Cu(II)] = 1 mM, Solid-phase Fe(II) = 88.6 mM, pH=7.5.

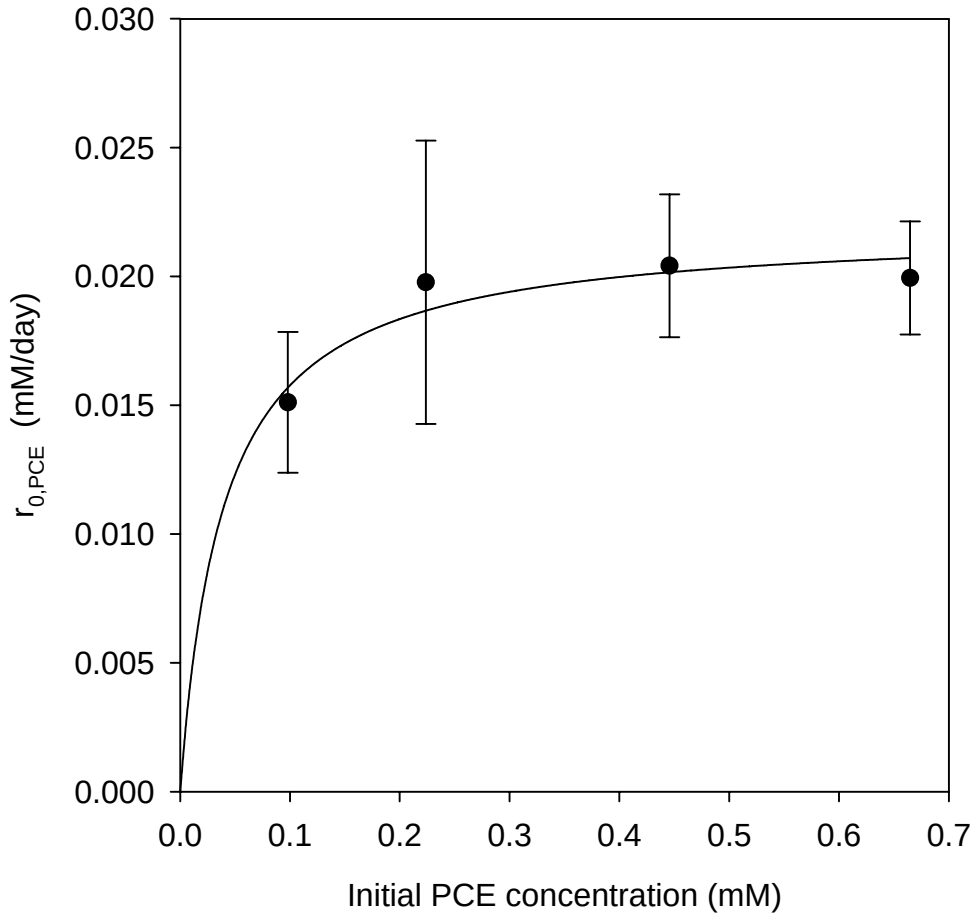

Figure 5.8 Dependence of initial degradation rate on initial PCE concentration. Error bars for R_0 represent 95 % confidential intervals. The solid line represents the fit of a saturation model: $r_{0,PCE} = \frac{r_{max,PCE} C_{PCE,0}}{\left(K_{m,PCE} + C_{PCE,0}\right)}$. The coefficients in this model are $r_{max,PCE}$ = 0.0219 (mM/day) and $K_{m,PCE}$ = 0.0391 (mM).

initial PCE concentration. Figure 5.8 clearly shows that the saturation model can appropriately express this relationship. It suggests that PCE dechlorination by the modified GR was controlled by the concentration of PCE adsorbed onto the surface of GR and that this surface concentration had a maximum concentration. These surface saturation reactions are known to occur on the surface of catalysts through the following three steps: adsorption of the target compound onto the catalyst surface, surface reaction, and desorption of reaction product. In addition, when the surface reaction was the rate-limiting step, the overall reaction rate with respect to initial PCE showed saturation behavior (81). This result is comparable to the dechlorination mechanism proposed by Cheng (49) in which a dehalogenation reaction occurs on the surface of a bimetallic reductant as illustrated in Figure 2.4. Surface saturation reaction was also observed in several studies on the reaction between chlorinated organics and solid reductant such as zero valent iron (ZVI) (53, 82, 83) cement slurries containing Fe(II) (54) and GR (28).

5.3.6 Reaction Products and Pathways

The reaction products of PCE degradation by GR-F(Cu) and GR-F(Pt) were studied. Based on the reduction pathway proposed by Arnold and co-workers (53). TCE, cis-DCE, trans-DCE, 1,1-DCE, VC, ethylene, acetylene, and ethane were measured at the point of about 95 % of PCE degradation. The experimental conditions were as follows: 0.247 mM of PCE, 82.7 mM of solid-phase Fe(II), 1 mM of Cu(II) or Pt(IV), and pH 7.5. Figure 5.9 shows the results of by-product analysis in which ethane was a major by-product of PCE degradation in both cases and any other possible by-products were not detected or below detection limits. The total recovery of organic carbon

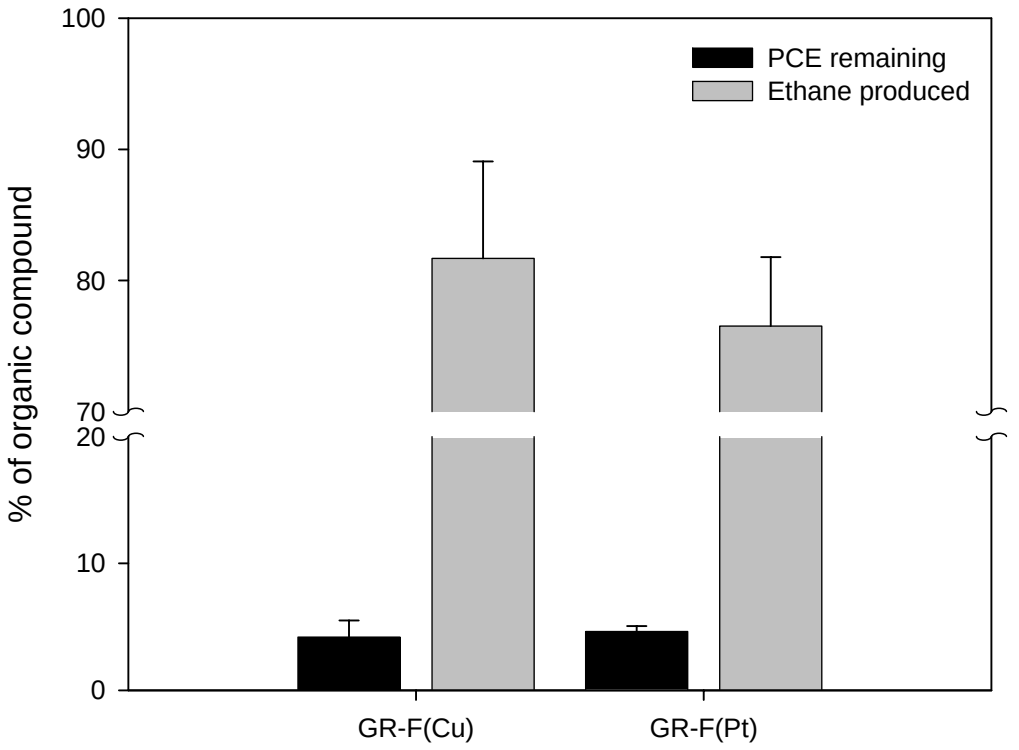

Figure 5.9 By-product analysis in PCE degradation by GR-F(Cu) and GR-F(Pt). Error bars represent standard deviation.

which was the sum of the concentration of PCE remaining and ethane produced, were 85.9 % for GR-F(Cu) and 81.1 % for GR-F(Pt). The following are possible explanations for the low recovery of carbon: 1) the loss of volatilized organic carbon during the experiment, 2) the formation of nondetectable compounds such as dichloroacetylene, chloroacetylene, and C_3 or C_4 carbon compounds, and 3) the inaccuracy of Henry's law constants (7, 8, 10, 13, 28, 82). The results shown in Figure 5.10 can be compared to those reported by Muftikian and co-workers (44), who observed that ethane was the only reaction product in the dechlorination of TCE using bimetallic reductant (Pd/Fe). Thus, ethane is proposed as the main reaction product and the following equation can be used to describe dechlorination of PCE by GR-F with Cu and Pt.

$$6Fe^{II}_3Fe^{III}_1(OH)_8 \cdot F + C_2Cl_4 \rightarrow 8Fe^{II}_1Fe^{III}_2O_4 + C_2H_6 + 6F^- + 4Cl^- + 10H^+ + 16H_2O \quad (5\text{-}14)$$

Unfortunately, it was difficult to propose the reduction pathway of PCE degradation using the results of reaction product analysis because ethane could be a product of hydrogenolysis as well as β-elimination, as shown in Figure 2.5.

Figure 5.10 shows the XRD analysis of GR-F(Cu) after it had reduced PCE. Only magnetite and GR-F were detected, which means that magnetite was the major oxidation product of GR-F. Lee (28) and Hansen (21) also observed that GR was transformed to magnetite during TCE dechlorination by GR-SO_4 and nitrate reduction by GR-Cl, respectively.

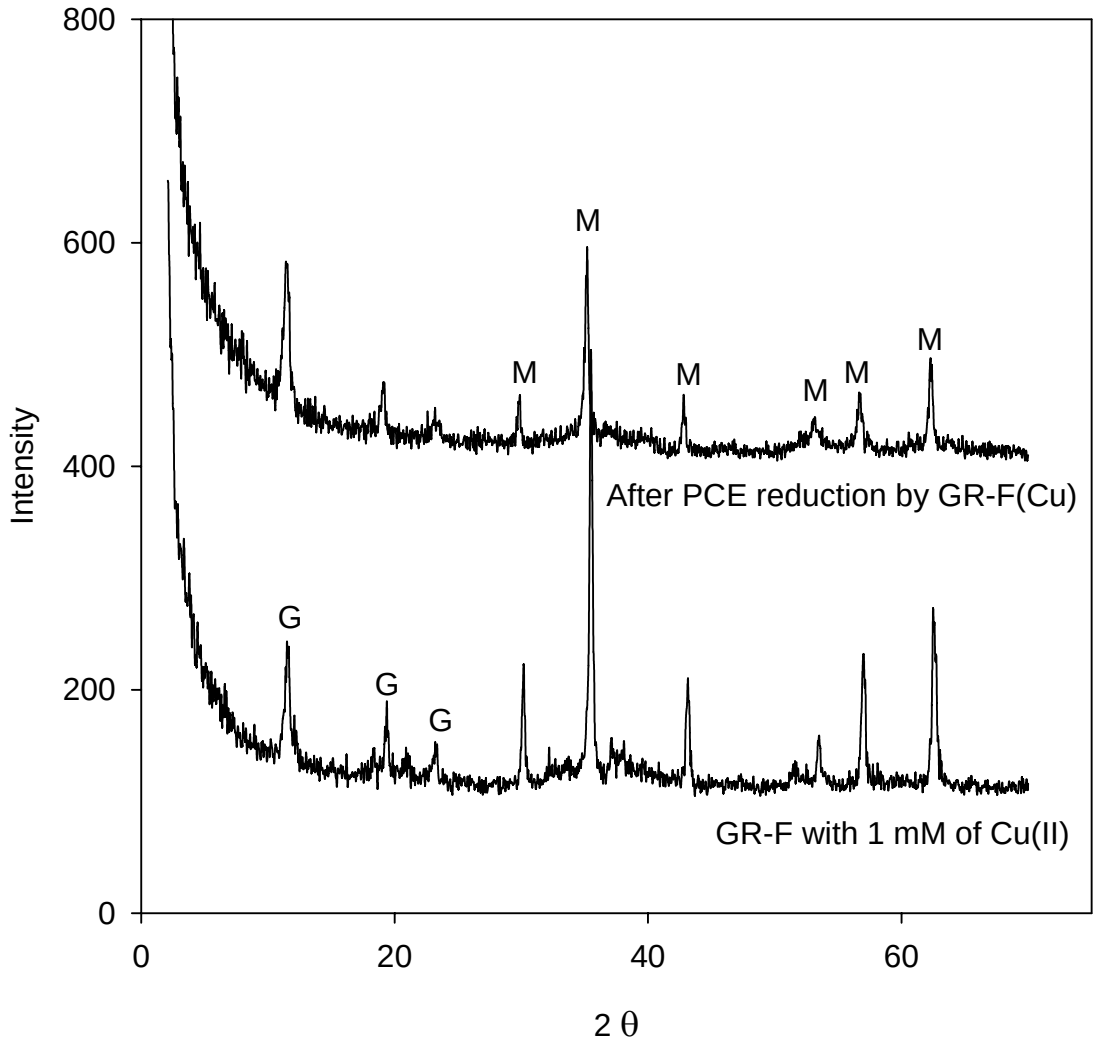

Figure 5.10 Results of XRD analysis for GR-F(Cu) after PCE degradation. G represents GR-F and M represents magnetite.

CHAPTER VI

NITRATE REDUCTION BY FLUORIDE GREEN RUST MODIFIED WITH COPPER OR PLATINUM

6.1 Introduction

Increasing nitrate concentration in groundwater is a considerable environmental problem, especially where groundwater is used as a source of drinking water. Excessive levels of nitrate can cause a serious illness called methemoglobinemia, which is also known as “blue baby syndrome”, because it interferes with the oxygen-carrying capacity of the child’s blood (11). Additionally, several studies reported that potentially carcinogenic N-nitroso compounds can be produced by reacting nitrate with amines or amides (84). For these reasons, maximum contaminant levels (MCLs) have been set at 10 mg NO_3^--N/L and 1.0 mg NO_2^--N/L by the United States Environmental Protection Agency (USEPA) (11). The primary sources of nitrate in groundwater are the excessive usage of chemical fertilizers and animal manure. Waste disposal practices associated with land application of sludge, wastewater effluents, municipal or industrial landfills, and septic tank systems are considered as additional sources of nitrate contamination (57, 84-86).

To remove nitrate from groundwater, physical, biological and chemical methods have been widely studied. The physico-chemical methods of ion exchange, reverse osmosis and electrodialysis have been shown to be stable, fast and easily automated processes. However, they have been considered not to be applicable to large scale

systems, because of high operational costs and the generation of concentrated brine wastes (12, 57). Biological denitrification has been used and has the environmental advantage of producing nitrogen gas as a final product, which is easily dispersed into the air phase. However, excessive production of biomass, need for a continual supply of electron donor for the growth of the microorganisms, and difficulty of operating the treatment system have been obstacles in the application of biological methods in water treatment (12, 57).

The chemical reduction of nitrate has received attention as an alternative to physico-chemical and biological methods in last decade because its reaction rate was faster than those of biological methods and it was cost-effective compared to other physico-chemical methods (57). Zero valent iron (ZVI) has been predominantly studied as a chemical reductant to remove nitrate (12, 59-63). In most cases, ZVI reduced nitrate to ammonium and its reaction rate was maximized at pH in the range of pH 2-5 and at low concentrations of dissolved oxygen (59-63).

In addition, green rusts (GRs) have been evaluated as chemical reductants for nitrate at neutral pH (20, 21). Green Rust (GR) is a layered Fe(II)-Fe(III) hydroxide solid phase with an appropriate anion in the interlayer. It was discovered as a transient corrosion product of iron pipe in early 1900 (31). It has been focused as an effective chemical reductant for organic and inorganic contaminants, including urinate (18), nitrate and nitrite (19-22), selenate (23), chromate (24, 25), and halogenated hydrocarbons (13, 26-29). An interesting observation was that its reactivity for dechlorinating chlorinated compounds was enhanced when it was contacted with a trace

metal such as Ag(I), Au(III), or Cu(II). The rate of dechlorination of GR with a trace metal was up to three orders of magnitude higher than for GR itself (13, 29, 30). Furthermore, it was revealed in Chapter IV of this study that GRs modified with Cu(II) or Pt(VI) also have higher reaction rates for nitrate reduction.

The goals of this study are: 1) to characterize nitrate reduction by fluoride green rust (GR-F) modified with Cu or Pt, and 2) to understand the reaction mechanism of nitrate reduction. The effect of pH, activating agent concentration, and initial nitrate concentration on nitrate reduction by GR-F modified with Cu and Pt were investigated.

6.2 Experimental Procedure

Fluoride green rust (GR-F) was synthesized using the partial air oxidation method developed by Refait and coworkers (69) and modified by Son (30). $Fe(OH)_2$ solid was freshly prepared by mixing 0.12 M of $FeCl_2$ and 0.2 M of NaOH in an anaerobic chamber and then 0.12 M of NaF was added into the $Fe(OH)_2$ suspension as an anion source. The mixture of $Fe(OH)_2$ and NaF was taken out of the chamber and oxidized by oxygen by allowing it to contact the air. During the oxidation of $Fe(OH)_2$, the pH in the solution was monitored. The oxidation process was stopped when the pH reached a maximum and began to drop. The synthesized GR-F was stored in the chamber to prevent further oxidation. In addition, all of the following experimental preparation steps were conducted in an anaerobic chamber.

GR-F was washed twice with deaerated deionized water (DDIW) to reduce the concentrations of undesirable ions before use. To maintain the pH in the experiment for determining pH effect, 0.1 M of biological pH buffer (CHES for pH 9 and CAPS for pH

11) instead of DDIW was added at the second washing step. The pH in the solution using biological buffers remained constant throughout the experiment.

The modification of GR-F was achieved by contacting GR-F and a trace metal for about 1 hr. A magnetic stirrer was used to provide homogenous conditions during the modification period. Generally, a trace metal concentration was set to 1 mM. In the experiment for the effect of Cu(II) concentration on nitrate reduction, 0.1 to 5 mM of Cu(II) concentration were obtained by adding appropriate amounts of 0.4 M of Cu(II) stock solution into 250 mL of GR suspension. GR-F modified with Pt or Cu will be identified as GR-F(Pt) and GR-F(Cu), respectively.

The batch kinetic experiment for nitrate reduction by GR-F(Cu) and GR-F(Pt) was conducted using a 250-mM polypropylene bottle (Nalgene) in an anaerobic chamber. The initial concentration of nitrate was set to 0.05, 0.1, 0.5, 1, and 1.2 mM by adding 0.0312, 0.0625, 0.312, 0.625, and 0.75 mL of 0.4 M nitrate stock solution using 1-mL or 0.1-mL micropipettes. During the reaction, the suspension of modified GR was continuously mixed using a magnetic stirrer. Samples of about 5 mL were taken at each sampling time and were filtered using 0.45-μm cellulose nitrate membrane filters. The degradation kinetics of nitrate reduction were determined by monitoring nitrate, nitrite and ammonium concentrations over time. The ammonium concentration was measured using the phenate method conducted within 4 hours of sampling (66). In some samples, nitrate and nitrite were also measured using an ion chromatograph (I.C.).

6.3 Results and Discussion

6.3.1 Treatment of Kinetic Data

In experiments with modified GR-F, nitrate was believed to enter the interlayer of GR-F by an anion exchange reaction and to be reduced while GR was oxidized to magnetite (21). In addition, the overall reaction was observed to occur in two steps; nitrate → nitrite → ammonium. Based on these two observations, the following sequential step reaction was proposed to describe kinetics of nitrate reduction by modified GR-F (equations 6-1 to 6-5). The first step is the exchange of nitrate with fluoride in GR (equation 6-1). The second step is the reduction of GR-NO_3 to form magnetite and nitrite (equation 6-2). Because the structure of magnetite does not have an interlayer, nitrite must be released into the aqueous phase. Equations 6-1 and 6-2 will be called nitrate reaction steps. The third and fourth steps are nitrite reduction steps. Nitrite is exchanged with fluoride (equation 6-3) and then nitrite is reduced to ammonium and GR is oxidized to magnetite (equation 6-4).

$$\text{Ion exchange reaction}: \ GR - F + NO_{3(aq)}^{-} \xrightarrow{k_1} GR - NO_3 + F_{(aq)}^{-} \qquad (6\text{-}1)$$

$$\text{Redox reaction}: \ GR - NO_3 \xrightarrow{k_2} \text{Magnetite} + NO_{2(aq)}^{-} \qquad (6\text{-}2)$$

$$\text{Ion exchange reaction}: \ GR - F + NO_{2(aq)}^{-} \xrightarrow{k_3} GR - NO_2 + F_{(aq)}^{-} \qquad (6\text{-}3)$$

$$\text{Redox reaction}: \ GR - NO_2 \xrightarrow{k_4} \text{Magnetite} + NH_{4(aq)}^{+} \qquad (6\text{-}4)$$

The overall reaction is summarized in equation 6-5.

$$NO_{3(aq)}^{-} \xrightarrow{k_1} GR-NO_3 \xrightarrow{k_2} NO_{2(aq)}^{-} \xrightarrow{k_3} GR-NO_2 \xrightarrow{k_4} NH_{4(aq)}^{+} \quad (6\text{-}5)$$

where, k_1 and k_3 are rate constants for anion exchange of nitrate and nitrite with GR-F, respectively, and k_2 and k_4 are reduction reaction rate constants for GR-NO_3 and GR-NO_2, respectively. This reaction model was developed based on the following assumptions: 1) each step is kinetically controlled and 2) the rate of reaction for each step can be expressed with a pseudo-first order kinetic model. Many ion exchange reactions are known to reach equilibrium, if other reactions do not occur. However, in this study, the nitrate exchange reaction was followed by a nitrate reduction reaction so ion exchange equilibrium was not observed.

To calculate the concentrations of NO_3^-, GR-NO_3, NO_2^-, GR-NO_2, NH_4^+ as functions of time in a batch system using this kinetic model, the following set of equations must be solved.

$$-\frac{dC_{NO_3}}{dt} = k_1 C_{NO_3} \quad (6\text{-}6)$$

$$-\frac{dC_{GR\text{-}NO_3}}{dt} = k_1 C_{NO_3} - k_2 C_{GR\text{-}NO_3} \quad (6\text{-}7)$$

$$-\frac{dC_{NO_2}}{dt} = k_2 C_{GR\text{-}NO_3} - k_3 C_{NO_2} \quad (6\text{-}8)$$

$$-\frac{dC_{GR\text{-}NO_2}}{dt} = k_3 C_{NO_2} - k_4 C_{GR\text{-}NO_2} \quad (6\text{-}9)$$

$$\frac{dC_{NH_4}}{dt} = k_4 C_{GR\text{-}NO_2} \tag{6-10}$$

where, C_{NO3} is the concentration of nitrate ion in solution, $C_{GR\text{-}NO3}$ is the concentration of nitrate green rust, C_{NO2} is the concentration of nitrite ion in solution, $C_{GR\text{-}NO2}$ is the concentration of nitrite green rust, and C_{NH4} is the concentration of ammonium ion in solution. All concentrations are measured in millimolar units. These equations were solved by a mathematical method using an integrating factor with the initial values of $C_{GR\text{-}NO3}$, C_{NO2}, $C_{GR\text{-}NO2}$, and C_{NH4} assumed to be equal to 0 and initial value of C_{NO3_init} assumed to be equal to whatever initial concentration was used in the experiment (87). The results are presented in equations 6-11 to 6-15.

$$C_{NO_3} = C_{NO_3\_init} \cdot e^{-k_1 \cdot t} \tag{6-11}$$

$$C_{GR\text{-}NO_3} = C_{NO_3\_init} \cdot \left[\frac{k_1}{(k_2 - k_1)} e^{-k_1 \cdot t} + \frac{k_1}{(k_1 - k_2)} e^{-k_2 \cdot t} \right] \tag{6-12}$$

$$C_{NO_2} = C_{NO_3\_init} \left[\frac{k_1 k_2 \cdot e^{-k_1 \cdot t}}{(k_2 - k_1)(k_3 - k_1)} + \frac{k_1 k_2 \cdot e^{-k_2 \cdot t}}{(k_1 - k_2)(k_3 - k_2)} + \frac{k_1 k_2 \cdot e^{-k_3 \cdot t}}{(k_1 - k_3)(k_2 - k_3)} \right] \tag{6-13}$$

$$C_{GR\text{-}NO_2} = C_{NO_3\_init} \left[\begin{array}{l} \frac{k_1 k_2 k_3 \cdot e^{-k_1 \cdot t}}{(k_2 - k_1)(k_3 - k_1)(k_4 - k_1)} + \frac{k_1 k_2 k_3 \cdot e^{-k_2 \cdot t}}{(k_1 - k_2)(k_3 - k_2)(k_4 - k_2)} + \\ \frac{k_1 k_2 k_3 \cdot e^{-k_3 \cdot t}}{(k_1 - k_3)(k_2 - k_3)(k_4 - k_3)} + \frac{k_1 k_2 k_3 \cdot e^{-k_4 \cdot t}}{(k_1 - k_4)(k_2 - k_4)(k_3 - k_4)} \end{array} \right] \tag{6-14}$$

$$C_{NH_4} = C_{NO_3\_init} - \left[C_{NO_3} - C_{GR\text{-}NO_3} - C_{NO_2} - C_{GR\text{-}NO_2} \right] \tag{6-15}$$

where C_{NO3_init} is the initial concentration of nitrate in solution.

The values of the rate constants (k_1, k_2, k_3, k_4) were obtained by conducting a nonlinear regression on aqueous phase nitrate, nitrite, and ammonium concentrations using the Gauss-Newton method coded in the nlinfit function of MATLAB® (MathWorks Inc.). The MATLAB function 'nlparci' was used to calculate 95% confidential levels of the rate constants. Figure 6.1 shows measured concentrations (symbols) and model predictions (lines) using the sequential step reaction for nitrate reduction by GR-F(Cu) at pH 9. There is a good fit between measured and modeled concentrations of nitrate, nitrite, and ammonium.

The rate constant of the reduction reaction could be normalized by the solid-phase concentration of Fe(II) with the assumption that solid-phase Fe(II) was large enough to remain constant during the reaction. The normalized rate constants for nitrate and nitrite reduction were expressed as $k_{2\_Fe(II)}$ and $k_{4\_Fe(II)}$, respectively.

However, in most cases, the nitrite reduction step was too fast to allow nitrite to accumulate in solution to detectable levels. This means that the nitrate reactions were the rate limiting steps in the overall reaction. Therefore, the following simplified sequential step reaction model was used when nitrite was not measured in solution;

$$NO^-_{3(aq)} \xrightarrow{k_1} GR\text{-}NO_3 \xrightarrow{k_2} NH^+_{4(aq)} \qquad (6\text{-}16)$$

The concentrations of all components were calculated using equations 6-17 to 6-19.

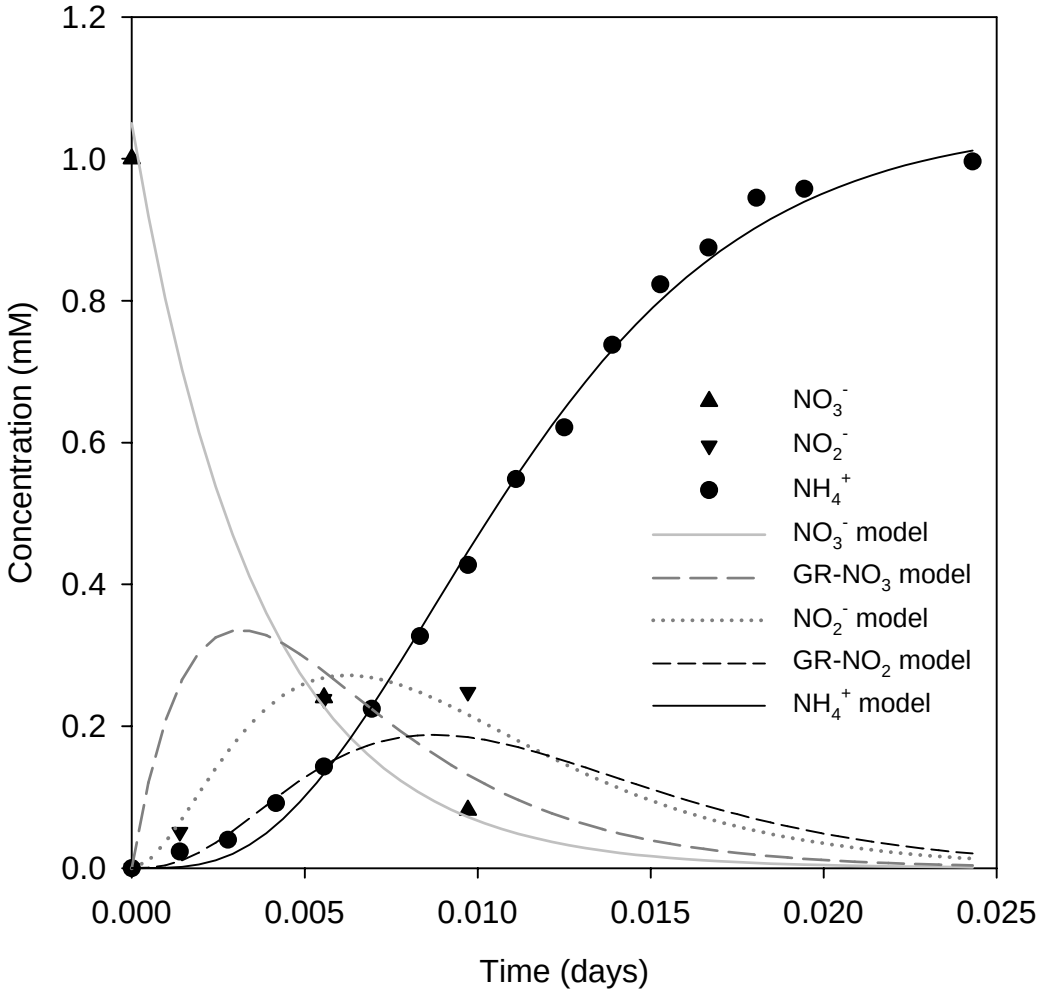

Figure 6.1 Experimental results and model simulations of nitrate reduction by GR-F(Cu) at pH 9 using a sequential step reaction model. Symbols represent the ion concentrations measured in liquid phase. Lines represent predictions of the kinetic model. C_{NO3_init} = 1 mM, Solid-phase Fe(II) = 83.3 mM, [Cu(II)] = 1 mM.

$$C_{NO_3} = C_{NO_3\_init} \cdot e^{-k_1 \cdot t} \quad (6\text{-}17)$$

$$C_{GR\text{-}NO_3} = C_{NO_3\_init} \cdot \left[\frac{k_1}{(k_2 - k_1)} e^{-k_1 \cdot t} + \frac{k_1}{(k_1 - k_2)} e^{-k_2 \cdot t} \right] \quad (6\text{-}18)$$

$$C_{NH_4} = C_{NO_3\_init} - \left[C_{NO_3} - C_{GR\text{-}NO_3} \right] \quad (6\text{-}19)$$

6.3.2 Effect of pH

The reaction rates of nitrate reduction by GR-F(Cu) and GR-F(Pt) were investigated at three different pH (pH 7.5, 9 and 11). Figure 6.2 shows the results of the experiments with GR-F(Cu) and the model predictions for concentrations of nitrate, nitrite, and ammonium. Nitrate reduction at pH 7.5 was described with the two-step model because nitrite was not detected, while experiments at pH 9 and pH 11 were described with a four-step model, because nitrite was detected. The rate constants and the solid-phase Fe(II) normalized rate constants are summarized in Table 6.1. The nitrate exchange reaction and the reduction of GR-NO_3 were fastest at pH 9, where the observed reduction rate constant of GR-NO_3 was almost four times faster than the slowest one, which was obtained at pH 7.5. Nitrite reduction at pH 9 was also relatively better than at pH 11. Normally, it was observed that all nitrate was transformed to ammonium by the modified GR- F within one and half hour.

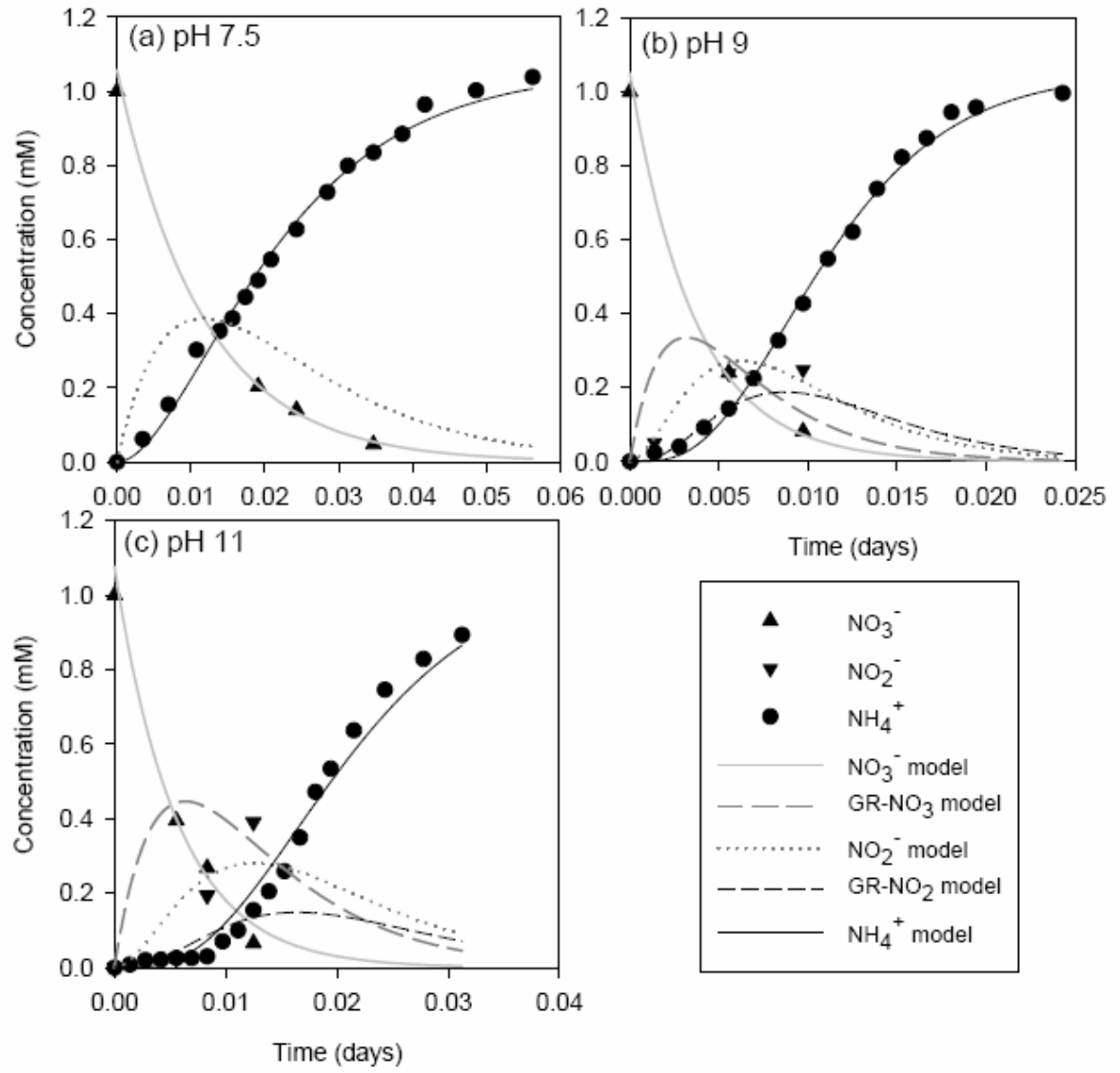

Figure 6.2 Results of kinetic experiments on nitrate reduction by GR-F(Cu) at various pH. The two-step reaction model was used for results at pH 7.5 and the four-step reaction model was used for results at pH 9 and pH 11. Symbols represent the concentrations measured in the liquid phase. Lines represent predictions of the kinetic model.

Table 6.1 Rate constants and solid-phase Fe(II)-normalized rate constants for nitrate reduction by GR-F(Cu) and GR-F(Pt) at various pH[a]

			Nitrate reduction step			Nitrite reduction step		
Exp.	reductant	pH[b]	k_1[c] (day^{-1})	k_2[c] (day^{-1})	$k_{2\_Fe(II)}$[d] ($M^{-1}day^{-1}$)	k_3[c] (day^{-1})	k_4[c] (day^{-1})	$k_{4\_Fe(II)}$[d] ($M^{-1}day^{-1}$)
24	GR-F(Cu)	7.3 – 7.6	85.3 (±12.6%)	85.7 (±18.1%)	1030	-	-	-
25	GR-F(Cu)	8.9 – 9.1	272 (±13.0%)	368 (±55.3%)	4420	343 (±20.7%)	414 (±71.9%)	4990
26	GR-F(Cu)	10.9 – 11.1	178 (±22.1%)	138 (±81.9%)	1660	165 (±69.4%)	287 (±204%)	3460
27	GR-F(Pt)	7.3 – 7.7	228 (±27.3%)	226 (±41.9%)	2810	-	-	-
28	GR-F(Pt)	8.9 – 9.1	230 (±22.0%)	352 (±44.9%)	4370	-	-	-
29	GR-F(Pt)	10.9 – 11.1	70.8 (±20.1%)	103 (±39.3%)	1280	-	-	-

[a] Initial nitrate concentration was 1 mM. The trace metal concentration was fixed to 1 mM in all cases. Solid-phase Fe(II) was 0.0831 M in exp. 24-26 and 0.0805 M in exp. 27-29.

[b] The pH range which was measured during the reaction period.

[c] Uncertainties represent 95 % confidence limits expressed in % relative to estimate for k_1, k_2, k_3, and k_4,. k_1 and k_3 describe the rates of exchange and k_2 and k_4 describe the rates of reduction reaction.

[d] Solid-phase Fe(II) normalized rate constants ($k_{2\_Fe(II)}$, and $k_{4\_Fe(II)}$) were calculated by dividing k_2, and k_4 by solid-phase Fe(II).

Figure 6.3 shows the effect of pH on nitrate reduction by GR-F(Pt). A two-step reaction model was used in all platinum modification cases and the rate constants obtained from modeling are presented in Table 6.1. The fastest rate constant for nitrate reduction with GR-F(Pt) was also observed at pH 9, where 1 mM of nitrate was completely transformed to ammonium in 25 minutes. The pH values remained relatively stable during the experiment.

The model simulations shown in Figures 6.2 and 6.3 illustrate that the sequential step reaction models provided relatively good descriptions for pH 7.5 and pH 9. However, there was quite a difference between the measured and simulated ammonium concentrations in the pH 11. The measured ammonium concentrations were lower than simulated values in the early stage of the reaction and were higher than simulated values in the later stage of reaction. This was due to the relatively lower rate of ammonium production at the beginning of reaction. Because ammonium production was the last step of the overall reaction, it might be delayed if additional steps occurred at pH 11 that were not included in the model.

These effects of pH on nitrate reduction by modified GR-F are analogous to the results reported by Gao and co-workers (88). They researched kinetics of nitrate reduction by hydrogen gas with a bimetallic catalyst (Pd-Cu) and reported that the rate increased above pH 2 to a maximum at pH 10. They also reported that nitrate reduction occurred according to the following sequential step reaction;

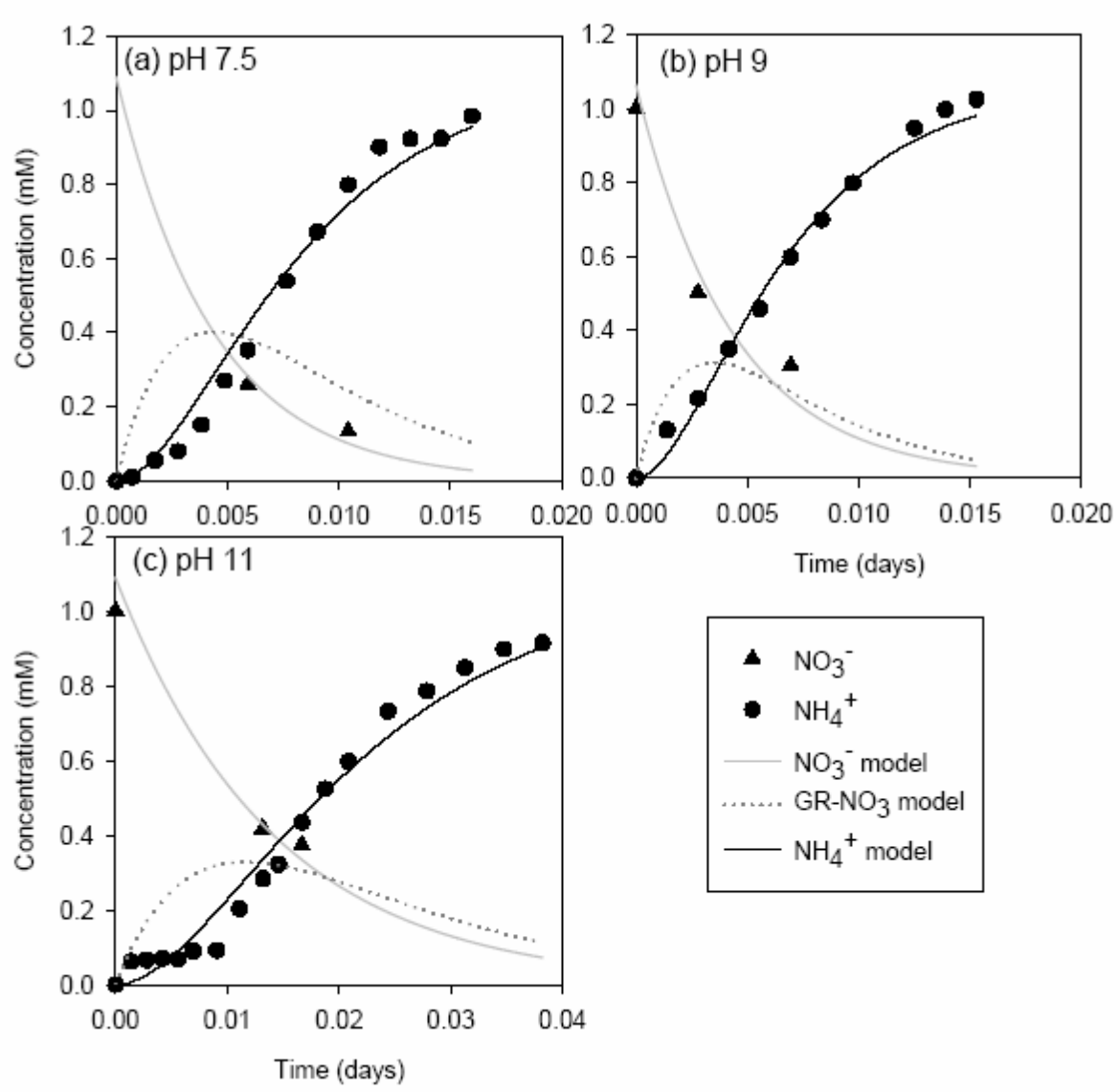

Figure 6.3 Results of kinetic experiments on nitrate reduction by GR-F(Pt) at various pH. The two-step reaction model was used for pH 7.5, pH 9, and pH 11. Symbols represent concentrations measured in the liquid phase. Lines represent predictions of the kinetic model.

$NO_3^- \rightarrow NO_2^- \rightarrow NO \rightarrow N_2$ or NH_4^+ (88). On the other hand, the rate of nitrate reduction by ZVI appears to decrease as pH increase (63).

The pH effects on nitrate reduction by GR-F(Cu) and GR-F(Pt) were quite different from those on PCE reduction, which are presented in Chapter V. First of all, the best condition for nitrate reduction by modified GR-F was at pH 9, while the best condition for dechlorination of PCE was at pH 11. Secondly, relative differences of reaction rates between experiments at different pH values were smaller for nitrate reduction than for PCE degradation. The ratio of the largest rate constant to smallest rate constant for nitrate reduction with GR-F(Cu) was 4, while it was almost 100 for PCE degradation. The rate of nitrate reduction by GR-F(Pt) at pH 9 was faster than that at pH 11 by a factor of 3.5, while the rate of PCE degradation at pH 11 was five times faster than that at pH 9. This means that nitrate reduction by modified GR-F was much less influenced by pH than was PCE degradation.

6.3.3 Effect of Cu(II) Concentration

The effect of Cu(II) concentration was investigated over the range of 0 to 5 mM. Figure 6.4 shows the results of nitrate reduction by GR-F(Cu) at each Cu(II) concentration and the concentrations predicted by the two-step kinetic model using coefficients determined by nonlinear regression. Table 6.2 presents the rate constants of two-step reaction model and the solid-phase Fe(II) normalized rate constants for nitrate reduction. The nitrate reduction rate was improved as Cu(II) additions were increased over the range of 0 to 2.5 mM, while the rate constant at 5 mM was slower than that at 2.5 mM.

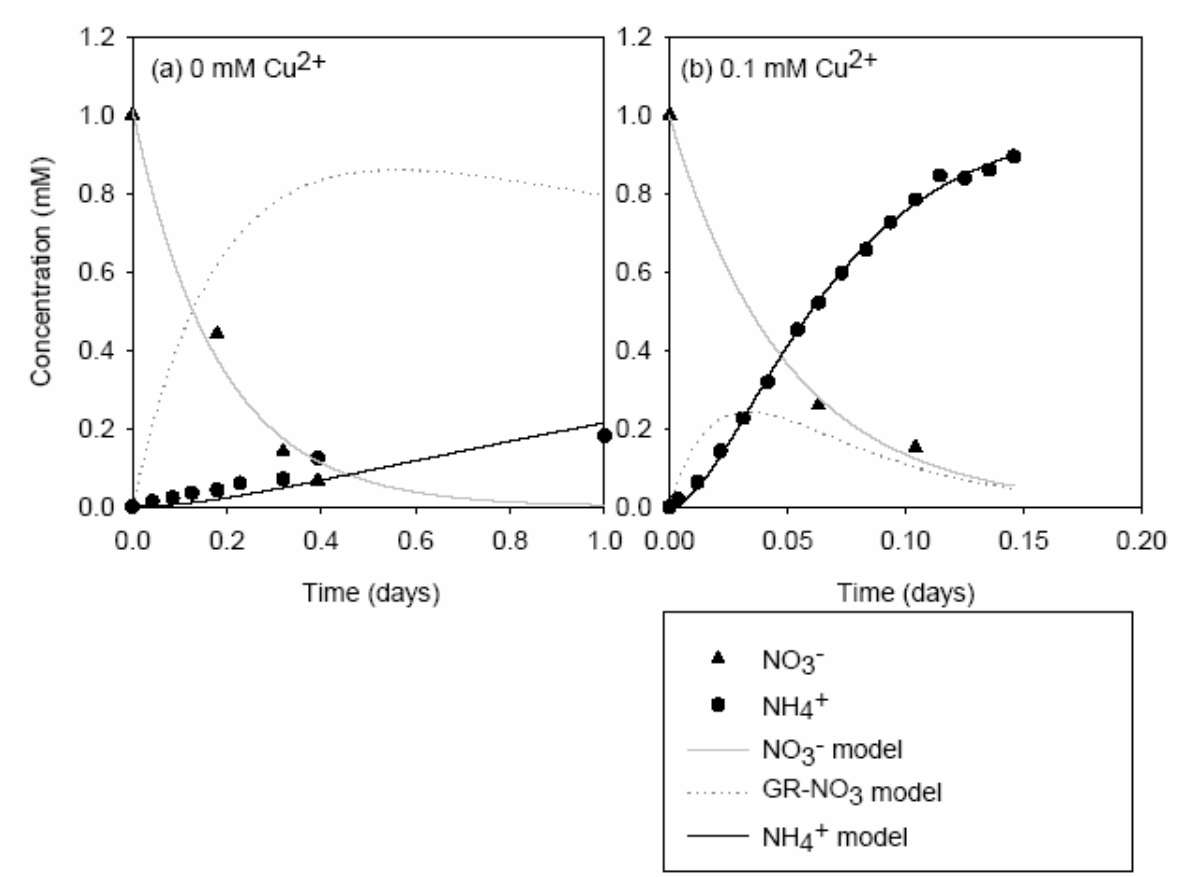

Figure 6.4 Results of kinetic experiments on nitrate reduction by GR-F(Cu) at various Cu(II) concentrations. Symbols represent concentrations measured in the liquid phase. Lines represent predictions of the two-step kinetic model.

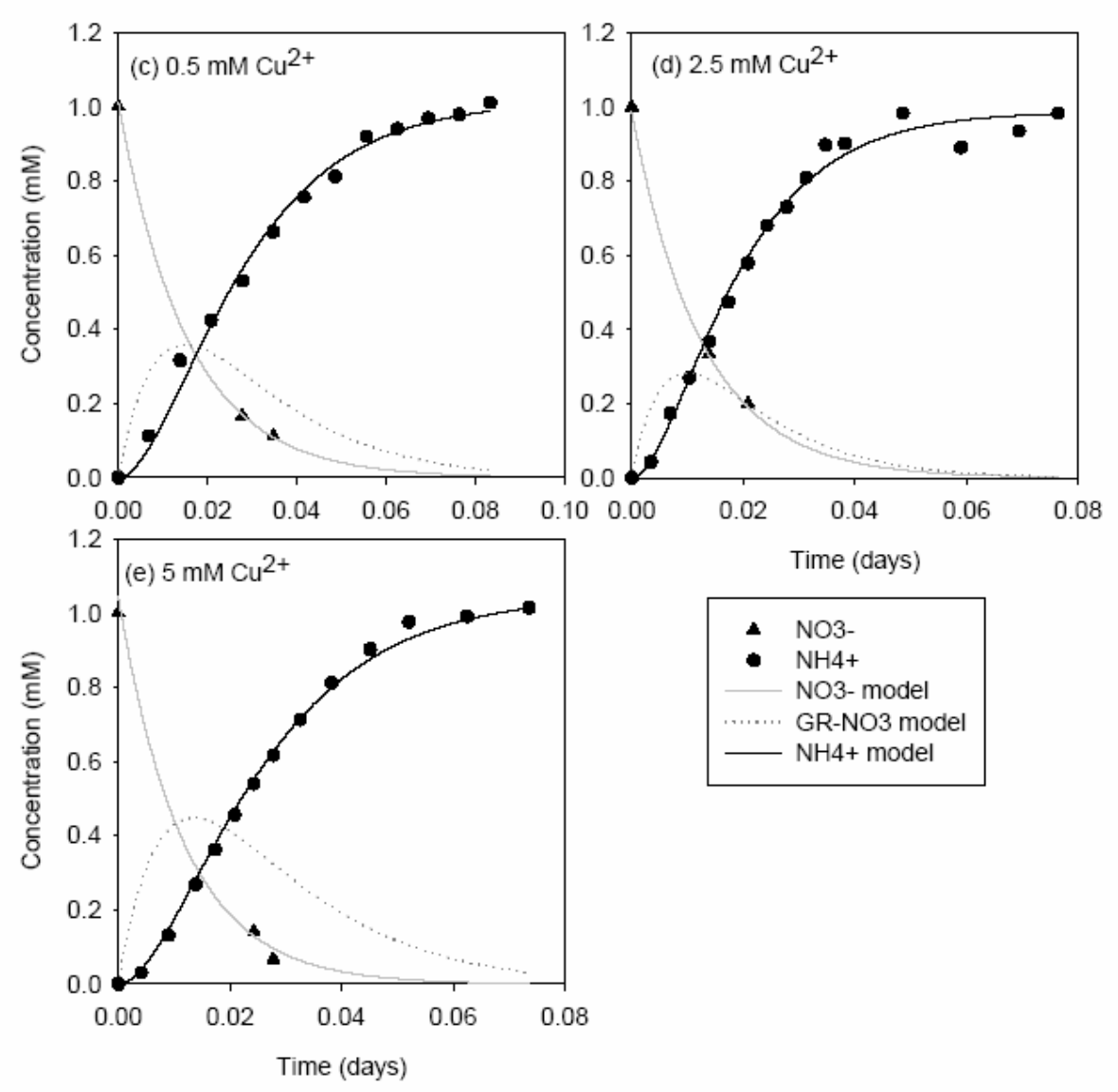

Figure 6.4 Continued.

The maximum value of $k_{2\_Fe(II)}$ was observed at 2.5 mM of Cu(II) and was almost three orders of magnitude larger than that for unmodified GR-F. The effect of Cu(II) concentration on solid-phase Fe(II)-normalized rate constants for nitrate reduction is illustrated in Figure 6.5.

Table 6.2 Rate constants and solid-phase Fe(II)-normalized rate constants for nitrate reduction by GR-F(Cu) at various Cu(II) concentrations[a]

Exp.	Cu(II) addition (mM)	Solid-phase Fe(II)[b] (M)	k_1[c] (day^{-1})	$k_{1\_Fe(II)}$[d] ($M^{-1}day^{-1}$)	k_2[c] (day^{-1})	$k_{2\_Fe(II)}$[d] ($M^{-1}day^{-1}$)
30	0	0.0886	5.52 (±17.4%)	62.3	0.29 (±44.3%)	3.29
31	0.1	0.0881	20.1 (±6.75%)	229	42.2 (±14.3%)	479
32	0.5	0.0860	64.3 (±16.3%)	748	69.7 (±24.0%)	811
24	1	0.0831	85.3 (±12.6%)	1026	85.7 (±18.1%)	1032
33	2.5	0.0754	78.8 (±13.9%)	1046	126 (±25.5%)	1672
34	5	0.0621	86.0 (±14.1%)	1384	62.4 (±16.1%)	1005

[a] Initial nitrate concentration was 1 mM. The pH range was set to 7.5. No buffer was used.

[b] Solid phase Fe(II) concentration after modification was calculated using the equation 5-5. Solid-phase Fe(II) before modification was 88.4 mM in exp. 24 and 88.6 mM in exp. 30-34.

[c] Uncertainties represent 95 % confidence limits expressed in % relative to estimate for k_1, and k_2,. k_1 is for the exchange reaction and k_2 is for the reduction reaction.

[d] Solid-phase Fe(II)-normalized rate constants ($k_{1\_Fe(II)}$ and $k_{2\_Fe(II)}$) were calculated by dividing k_1, and k_2 by solid-phase Fe(II) concentration.

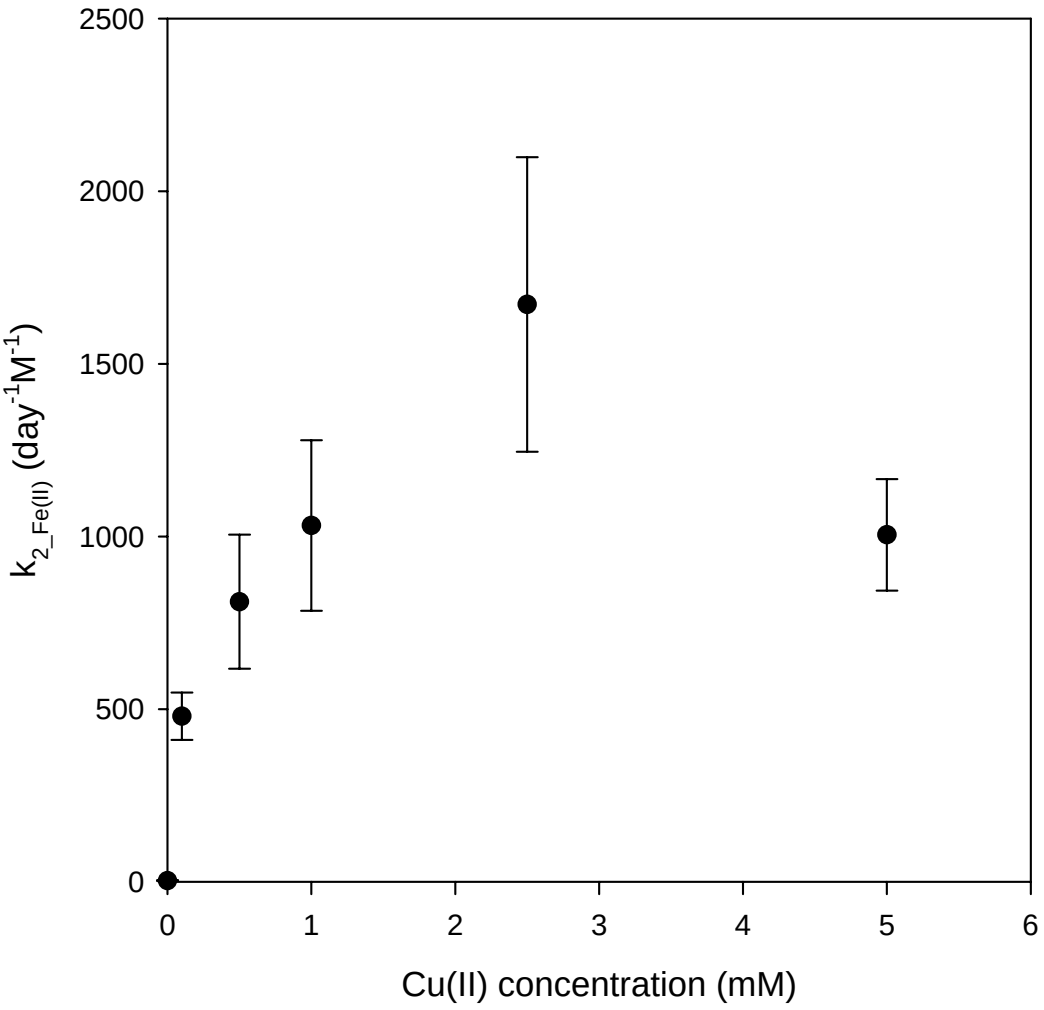

Figure 6.5 Dependence of solid-phase Fe(II) normalized nitrate reduction rate of GR-NO_3, $k_{2\_Fe(II)}$, on Cu(II) concentration. Error bars for $k_{2\_Fe(II)}$ represent 95% confidential intervals.

The rate constant for nitrate exchange, k_1, clearly increased with increasing Cu(II) concentration over the range of 0 mM to 1 mM (Table 6.2). This result is somewhat unexpected, because it was generally believed that Cu(II) would not affect the rate constant for the exchange reaction (k_1), but would affect the rate constant for the reduction reaction (k_2). This means that the reaction rate of the exchange reaction was affected by the rate of nitrate reduction. This result may be explained by considering that the ion exchange reaction is actually reversible, although the model in equation 6-5 assumes that it is irreversible. If the ion exchange reactions are reversible, the net rate would depend on the difference between the forward and reverse rates. The reverse rate would depend on the concentration of GR-NO_3. If the reduction rates are more rapid, the concentrations of GR-NO_3 would be lower, resulting in lower reverse reactions and higher net reactions of ion exchange. This would be shown in higher values of k_1.

The rate constant for nitrate reduction increased with increasing Cu(II) concentration over the range of 0 to 2.5 mM and then decreased at Cu(II) concentrations above 2.5 mM. This trend is the same as was observed for PCE degradation by modified GR-F. This can be explained in terms of two aspects of the proposed mechanism for modification of the GR: (1) the Cu(II) that was reduced to elemental Cu by GR-F was deposited on the surface of GR-F and (2) nitrate reduction occurred only on the surface of deposited Cu. Therefore, the rate of reduction is expected to be dependent on the concentration of elemental Cu on the surface of GR. Similar behavior has been reported by Lin and coworkers (46). They used iron with Ru (Ru/Fe) for dechlorination of trichloroethylene (TCE) and observed that the rate constant increased from 0.264 to 2.4

h^{-1} with increasing amounts of Ru over the rang of 0.25 to 1.5 % (w/w). However, the rate constant decreased to 1.8 h^{-1} at 2 % Ru. In addition, the surface area of Ru/Fe was observed to decrease from 1.66 to 1.44 m^2/g when Ru increased from 1.5 to 2 %. They proposed that the reason for this was the aggregation of Ru particles. They mentioned that increasing Ru resulted in an increase in the number of fine Ru particles at lower Ru addition rates, whereas fine Ru particles were aggregated into larger ones at higher Ru addition rates. If a similar mechanism occurred on GR, aggregated Cu particles at high Cu addition rates could explain the low reactivity of GR-F(Cu) at higher Cu(II) doses that was observed in this study. In other words, the aggregation of Cu could reduce the surface area of Cu on GR. This could be supported by further study that would analyze Cu speciation, measure the surface area of modified GR, and characterize the morphology of the modified GR particles with SEM.

6.3.4 Effect of Initial Nitrate Concentration

The effect of initial nitrate concentration on nitrate reduction by GR-F(Cu) was studied over the range of 0.05 to 1.2 mM and the results are shown in Figure 6.6. A two-step reaction model was used to describe the kinetic behavior. The rate constants for these experiments are presented in Table 6.3. The rate constants for nitrate reduction decreased as initial nitrate concentrations increased. The reduction rate constant (k_2) decreased from 210 to 77.2 day^{-1} as initial nitrate concentration increased from 0.05 to 1.2 mM.

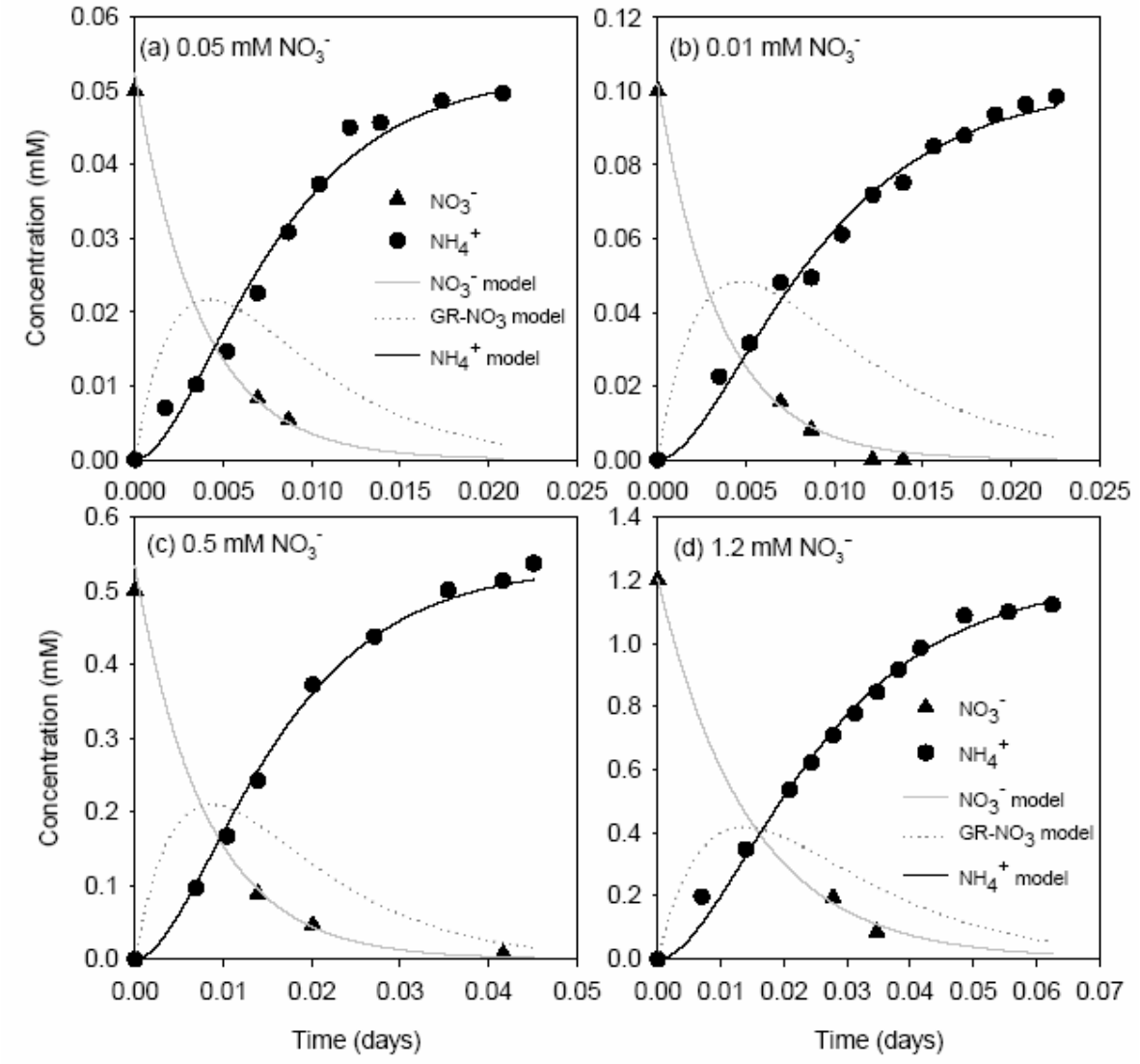

Figure 6.6 Results of kinetic experiments on nitrate reduction by GR-F(Cu) at various initial nitrate concentrations. Symbols represent concentrations measured in the liquid phase. Lines represent predictions of the two-step kinetic model.

Table 6.3 Rate constants and solid-phase Fe(II)-normalized rate constants for nitrate reduction by GR-F(Cu) at various initial nitrate concentrations[a]

exp	NO_{3_init} (mM)	solid-phase Fe(II)[b] (M)	k_1[c] (day^{-1})	$k_{1\_Fe(II)}$[d] ($M^{-1}day^{-1}$)	k_2[c] (day^{-1})	$k_{2\_Fe(II)}$[d] ($M^{-1}day^{-1}$)
35	0.05	0.0838	270 (±28.1%)	3222	210 (±36.2%)	2506
36	0.1	0.0838	280 (±19.7%)	3341	160 (±21.9%)	1909
37	0.5	0.0838	125 (±17.6%)	1486	109 (±24.4%)	1295
24	1	0.0831	85.3 (±12.6%)	1026	85.7 (±18.1%)	1032
38	1.2	0.0838	69.0 (±15.6%)	823	77.2 (±22.5%)	921

[a] Cu(II) concentration was fixed at 1 mM in all cases. The pH was set to 7.5. No buffer was used.

[b] Solid phase Fe(II) concentration after modification was calculated using the equation 5-5. Solid-phase Fe(II) concentration before modification was 88.4 mM in exp. 24 and 89.1 mM in exp. 35-38.

[c] Uncertainties represent 95 % confidence limits expressed in % relative to estimate for k_1, and k_2,. k_1 is the rate constant for the exchange reaction and k_2 is the rate constant for the reduction reaction.

[d] Solid-phase Fe(II)-normalized rate constants ($k_{1\_Fe(II)}$ and $k_{2\_Fe(II)}$) were calculated by dividing k_1 and k_2 by the concentration of solid-phase Fe(II).

Initial reduction rates were calculated by multiplying the reduction rate constant by the initial nitrate concentration and were found to be nonlinearly related to initial nitrate concentrations, as shown in Figure 6.7. This relationship was described with the following saturation model,

$$r_{0\_nitrate} = \frac{r_{max\_nitrate} C_{nitrate\_init}}{\left(K_{m\_nitrate} + C_{nitrate\_init}\right)} \tag{6-20}$$

where $r_{0\_nitrate}$ is the initial degradation rate, $r_{max\_nitrate}$ is the maximum initial degradation rate, $K_{m\_nitrate}$ is the nitrate concentration at its half maximal degradation rate, and $C_{nitrate,init}$ is the initial nitrate concentration. The values of $r_{max\_nitrate}$ and $K_{m\_nitrate}$ obtained through nonlinear regression using MATLAB are 174(±23.2%) mM/day and 1.028(±44.5%) mM, respectively. This result means that nitrate reduction was a surface saturation reaction in which reduction rate approaches a maximum value at high nitrate concentration and the reaction kinetics shift from first-order to zeroth-order. Furthermore, the results of these experiments might be also useful in estimating reaction rates at higher concentrations.

The surface saturation reaction in nitrate reduction was expected because nitrate reduction by modified GR-F occurred through the sequential steps of ion exchange and reduction. In addition, this kind of behavior has also been observed in several studies on the reaction between chlorinated organics and solid reductants such as zero valent iron (ZVI) (53, 82, 83), cement slurries containing Fe(II) (54), and GR (28).

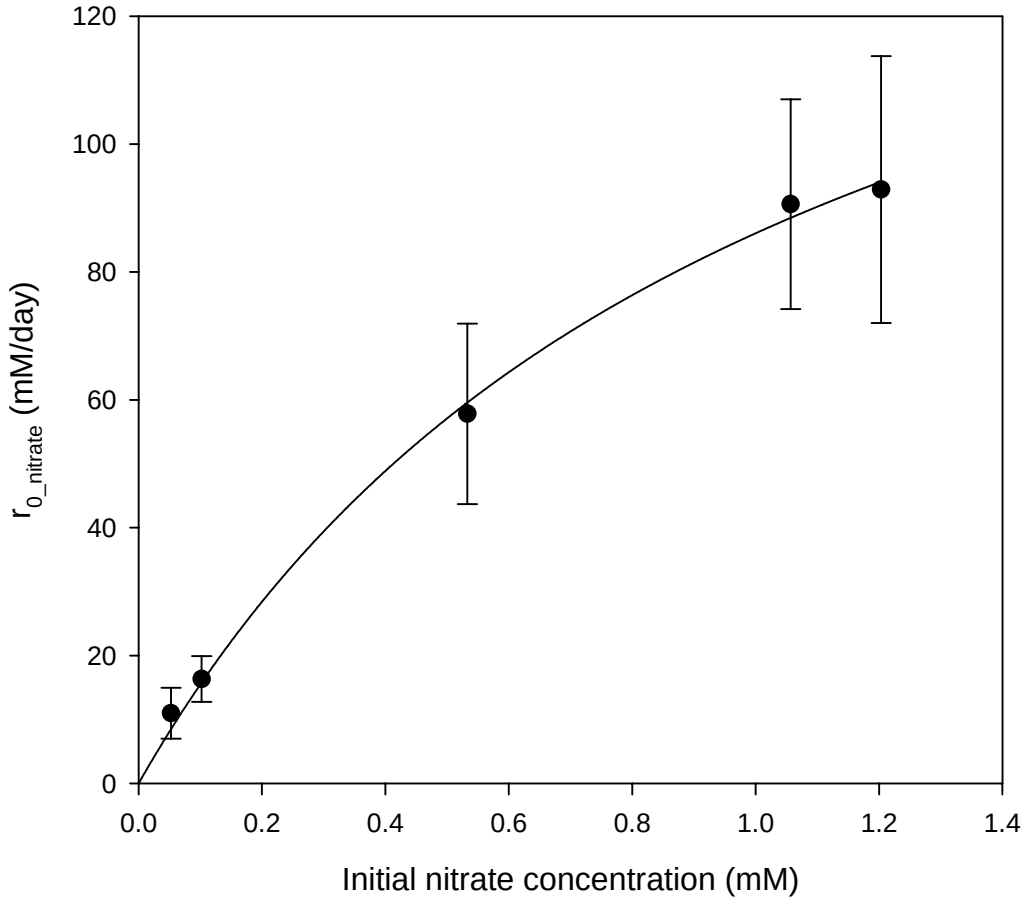

Figure 6.7 Dependence of initial nitrate reduction rate on initial nitrate concentration. Error bars for $r_{0\_nitrate}$ represent 95 % confidential intervals. The solid line represents predictions of a saturation model: $r_{0\_nitrate} = \frac{r_{max\_nitrate} C_{nitrate,0}}{\left(K_{m\_nitrate} + C_{nitrate,0}\right)}$.

CHAPTER VII

SUMMARY AND CONCLUSIONS

Green rusts, a group of layered Fe(II)-Fe(III) hydroxide salts, have been observed to be effective reductants for degrading organic and inorganic contaminants under suboxic conditions. Furthermore, the addition of a transition metal to GRs can produce high-activity modified green rusts (HMGRs) that demonstrate higher degradation rates. The goal of this study was to develop and characterize HMGRs as reductants for PCE and nitrate. This goal was accomplished through the following three objectives: 1) develop modification methods to produce HMGRs; 2) characterize reduction kinetics of PCE by HMGRs; 3) characterize reduction kinetics of nitrate by HMGRs. The results of this research would be very useful in developing cost-effective treatment technologies for contaminated groundwater. The specific conclusions obtained from the research are as follows:

7.1 Development of High-activity Modified Green Rust (Chapter IV)

Screening tests were conducted to determine the most promising HMGRs for degradation of PCE and nitrate. Five types of GRs (GR-Cl, GR-SO_4, GR-CO_3, GR-F, and GR-Br) were used and each GR was contacted with 10 metals (Ba, Mn, Co, Ni, Pt, Cu, Ag, Zn, Ti, and Pb).

Four trace metals (Pt, Cu, Ag, and Pb) were found to be effective in improving the degradation rates of PCE. Pt appeared to be the most effective activating agent for all types of GRs. The rate of PCE degradation by GRs with Pt was improved by up to three

orders of magnitude. Cu was an effect trace metal for activating GR-F and GR-CO_3. The solid-phase Fe(II) normalized first-order rate constant for PCE degradation by GR-F(Cu) was two orders of magnitude larger than that for GR-F. Ag showed the capability of enhancing the reactivity of GR-CO_3 and GR-SO_4 and Pb was an effective additive for GR-CO_3, GR-Cl, and GR-Br. In particular, all PCE added was completely removed by GR-Cl(Pt), GR-CO_3(Ag), GR-CO_3(Pb), and GR-F(Pt) within 10 days. PCE removed by GR modified with Pt or Cu was mainly reduced to dichloroacetylene through the reductive β-elimination pathway and PCE removed by GR with Ag or Pb was primarily reduced to TCE through the hydrogenolysis pathway.

GR-F(Pt) and GR-F(Cu) were selected as reductants for further study based on kinetics of PCE degradation and extent of production of intermediates. Pt and Cu could effectively enhance the reactivity of GR-Cl, GR-CO_3, GR-F and GR-Br and produce non-chlorinated by-products. GR-F was selected because only GR-F showed an enhancement of activity by both Pt and Cu.

Only Pt and Cu showed the capability of improving reduction kinetics of nitrate. Pt was an effective activating agent for all GRs. The rate of nitrate reduction by GR-Br(Pt), GR-SO_4(Pt), GR-Cl(Pt), GR-F(Pt), and GR-CO_3(Pt) were approximately 12.9 – 224 times faster than those of unmodified GRs. Cu was an effective activating agent for GR-Cl and GR-F. The Fe(II)-normalized rate constant of GR-F(Cu) was increased by a factor of 14.2 compared to GR-F.

GR-F(Pt) and GR-F(Cu) were chosen as effective HMGRs for nitrate reduction. The reactivity of GR-F was improved by both Pt and Cu, while the reactivity of GR-SO_4

and GR-Cl was improved by Cu, but much less than was observed with Pt. Even though GR-Br(Pt) showed the fastest reduction rate, GR-Br was not considered for further study during the characterization phase because it was less pure than the other HMGRs.

7.2 Reductive Dechlorination of Tetrachloroethylene by Fluoride Green Rust Modified with Copper or Platinum (Chapter V)

Modified GR-Fs were examined by XRD analysis and iron measurement. The trace metal ion added into GR-F was initially reduced to the metallic element, which was deposited on the surface of GR-F, while GR-F was transformed to magnetite. In addition, dissolution of GR-F was observed during modification by hydrogen ion produced as a byproduct of GR reduction. Therefore, some GR and magnetite reacted with H^+ to produce Fe(II) in solution. The overall reaction for the modification of GR-F by Cu was proposed in equation 5-8.

Degradation of PCE by GR-F(Cu) and GR-F(Pt) was characterized further using a batch reactor system. The degradation kinetics were reasonably described by a pseudo-first-order rate law. The effect of pH on PCE dechlorination by GR-F(Cu) and GR-F(Pt) was studied over the range of pH from 7.5 to 11. The reaction kinetics were the fastest at pH 11 in both cases and 0.245 mM of PCE added was completely reduced in 0.5 day. The reaction rates of GR-F(Cu) increased as pH increased, whereas rates of GR-F(Pt) varied in the order: pH 11 > pH 7.5 > pH 9. In particular, it was observed that a second-order kinetic model was more applicable for PCE reduction by GR-F(Pt) at pH 11 than a first-order model. This behavior was caused by a lower amount of GR-F being present at the later reaction times as the result of it reacting with water as well as PCE.

The effect of the initial concentration of Cu(II) on reductive dechlorination of PCE by GR-F was investigated over the range of 0 to 7.5 mM at pH 7.5. Increasing addition of Cu(II) over the range of 0 to 5 mM resulted in improving the reduction kinetics by a factor of more than 400. However, the rate at 7.5 mM of Cu(II) was unexpectedly decreased by a factor of 1.5 compared to that at 5 mM of Cu(II).

PCE degradation kinetics by GR-F(Cu) were also affected by initial PCE concentration. The Fe(II)-normalized pseudo-first-order rate constants decreased by a factor of 5 as initial PCE concentrations increased from 0.1 to 0.707 mM. On the other hand, initial reaction rate seemed to approach a limiting value at high PCE concentrations. This is evidence that the rate of PCE dechlorination by the modified GR can be described by a surface saturation reaction model, in which the rate of PCE dechlorination is controlled by the concentration of PCE adsorbed onto the surface of GR and that this surface concentration has a maximum concentration. This is consistent with the dechlorination mechanism that occurs on the surface of a bimetallic reductant.

PCE was mainly reduced to ethane and GR-F was transformed to magnetite during reductive dechlorination of PCE by GR-F(Cu) and GR-F(Pt). Unfortunately, it is difficult to propose the reduction pathway of PCE degradation using the results of reaction product analysis because no intermediates were observed except for ethane, which could be a product of hydrogenolysis or β-elimination.

7.3 Nitrate Reduction by Fluoride Green Rust Modified with Copper or Platinum (Chapter VI)

Kinetics of degradation of nitrate by GR-F(Cu) and GR-F(Pt) was described with a reaction model having four sequential steps that were well described by first-order kinetics.

$$NO^-_{3(aq)} \xrightarrow{k_1} GR - NO_3 \xrightarrow{k_2} NO^-_{2(aq)} \xrightarrow{k_3} GR - NO_2 \xrightarrow{k_4} NH^+_{4(aq)}$$

When the nitrite reduction step was too fast to allow nitrite to accumulate in solution to detectable levels, a simplified reaction model with two sequential steps was used.

The reaction rates of nitrate reduction by GR-F(Cu) and GR-F(Pt) were investigated at three different pH (pH 7.5, 9 and 11). The four-step reaction model was used for GR-F(Cu) at pH 9 and pH 11, while the two-step reaction model was used to describe kinetics under all other conditions. The reduction of GR-NO_3 by Cu-modified GR was the most rapid at pH 9, being almost four times faster than that at pH 7.5. The reduction of GR-NO3 by Pt-modified GR was fastest at pH 9 and slowest at pH 11. Unfortunately, neither kinetic model fit the data at pH 11 very well. This was due to the relatively lower rate of ammonium production at the beginning of reaction that was caused by additional steps that were not included in the model.

Kinetics of nitrate reduction by GR-F(Cu) was affected by Cu(II) concentration. The reaction rates of GR-NO_3 increased as Cu(II) additions increased from 0 to 2.5 mM , while the rate at 5 mM was slower than that at 2.5 mM. Two possible reasons were

proposed for this behavior. This might be due to the potential aggregation of Cu particles on GR, which would reduce the surface area of Cu.

The effect of initial nitrate concentration on nitrate reduction by GR-F(Cu) was studied over the range of 0.05 to 1.2 mM. The reduction rate constant of GR-NO_3 decreased from 210 to 77.2 day^{-1} as initial nitrate concentration increased. Initial reduction rates obtained by multiplying the reduction rate constant by the initial nitrate concentration were nonlinearly related to initial nitrate concentrations and the relationship was successfully described by a saturation model. The maximum initial degradation rate was 174 mM/day and half-saturation constant was 1.03 mM.

7.4 Recommendation for Future Works

Several directions for future research are suggested;

1) Investigation of the mechanism of GR modification to understand the deposition of an activating agent on the surface area of GR and to determine the optimal conditions for modification.

2) Characterization of the removal efficiency and settling behavior of HMGRs in continuous flow reactor systems.

3) Evaluation of the feasibility of using HMGR to reduce other chlorinated compounds and toxic metals.

LITERATURE CITED

(1) LaGerga, M. D.; Buckingham, P. L.; Evans, J. C. *Hazardous Waste Management* ; McGraw-Hill: New York, NY, 1994.

(2) White, P. A.; Claxton, L. D. *Mutation Research* **2004**, *567*, 227-345.

(3) Zoller, U. *Groundwater Contamination and Control*; Marcel Dekker: New York, NY, 1994.

(4) Hill, M. K. *Understanding Environmental Pollution*; Cambridge: Cambridge, United Kingdom, 2004.

(5) Heidrich, S.; Schirmer, M.; Weiss, H.; Wycisk, P.; Grossmann, J.; Kaschl, A. *Toxicology* **2004**, *205*, 143-155.

(6) U.S.EPA, *A Review of Contaminant Occurrence in Public Water Systems; EPA 816-R-99-006*; Office of Water, Washington, D.C., 1999.

(7) Butler, E. C.; Hayes, K. F. *Environmental Science and Technology* **1999**, *33*, 2021-2027.

(8) Campbell, T. J.; Burris, D. R.; Roberts, A. L.; Wells, J. R. *Environmental Toxicology and Chemistry* **1997**, *16*, 625-630.

(9) U.S.EPA, *Cleaner Technologies Substitutes Assessment: Professional Fabricare Processes; EPA 744-B-98-001*; Office of Pollution Prevention and Toxics Economics, Exposure and Technology Division, Washington, D.C., 1998.

(10) O'Loughlin, E. J.; Burris, D. R.; Delcomyn, C. A. *Environmental Science and Technology* **1999**, *33*, 1145-1147.

(11) U.S.EPA. *National Primary Drinking Water Regulations*; EPA 811-F-95-002-C; Office of Ground Water & Drinking Water, Washington, D.C., 1995.

(12) Choe, S.; Chang, Y.; Hwang, K.; Khim, J. *Chemosphere* **2000**, *41*, 1307-1311.

(13) O'Loughlin, E.; Kemner, K. M.; Burris, D. R. *Environmental Science and Technology* **2003**, *37*, 2905-2912.

(14) Erbs, M.; Hansen, H. C. B.; Olsen, C. E. *Environmental Science and Technology* **1999**, *33*, 307-311.

(15) Drissi, S. H.; Refait, P.; Abdelmoula, M.; Genin, J. M. R. *Corrosion Science* **1995**, *37*, 2025-2041.

(16) Phillips, D. H.; Watson, D. B.; Roh, Y.; Gu, B. *Journal of Environmental Quality* **2003**, *32*, 2033-2045.

(17) Kamolpornwijit, W.; Liang, L.; Moline, G. R.; Hart, T.; West, O. R. *Environmental Science and Technology* **2004**, *38*, 5757-5765.

(18) O'Loughlin, E. J.; Kelly, S. D.; Cook, R. E.; Csencsits, R.; Kemner, K. M. *Environmental Science and Technology* **2003**, *37*, 721-727.

(19) Hansen, H. C. B.; Koch, C. B.; Nancke-Krogh, H.; Borggaard, O. K.; Sorensen, J. *Environmental Science and Technology* **1996**, *30*, 2053-2056.

(20) Hansen, H. C. B.; Koch, C. B. *Clay Minerals* **1998**, *33*, 87-101.

(21) Hansen, H. C. B.; Guldberg, S.; Erbs, M.; Koch, C. B. *Applied Clay Science* **2001**, *18*, 81-91.

(22) Hansen, H. C. B.; Borggaard, O. K.; Sorensen, J. *Geochimica et Cosmochimica Acta* **1994**, *58*, 2599-2608.

(23) Johnson, T. M.; Bullen, T. D. *Geochimica et Cosmochimica Acta* **2003**, *67*, 413-419.

(24) Williams, A. G. B.; Scherer, M. M. *Environmental Science and Technology* **2001**, *35*, 3488-3494.

(25) Legrand, L.; Figuigui, A. E.; Mercier, F.; Chausse, A. *Environmental Science and Technology* **2004**, *38*, 4587-4595.

(26) Marchal, F. Dechlorination of PCE by Mixtures of Green Rust and Zero-valent Iron, M.S. Thesis, Texas A&M University, College Station, TX, 2002.

(27) Lee, W.; Batchelor, B. *Environmental Science and Technology* **2003**, *37*, 535-541.

(28) Lee, W.; Batchelor, B. *Environmental Science and Technology* **2002**, *36*, 5348-5354.

(29) O'Loughlin, E. J.; Burris, D. R. *Environmental Toxicology and Chemistry* **2004**, *23*, 41-48.

(30) Son, S. Reductive Dechlorination of Chlorinated Hydrocarbons using Fe(II) and Modified Green Rusts in Degradative Solidification/Stabilization, Ph.D. Dissertation, Texas A&M University, College Station, TX, 2002.

(31) Rives, V. *Layered Double Hydroxides: Present and Future*; Nova Science Publishers: New York, NY, 2001.

(32) Genin, J. M. R.; Ruby, C. *Solid State Sciences* **2004**, *6*, 705-718.

(33) Simon, L.; Francois, M. *Solid State Sciences* **2003**, *5*, 327-334.

(34) Peulon, S.; Legrand, L.; Antony, H.; Chausse, A. *Electrochemistry Communications* **2003**, *5*, 208-213.

(35) O'loughlin, E. J.; Kelly, S. D.; Kemner, K. M.; Csencsits, R.; Cook, R. E. *Chemosphere* **2003**, *53*, 437-446.

(36) Puls, R. W.; Paul, C. J.; Powell, R. M. *Applied Geochemistry* **1999**, *14*, 989-1000.

(37) Abdelouas, A.; Lutze, W.; Nuttall, E.; Gong, W. *Surface Geosciences* **1999**, *328*, 315-319.

(38) Roberts, A. L.; Totten, L. A.; Arnold, W. A.; Burris, D. R.; Campbell, T. J. *Environmental Science and Technology* **1996**, *30*, 2654-2659.

(39) O'Hannesin, S. F.; Gillham, R. W. *Ground Water* **1998**, *36*, 164-170.

(40) U.S.EPA, *Permeable Reactive Barrier Technologies for Contaminant Remediation*; EPA 600-R-98-125; Office of Research and Development, Washington, D.C., 1998.

(41) Zhang, W.; Wang, C.; Lien, H. *Catalysis Today* **1998**, *40*, 387-395.

(42) Fennelly, J. P.; Roberts, A. L. *Environmental Science and Technology* **1998**, *32*, 1980-1988.

(43) Kim, Y.; Caraway, E. R. *Environmental Science and Technology* **2000**, *34*, 2014-2017.

(44) Muftikian, R.; Fernando, Q.; Korte, N. *Water Research* **1995**, *29*, 2434-2439.

(45) Wan, C.; Chen, Y. H.; Wei, R. *Environmental Toxicology and Chemistry* **1999**, *18*, 1091-1096.

(46) Lin, C. J.; Lo, S. L.; Liou, Y. H. *Journal of Hazardous Materials* **2004**, *B116*, 219-228.

(47) Lien, H.; Zhang, W. *Journal of Environmental Engineering* **1999**, *125*, 1042-1047.

(48) Matheson, L. J.; Tratnyek, P. G. *Environmental Science and Technology* **1994**, *28*, 2045-2053.

(49) Cheng, I. F.; Fernando, Q.; Korte, N. *Environmental Science and Technology* **1997**, *31*, 1074-1078.

(50) Vogel, T. M.; Criddle, C. S.; McCarty, P. L. *Environmental Science and Technology* **1987**, *21*, 722-736.

(51) Atkins, R. C.; Carey, F. A. *Organic Chemistry: A Brief Course*; McGraw-Hill: New York, NY, 1997.

(52) Cervini-Silva, J.; Larson, R. A.; We, J.; Stucki, J. W. *Chemosphere* **2000**, *47*, 971-976.

(53) Arnold, W. A.; Roberts, A. L. *Environmental Science and Technology* **2000**, *34*, 1794-1805.

(54) Hwang, I.; Batchelor, B. *Chemosphere* **2002**, *48*, 1019-1027.

(55) Lee, W.; Batchelor, B. *Environmental Science and Technology* **2002**, *36*, 5147-5154.

(56) Lee, W.; Batchelor, B. *Chemosphere* **2004**, *56*, 999-1009.

(57) Luk, G. K.; Au-Yeung, W. C. *Advances in Environmental Research* **2002**, *6*, 441-453.

(58) Rittmann, B. E.; McCarty, P. L. *Environmental Biotechnology: Principles and Applications*; McGraw-Hill: New York, NY, 2001.

(59) Westerhoff, P.; James, J. *Water Research* **2003**, *37*, 1818-1830.

(60) Huang, C.; Wang, H.; Chiu, P. *Water Research* **1998**, *32*, 2257-2264.

(61) Choe, S.; Liljestrand, H. M.; Khim, J. *Applied Geochemistry* **2004**, *19*, 335-342.

(62) Yang, G. C. C.; Lee, H. *Water Research* **2005**, *39*, 884-894.

(63) Alowitz, M. J.; Scherer, M. M. *Environmental Science and Technology* **2002**, *36*, 299-306.

(64) Ottley, C. J.; Davison, W.; Edmunds, W. M. *Geochimica et Cosmochimica Acta* **1997**, *61*, 1819-1828.

(65) Clark, W. M. *Oxidation-Reduction Potentials of Organic Systems*; Williams & Wilkins, Baltimore, MD, 1960.

(66) Clesceri, L. S.; Greenberg, A. E.; Eaton, A. D. *Standard Methods for the examination of water and wastewater, 19th edition*; American Public Health Association: Boston, MA, 1995.

(67) Refait, P. H.; Genin, J. M. R. *Corrosion Science* **1993**, *34*, 797-819.

(68) Olowe, A. A.; Genin, J. M. G. *Corrosion Science* **1991**, *32*, 965-984.

(69) Refait, P. H.; Drissi, S. H.; Pytkiewicz, J.; Genin, J. M. R. *Corrosion Science* **1997**, *39*, 1699-1710.

(70) Gibbs, C. R. *Analytical Chemistry* **1976**, *48*, 1197-1201.

(71) Staudinger, J.; Roberts, P. V. *Chemosphere* **2001**, *44*, 561-576.

(72) Mackay, D.; Shiu, W. Y. *Journal of Physical and Chemical Reference Data* **1981**, *10*, 1175-1199.

(73) Refaut, P. H.; Genin, J. M. R. *Corrosion Science* **1993**, *34*, 797-819.

(74) Loyaux-Lawniczak, S.; Refait, P.; Ehrhardt, J. J.; Lecomte, P.; Genin, J. M. R. *Environmental Science and Technology* **2000**, *34*, 438 -443.

(75) Refait, P.; Simon, L.; Genin, J. M. G. *Environmental Science and Technology* **2000**, *34*, 819 -825.

(76) Hwang, I. Fe(II)-based Reductive Dechlorination of Tetrachloroethylene in Soils Treated by Degradative Solidification/Stabilization, Ph.D. Dissertation, Texas A&M University, College Station, TX, 2000.

(77) Chai, J. C.; Miura, N. *Journal of Hazardous Materials* **2004**, *110*, 85-92.

(78) Ding, Y.; Schuring, J. R.; Chan, P. C. *Practice Periodical of Hazardous, Toxic & Radioactive Waste Management* **1999**, *3*, 69-76.

(79) Prakash, S. M.; Gupta, S. K. *Bioresource Technology* **2000**, *72*, 47-54.

(80) Grittini, C.; Malcomson, M.; Fernando, Q.; Korte, N. *Environmental Science and Technolgoy* **1995**, *29*, 2898-2900.

(81) Fogler, H. S. *Elements of Chemical Reaction Engineering*; third ed.; Prentice Hall: Upper Saddle River, NJ, 1999.

(82) Schafer, D.; Kober, R.; Dahmke, A. *Journal of Contaminant Hydrology* **2003**, *65*, 183-202.

(83) Janda, V.; Vaseka, P.; Bizova, J.; Belohlav, Z. *Chemosphere* **2004**, *54*, 917-925.

(84) Canter, L. W. *Nitrates in Groundwater*; CRC Press: Boca Raton, FL, 1997.

(85) Fanning, J. C. *Coordination Chemistry Reviews* **2000**, *199*, 159-179.

(86) Haugen, K. S.; Semmens, M. J.; Novak, P. J. *Water Research* **2002**, *36*, 3497-3506.

(87) Capellos, C.; Bielski, B. H. J. *Kinetic Systems: Mathematical Description of Chemical Kinetics in Solution*; John Wiley & Sons: New York, NY, 1972.

(88) Gao, W.; Guan, N.; Chen, J.; Guan, X.; Jin, R.; Zeng, H.; Liu, Z.; Zhang, F. *Applied Catalysis B: Environmental* **2003**, *46*, 341-351.

APPENDIX A

NOTATION

The following symbols are used in this dissertation:

$C_{Fe(II)-GR}$	Concentration of solid-phase Fe(II) in the suspension of GR;
C_{GR-NO2}	Concentration of GR-NO_2;
C_{GR-NO3}	Concentration of GR-NO_3;
$C_{L,PCE}$	Concentration of PCE in solution;
$C_{L,PCE,init}$	Initial concentration of PCE in solution;
C_{NH4}	Concentration of ammonium ion;
C_{NH4_init}	Initial concentration of ammonium ion;
$C_{nitrate,0}$	Initial nitrate concentration;
C_{NO2}	Concentration of nitrite ion
C_{NO2_init}	Initial concentration of nitrite ion;
C_{NO3}	Concentration of nitrate ion;
C_{NO3_init}	Initial concentration of nitrate ion;
$C_{T,PCE}$	Concentration of PCE in all phases of the system;
GR	Green rust;
GR-Br	Bromide green rust;
GR-Br(Pb)	Pb(II)-modified bromide green rust;
GR-Br(Pt)	Pt(IV)-modified bromide green rust;
GR-Cl	Chloride green rust;
GR-Cl(Cu)	Cu(II)-modified chloride green rust;
GR-Cl(Pb)	Pb(II)-modified chloride green rust;
GR-Cl(Pt)	Pt(IV)-modified chloride green rust;
GR-CO_3	Carbonate green rust;

GR-CO_3(Ag)	Ag(I)-modified carbonate green rust;
GR-CO_3(Cu)	Cu(II)-modified carbonate green rust;
GR-CO_3(Pb)	Pb(II)-modified carbonate green rust;
GR-CO_3(Pt)	Pt(IV)-modified carbonate green rust;
GR-F	Fluoride green rust;
GR-F(Cu)	Cu(II)-modified fluoride green rust
GR-F(Pt)	Pt(IV)-modified fluoride green rust;
GR-SO_4	Sulfate green rust;
GR-SO_4(Ag)	Ag(I)-modified sulfate green rust;
GR-SO_4(Pt)	Pt(IV)-modified sulfate green rust;
H_{PCE}	Dimensionless Henry's law constant for PCE;
k_1	Rate constant for anion exchange of nitrate with GR-F;
k_2	Rate constant for reduction of GR-NO_3;
$k_{2\_Fe(II)}$	Solid-phase Fe(II)-normalized rate constants for nitrate reduction;
k_3	Rate constant for anion exchange of nitrite with GR-F;
k_4	Rate constant for reduction of GR-NO_2;
$k_{4\_Fe(II)}$	Solid-phase Fe(II)-normalized rate constants for nitrite reduction;
$k_{app,PCE,half}$	Apparent half-order rate constant for PCE dechlorination;
$k_{app,PCE,second}$	Apparent second-order rate constant for PCE dechlorination;
k_{app_NO3}	Apparent pseudo-first-order rate constant for nitrate reduction;
k_{app_PCE}	Apparent pseudo-first-order rate constant for PCE dechlorination;
$K_{m,PCE}$	PCE concentration at its half maximal degradation rate;
$K_{m\_nitrate}$	Nitrate concentration at its half maximal degradation rate;
k_{NO3}	Second-order rate constant for nitrate reduction or solid-phase Fe(II)-normalized first-order rate constant for nitrate reduction ;

k_{PCE}	Second-order rate constant for PCE dechlorination or solid-phase Fe(II)-normalized first-order rate constant for PCE dechlorination;
$K_{S,PCE}$	Solid phase partition coefficient of PCE;
P_{PCE}	Partitioning factor for PCE;
$r_{0,PCE}$	Initial rate of PCE dechlorination;
$r_{0\_nitrate}$	Initial rate of nitrate reduction;
Ratio of k_{NO3}	Ratio of k_{NO3} for GR with a trace metal to k_{NO3} for control;
Ratio of k_{PCE}	Ratio of k_{PCE} for GR with a trace metal to k_{PCE} for control;
$r_{max,PCE}$	Maximum rate for PCE degradation;
$r_{max\_nitrate}$	Maximum rate for nitrate reduction;
V_g	Volume of the gas phase;
V_l	Volume of the liquid phase;

APPENDIX B

EVALUATION OF SYNTHEIC METHOD FOR GR-F

GR-F was synthesized by partially oxidizing $Fe(OH)_2$ with oxygen in the presence of dissolved Cl^- and F^-. The type of GR that was produced was determined by calculating anion concentrations before and after GR synthesis and assuming that all of the anion removed from solution was placed in interlayer of GR. Applying this method showed that 98% of GR formed was GR-F.

This appendix provides additional evidence that GR-F was produced rather than GR-Cl. First, it was observed that the concentration of F^- increased as the concentration of NH_4^+ produced by reduction of nitrate by GR-F increased. Table B.1 shows that when 0.373 mM of ammonium was produced, the concentration of F^- increased from 3.17 to 4.61 mM. This implies that the reductant responsible for nitrate reduction was not GR-Cl but GR-F.

Table B.1 Concentrations of ammonium and fluoride during nitrate reduction by GR-F[a]

Time (hr)	NH_4^+ measured (mM)	NH_4^+ change[b] (mM)	F^- measured (mM)	F^- change[c] (mM)
0.03	0.062	0	3.17	0
0.13	0.068	0.005	3.51	0.34
0.32	0.284	0.222	4.30	1.12
0.40	0.435	0.373	4.61	1.43

[a] The results of measuring ammonium and fluoride during the nitrate reduction by GR-F(Pt) at pH 11 (exp. 29)

[b] The NH_4^+ concentration change was calculated by subtracting concentration of NH_4^+ measured at 0.03 hr from concentration of NH_4^+ measured at each time.

[c] The F^- concentration change was calculated by subtracting the concentration of F^- measured at 0.03 hr from the concentration of F^- measured at each time.

Second, the affinity of GR for the fluoride ion was observed to be stronger than that for the chloride ion. This means that production of GR-F would be preferred when both F^- and Cl^- are present. The higher affinity of GR for F^- over Cl^- was confirmed by ion exchange experiment. Once GR-Cl was synthesized, it was contacted with various concentration of F^- for 1 hr. The results shown in Table B.2 clearly show that GR exchanged Cl^- for F^- .

Table B.2 The results of F- exchange with GR-Cl.

before reaction		after reaction		Exchanged conc.		ratio of
$Cl^-_{(aq)}$ (mM)	$F^-_{(aq)}$ (mM)	$Cl^-_{(aq)}$ (mM)	$F^-_{(aq)}$ (mM)	Cl^- [a] (mM)	F^- [b] (mM)	F^- to Cl^- [c]
19.5	0	19.5	0	0	0	-
19.5	5	22.4	1.8	2.8	3.2	1.15
19.5	10	24.5	4.1	5.0	5.9	1.18
19.5	15	26.6	7.2	7.0	7.8	1.11
19.5	17.5	27.4	8.7	7.9	8.8	1.12
19.5	20	28.0	10.2	8.5	9.8	1.16
19.5	22.5	28.7	11.9	9.2	10.6	1.15
19.5	25	29.2	13.5	9.7	11.5	1.19
19.5	30	29.9	15.8	10.4	14.2	1.37

[a] Exchanged concentration of Cl^- was calculated by subtracting that in solution before reaction from that in solution after reaction.

[b] Exchanged concentration of F^- was calculated by subtracting that in solution after reaction from that in solution before reaction .

[c] The ratio of exchanged F- to exchanged Cl-.

APPENDIX C

C.1 COMPUTER PROGRAM (MATLAB®) TO PREDICT PSEUDO-FIRST-ORDER RATE CONSTANT FOR PCE DECHLORINATION

```
disp('First order kinetic model for PCE degradation by green rust')
% Calculation of rate constant and 95% confidence limits
data=load('exp19.txt'); % load the data stored in exp19.txt
t=data(:,1); % measured values of time (days)
c=data(:,2); % measured values of PCE (mM)
plot(t, c, 'x')
hold on

[beta,r,j]=nlinfit(t,c,@rateeqn_first_kinetic, [0.260 0.002] );
% nonlinear regression with 'nlinfit' function
ci=nlparci(beta,r,j); % 95% confidential level
beta
ci=ci'
sum_of_square=sum(r.^2)

dt=(max(t)-min(t))/100;
tp=min(t):dt:max(t);
   for      i=1:size(tp,2)
            ca0=beta(1);
            k=beta(2);
            cestp(i)=ca0*exp(-k*tp(i));  % 1st order
   end

plot(tp, cestp )
  hold off
```

```
function  cest=rateeqn_first_kinetic(beta, t)
ca0=beta(1);
k=beta(2);
cest=ca0*exp(-k*t);   % calculation PCE with analytical solution in first order model
```

C.2 COMPUTER PROGRAM (MATLAB®) TO PREDICT HALF-ORDER RATE CONSTANT FOR PCE DECHLORINATION

```
disp('half order kinetic model for PCE degradation by green rust')
% Calculation of rate constant and 95% confidence limits
data=load('exp22.txt'); load the data stored in exp22.txt
t=data(:,1); % measured values of time (days)
c=data(:,2); % measured values of PCE (mM)
plot(t, c, 'x')
hold on
cb0=0.0886;

[beta,r,j]=nlinfit(t,c,@rateeqn_half_kinetic, [0.2235 0.0885] );
% nonlinear regression with 'nlinfit' function
ci=nlparci(beta,r,j); % 95% confidential level
beta
ci=ci'
sum_of_square=sum(r.^2)

dt=(max(t)-min(t))/100;
tp=min(t):dt:max(t);
   for      i=1:size(tp,2)
            ca0=beta(1);
            k=beta(2);
            cestp(i)=(sqrt(ca0)-k*tp(i)/2).^2; % half order
   end

plot(tp, cestp )
hold off
```

```
function  cesthf=rateeqn_half_kinetic(beta, t)
ca0=beta(1);
k=beta(2);
cbesthf=(sqrt(ca0)-k*t/2).^2; % calculation PCE with analytical solution in half order model
```

C.3 COMPUTER PROGRAM (MATLAB®) TO PREDICT SECOND-ORDER RATE CONSTANT FOR PCE DECHLORINATION

```
disp('Second order kinetic model for PCE degradation by green rust')
% Calculation of rate constant and 95% confidence limits
data=load('exp23.txt'); load the data stored in exp23.txt
t=data(:,1); % measured values of time (days)
c=data(:,2); % measured values of PCE (mM)
plot(t, c, 'x')
hold on

[beta,r,j]=nlinfit(t,c,@rateeqn_second_kinetic, [0.2235 0.0885] );
% nonlinear regression with 'nlinfit' function
ci=nlparci(beta,r,j); % 95% confidential level
beta
ci=ci'
sum_of_square=sum(r.^2)

dt=(max(t)-min(t))/100;
tp=min(t):dt:max(t);
   for      i=1:size(tp,2)
            ca0=beta(1);
            k=beta(2);
            cestp(i)=(ca0)./(1+2*k*ca0*tp(i)); %2nd order
   end

plot(tp, cestp )
hold off
```

```
function  cest=rateeqn_second_kinetic(beta, t)
ca0=beta(1);
k=beta(2);
 cbest=(ca0)./(1+2*k*ca0*t); % calculation PCE with analytical solution in second order model
```

C.4 COMPUTER PROGRAM (MATLAB®) TO PREDICT RATE CONSTANTS IN TWO STEP REACTION MODEL FOR NITRATE REDUCTION

```
disp('Nitrate reduction in two step reaction model')
%Calculation of rate constant and 95% confidence limits
data=load('exp36.txt'); % load the data stored in exp36.txt
tmeas=data(:,1); % measured values of time (days)
cmeas=data(:,2); % measured values of nitrate and ammonium (mM)
plot(tmeas, cmeas, 'x')
hold on

[beta,r,j]=nlinfit(tmeas, cmeas,@rateeqnnitrate_two_step, [ 0.1  270  150] );
% nonlinear regression with 'nlinfit' function
ci=nlparci(beta,r,j); % 95% confidential level
beta
ci=ci'
sum_of_square=sum(r.^2)

dt=(max(tmeas)-min(tmeas))/50;
%tp=min(tmeas):dt:3;
tp=min(tmeas):dt:max(tmeas);
   for      i=1:size(tp,2)
            ca0=beta(1);
             k1=beta(2);
            k2=beta(3);
            camodeltp(i)=ca0*exp(-k1*tp(i));% nitrate
            cbmodeltp(i)=(ca0*k1)./(k2-k1)*(exp(-k1*tp(i))-exp(-k2*tp(i))); % GR-NO3
            ccmodeltp(i)=ca0-camodeltp(i)-cbmodeltp(i); % ammonium
   end
plot(tp, camodeltp, tp,cbmodeltp,tp,ccmodeltp)
hold off
```

```
function  cmodel=rateeqnnitrate_two_step(beta, t)
data=load('exp36.txt');
t=data(:,1);
ca0=beta(1);
k1=beta(2);
k2=beta(3);
%camodel(i)=ca0*exp(-k1*t);   the equation to calculate NO3(aq)
%cbmodel(i)=(ca0*k1)./(k2-k1)*(exp(-k1*t)-exp(-k2*t));
%The equation to calculate GR-NO3(s)
%ccmodel(i)=ca0-camodel-cbmodel; The equation to calculate NH4(aq)

   for      i=1:3
            camodela(i)=ca0*exp(-k1*t(i));
   end
camodela=camodela';

   for      i=4:16
            camodelb(i)=ca0*exp(-k1*t(i));
            cbmodelb(i)=(ca0*k1)./(k2-k1)*(exp(-k1*t(i))-exp(-k2*t(i)));
            ccmodel(i)=ca0-camodelb(i)-cbmodelb(i);
   end
ccmodel=ccmodel';

cmodel=[camodela(1:3);ccmodel(4:16)];
```

C.5 COMPUTER PROGRAM (MATLAB®) TO PREDICT RATE CONSTANTS IN FOUR-STEP REACTION MODEL FOR NITRATE REDUCTION

```
disp('Nitrate reduction in four step reaction model')
%Calculation of rate constant and 95% confidence limits
data=load('exp25.txt'); % load the data stored in exp25.txt
tmeas=data(:,1); % measured values of time (days)
cmeas=data(:,2); % measured values of nitrate, nitrite, and ammonium (mM)
plot(tmeas, cmeas, 'x')
hold on

%ca=C_no3, cb=C_GR_no3, cc=C_no2, cd=C_GR_no2, ce=C_nh4
%ca0=beta(1), k1=beta(2), k2=beta(3), k3=beta(4), k4=beta(5)

[beta,r,j]=nlinfit(tmeas, cmeas,@rateeqnnitrate_four_step, [ 1  220  130  160  290] );
% nonlinear regression with 'nlinfit' function
ci=nlparci(beta,r,j); % 95% confidential level
beta
ci=ci'
sum_of_square=sum(r.^2)

dt=(max(tmeas)-min(tmeas))/50;
tp=min(tmeas):dt:max(tmeas);
   for      i=1:size(tp,2)
            ca0=beta(1);
            k1=beta(2);
            k2=beta(3);
            k3=beta(4);
            k4=beta(5);
            camodeltp(i)=ca0*exp(-k1*tp(i));% nitrate
            cbmodeltp(i)=(ca0*k1)./(k2-k1)*(exp(-k1*tp(i))-exp(-k2*tp(i))); % GR-NO3
            ccmodeltp(i)=((k1*k2*ca0)./((k2-k1)*(k3-k1))*exp(-k1*tp(i)))+((k1*k2*ca0)./((k1-
                        k2)*(k3-k2))*exp(-k2*tp(i)))+((k1*k2*ca0)./((k1-k3)*(k2-k3))*exp(-
                        k3*tp(i))); % nitrite
            cdmodeltp(i)=(k1*k2*k3*ca0)*(1./((k2-k1)*(k3-k1)*(k4-k1))*exp(-k1*tp(i))+1./((k1-
                        k2)*(k3-k2)*(k4-k2))*exp(-k2*tp(i))+1./((k1-k3)*(k2-k3)*(k4-
                        k3))*exp(-k3*tp(i))+1./((k1-k4)*(k2-k4)*(k3-k4))*exp(-
                        k4*tp(i)));  %GR-NO2
```

```
        cemodeltp(i)=ca0-camodeltp(i)-cbmodeltp(i)-ccmodeltp(i)-cdmodeltp(i);
                % ammonium
   end
plot(tp, camodeltp, tp,cbmodeltp,tp,ccmodeltp,tp, cdmodeltp, tp,cemodeltp)
hold off
```

```
function  cmodel=rateeqnnitrate_four_step(beta, t)
data=load('exp25.txt');
t=data(:,1);
ca0=beta(1);
k1=beta(2);
k2=beta(3);
k3=beta(4);
k4=beta(5);
%ca=C_no3, cb=C_GR_no3, cc=C_no2, cd=C_GR_no2, ce=C_nh4
% the equation to calculate NO3(aq)
%camodel(i)=ca0*exp(-k1*t);
% the equation to calculate GR-NO3
%cbmodel(i)=(ca0*k1)./(k2-k1)*(exp(-k1*t)-exp(-k2*t));
% the equation to calculate NO2(sq)
%ccmodel(i)=(k1*k2*ca0)./((k2-k1)*(k3-k1))*exp(-k1*t)+(k1*k2*ca0)./((k1-k2)*(k3-
k2))*exp(-k2*t)+(k1*k2*ca0)./((k1-k3)*(k2-k3))*exp(-k3*t);
% the equation to calculate GR-NO2
%cdmodel(i)=(k1*k2*k3*ca0)*(1./((k2-k1)*(k3-k1)*(k4-k1))*exp(-k1*t+1./((k1-k2)*(k3-
k2)*(k4-k2))*exp(-k2*t+1./((k1-k3)*(k2-k3)*(k4-k3))*exp(-k3*t+1./((k1-k4)*(k2-k4)*(k3-
k4))*exp(-k4*t));
% the equation to calculate ammonium
%cemodel(i)=ca0-camodel-cbmodel-ccmodel-cdmodel;

   for     i=1:3
           camodela(i)=ca0*exp(-k1*t(i));
   end
camodela=camodela';

   for     i=4:7
           ccmodelb(i)=(k1*k2*ca0)*(1./((k2-k1)*(k3-k1))*exp(-k1*t(i))+1./((k1-k2)*(k3-
                   k2))*exp(-k2*t(i))+1./((k1-k3)*(k2-k3))*exp(-k3*t(i)));
   end
ccmodelb=ccmodelb';
```

```
   for      i=8:23
            camodelc(i)=ca0*exp(-k1*t(i));
            cbmodelc(i)=(ca0*k1)./(k2-k1)*(exp(-k1*t(i))-exp(-k2*t(i)));
            ccmodelc(i)=(k1*k2*ca0)*(1./((k2-k1)*(k3-k1))*exp(-k1*t(i))+1./((k1-k2)*(k3-
                        k2))*exp(-k2*t(i))+1./((k1-k3)*(k2-k3))*exp(-k3*t(i)));
            cdmodelc(i)=(k1*k2*k3*ca0)*(1./((k2-k1)*(k3-k1)*(k4-k1))*exp(-k1*t(i))+1./((k1-
                        k2)*(k3-k2)*(k4-k2))*exp(-k2*t(i))+1./((k1-k3)*(k2-k3)*(k4-
                        k3))*exp(-k3*t(i))+1./((k1-k4)*(k2-k4)*(k3-k4))*exp(-k4*t(i)));
            cemodelc(i)=ca0-camodelc(i)-cbmodelc(i)-ccmodelc(i)-cdmodelc(i);
   end
cemodelc=cemodelc';
cmodel=[camodela(1:3);ccmodelb(4:7);cemodelc(8:23)];
```

C.6 COMPUTER PROGRAM (MATLAB®) FOR SATURATION MODEL

```
disp('saturation model')
%model to express the saturation relationship between reaction rate and initial PCE or nitrate
data=load('task11.txt'); % load the data stored in task11.txt
cinit=data(:,1); % initial concentration of target compound
rate=data(:,2); % initial reaction rate
plot(cinit, rate, 'x')
hold on

%rmax=beta(1), k=beta(2);

[beta,r,j]=nlinfit(cinit, rate,@saturationeqn1, [ 200 1] );
% nonlinear regression with 'nlinfit' function
ci=nlparci(beta,r,j); %95% confidential level
beta
ci=ci'
sum_of_square=sum(r.^2)

dc=(max(cinit)-min(cinit))/50;
cp=min(cinit):dc:max(cinit);
   for      i=1:size(cp,2)
            rmax=beta(1);
            k=beta(2);
            rmodelp(i)=(rmax*cp(i))./(k+cp(i));
   end

plot(cp, rmodelp)
hold off
```

```
function  rmodel=saturationeqn1(beta, cinit)
rmax=beta(1);
k=beta(2);
rmodel=(rmax*cinit)./(k+cinit); % saturation model
```

APPENDIX E

TABULATED DATA

1. Screening experiments

Table E.1 PCE dechlorination by five types of GRs with 10 trace metals (task1)

exp. 1		10^{th} day		39^{th} day	
	Trace metal	PCE (mM)	STDEV	PCE (mM)	STDEV
Blank		0.205	0.0001	0.188	0.0090
Control		0.201	0.0037	0.194	0.0027
GR-Cl	Ba	0.208	0.0022	0.201	0.0013
	Mn	0.206	0.0047	0.193	0.0013
	Co	0.210	0.0010	0.184	0.0204
	Ni	0.204	0.0086	0.168	0.0361
	Pt	0.007		0.006	0.0000
	Cu	0.199	0.0031	0.178	0.0029
	Ag	0.199	0.0030	0.173	0.0076
	Zn	0.199	0.0046	0.195	0.0047
	Ti	0.202	0.0054	0.197	0.0030
	Pb	0.122	0.0083	0.037	0.0048

exp. 2		10^{th} day		44^{th} day	
	Trace metal	PCE (mM)	STDEV	PCE (mM)	STDEV
Blank		0.192	0.0025	0.196	0.0054
Control		0.196	0.0011	0.199	0.0018
GR-SO_4	Ba	0.199	0.0014	0.198	0.0045
	Mn	0.199	0.0008	0.201	0.0019
	Co	0.194	0.0029	0.195	0.0033
	Ni	0.195	0.0018	0.199	0.0037
	Pt	0.152	0.0023	0.091	0.0040
	Cu	0.187	0.0020	0.162	0.0043
	Ag	0.056	0.0121	0.011	0.0060
	Zn	0.202	0.0036	0.182	0.0030
	Ti	0.198	0.0020	0.194	0.0045
	Pb	0.195	0.0002	0.187	0.0020

Table E.1 Continued

exp. 3		10th day		42th day	
	Trace metal	PCE (mM)	STDEV	PCE (mM)	STDEV
Blank		0.215	0.0023	0.199	0.0001
Control		0.209	0.0038	0.193	0.0049
GR-CO_3	Ba	0.215	0.0011	0.192	0.0239
	Mn	0.216	0.0004	0.196	0.0045
	Co	0.217	0.0037	0.197	0.0121
	Ni	0.202	0.0038	0.187	0.0031
	Pt	0.010	0.0019	0.007	
	Cu	0.186	0.0003	0.009	0.0020
	Ag	0.009		0.007	
	Zn	0.213	0.0000	0.202	0.0038
	Ti	0.209	0.0054	0.201	0.0055
	Pb	0.009		0.007	

exp. 4		10.3th day		46th day	
	Trace metal	PCE (mM)	STDEV	PCE (mM)	STDEV
Blank		0.209	0.0030	0.195	0.0104
Control		0.208	0.0072	0.202	0.0017
GR-F	Ba	0.212	0.0025	0.211	0.0028
	Mn	0.211	0.0011	0.204	0.0059
	Co	0.212	0.0002	0.205	0.0004
	Ni	0.211	0.0019	0.205	0.0017
	Pt	0.008	-	0.004	0.0000
	Cu	0.010	0.0035	0.004	0.0000
	Ag	0.203	0.0015	0.187	0.0028
	Zn	0.212	0.0042	0.206	0.0061
	Ti	0.211	0.0032	0.203	0.0022
	Pb	0.184	0.0228	0.161	0.0097

exp. 5		9.8th day		42th day	
	Trace metal	PCE (mM)	STDEV	PCE (mM)	STDEV
Blank		0.206	0.0014	0.202	0.0064
Control		0.209	0.0067	0.209	0.0072
GR-Br	Ba	0.216	0.0015	0.207	0.0066
	Mn	0.213	0.0018	0.205	0.0091
	Co	0.216	0.0004	0.208	0.0111
	Ni	0.212	0.0061	0.204	0.0061
	Pt	0.007	0.0011	0.005	0.0000
	Cu	0.219	0.0000	0.207	0.0040
	Ag	0.213	0.0057	0.204	0.0059
	Zn	0.217	0.0101	0.212	0.0108
	Ti	0.220	0.0015	0.224	0.0040
	Pb	0.160	0.0008	0.057	0.0042

Table E.2 Nitrate reduction by five types of GRs with 10 trace metals (task2)

exp.6	nitrate(mM) 1st	2nd	exp. 7	nitrate(mM) 1st	2nd	exp. 8	nitrate(mM) 1st	2nd
control	0	0	control	0	0	control	0	0
GR-Cl	0.094	0.508	GR-SO_4	0.027	0.135	GR-CO_3	0.033	0.356
GR-Cl (Ba)	0.051	0.339	GR-SO_4 (Ba)	0.020	0.052	GR- CO_3 (Ba)	0.010	0.338
GR-Cl (Mn)	0.094	0.405	GR-SO_4 (Mn)	0.019	0.024	GR- CO_3 (Mn)	0.015	0.366
GR-Cl (Co)	0.115	0.419	GR-SO_4 (Co)	0.012	0.162	GR-CO_3 (Co)	0.045	0.383
GR-Cl (Ni)	0.107	0.385	GR-SO_4 (Ni)	0.014	0.032	GR-CO_3 (Ni)	0.000	0.251
GR-Cl (Pt)	1.722	2.111	GR-SO_4 (Pt)	1.825	2.039	GR-CO_3 (Pt)	1.029	1.932
GR-Cl (Cu)	0.225	1.271	GR-SO_4 (Cu)	0.553	1.024	GR-CO_3 (Cu)	0.660	1.605
GR-Cl (Ag)	0.118	0.429	GR-SO_4 (Ag)	0.019	0.346	GR-CO_3 (Ag)	0.056	0.478
GR-Cl (Zn)	0.085	0.136	GR-SO_4 (Zn)	0.018	0.090	GR-CO_3 (Zn)	0.000	0.065
GR-Cl (Ti)	0.080	0.472	GR-SO_4 (Ti)	0.044	0.056	GR-CO_3 (Ti)	0.033	0.386
GR-Cl (Pb)	0.094	0.394	GR-SO_4 (Pb)	0.054	0.177	GR-CO_3 (Pb)	0.084	0.461

exp. 9	nitrate(mM) 1st	2nd	exp. 10	nitrate(mM) 1st	2nd
control	0	0	control	0	0
GR-F	0.333	0.959	GR-Br	0.610	1.763
GR-F (Ba)	0.158	0.721	GR-Br (Ba)	0.436	1.486
GR-F (Mn)	0.086	0.361	GR-Br (Mn)	0.257	1.550
GR-F (Co)	0.097	0.461	GR-Br (Co)	0.622	1.750
GR-F (Ni)	0.206	0.611	GR-Br (Ni)	0.481	1.606
GR-F (Pt)	1.629	1.531	GR-Br (Pt)	2.033	1.978
GR-F (Cu)	1.688	1.600	GR-Br (Cu)	1.253	1.917
GR-F (Ag)	0.257	0.866	GR-Br (Ag)	0.411	1.709
GR-F (Zn)	0.311	1.376	GR-Br (Zn)	0.111	1.833
GR-F (Ti)	0.309	1.071	GR-Br (Ti)	0.517	1.689
GR-F (Pb)	0.092	0.272	GR-Br (Pb)	0.833	1.861

2. Characterization experiments

Table E.3 PCE dechlorination by GR-F(Cu) or GR-F(Pt) (task 3-6)

	exp. 11			exp. 12	
time (day)	PCE (mM)	STDEV	time (day)	PCE (mM)	STDEV
0	0.248		0	0.247	
0.3	0.214	0.0056	0.1	0.210	0.0019
0.9	0.199	0.0101	0.2	0.189	0.0007
1.3	0.210	0.0040	0.4	0.173	0.0014
1.8	0.193	0.0121	1.0	0.109	0.0070
2.2	0.185	0.0045	1.2	0.099	0.0070
3.0	0.157	0.0188	1.4	0.092	0.0034
4.8	0.143	0.0129	1.5	0.086	0.0025
6.9	0.110	0.0143	2.0	0.081	0.0025
9.9	0.113	0.0022	3.1	0.031	0.0031
13.8	0.064	0.0168	5.2	0.004	0.0004
22.5	0.034	0.0005			

	exp. 13			exp. 14	
time (day)	PCE (mM)	STDEV	time (day)	PCE (mM)	STDEV
0	0.247		0	0.247	
0.04	0.197	0.0063	5.1	0.218	0.0030
0.09	0.124	0.0103	13.0	0.210	0.0030
0.13	0.068	0.0008	20.0	0.206	0.0053
0.17	0.037	0.0015	23.0	0.209	0.0040
0.21	0.023	0.0004	31.0	0.204	0.0029
0.25	0.009	0.0010	41.0	0.209	0.0028
0.32	0.004	0.0008	52.0	0.212	0.0041
0.38	0.002	0.0005	62.1	0.212	0.0008

	exp. 15			exp. 16	
time (day)	PCE (mM)	STDEV	time (day)	PCE (mM)	STDEV
0	0.245		0	0.245	
0.9	0.221	0.0031	0.3	0.228	0.0068
1.8	0.216	0.0026	1.0	0.209	0.0046
4.3	0.210	0.0074	1.3	0.201	0.0017
5.8	0.202	0.0057	1.9	0.179	0.0057
6.9	0.206	0.0051	2.8	0.149	0.0038
9.8	0.203	0.0033	4.4	0.097	0.0010
13.8	0.199	0.0047	5.1	0.083	0.0021
16.9	0.190	0.0047	6.1	0.071	0.0050
20.9	0.186	0.0066	7.1	0.043	0.0031
			9.9	0.017	0.0053

Table E.3 Continued

	exp. 17			exp. 18	
time (day)	PCE (mM)	STDEV	time (day)	PCE (mM)	STDEV
0	0.247		0	0.1	
0.9	0.226	0.0017	1.0	0.0769	0.0022
1.9	0.214	0.0052	2.1	0.0742	0.0040
4.3	0.150	0.0015	3.0	0.0688	0.0081
5.8	0.136	0.0014	4.0	0.0525	0.0085
7.0	0.116	0.0034	5.0	0.0484	0.0121
8.9	0.083	0.0048	6.0	0.0385	0.0065
10.8	0.077	0.0094	9.1	0.0239	0.0128
13.9	0.063	0.0071	12.0	0.0115	0.0016
16.9	0.036	0.0089			
19.9	0.014	0.0012			

	exp. 19			exp. 20	
time (day)	PCE (mM)	STDEV	time (day)	PCE (mM)	STDEV
0	0.465		0	0.707	
1.0	0.402	0.0052	0.9	0.612	0.0073
2.0	0.391	0.0115	2.8	0.579	0.0237
3.9	0.375	0.0010	4.8	0.572	0.0058
5.9	0.354	0.0211	7.9	0.555	0.0185
10.9	0.319	0.0477	12.9	0.503	0.0130
15.9	0.227	0.0283	17.8	0.422	0.0469
20.9	0.145	0.0345	21.8	0.341	0.0442
26.9	0.130	0.0364	27.8	0.293	0.0330
35.0	0.062	0.0098	46.1	0.141	0.0228
53.2	0.033	0.0283	53.1	0.110	0.0216

	exp. 21			exp. 22	
time (day)	PCE (mM)	STDEV	time (day)	PCE (mM)	STDEV
0	0.247		0	0.247	
0.02	0.188	0.0019	0.1	0.206	0.0036
0.03	0.152	0.0017	0.3	0.170	0.0040
0.05	0.139	0.0013	0.5	0.103	0.0003
0.07	0.124	0.0091	0.7	0.067	0.0058
0.07	0.109	0.0021	0.8	0.036	0.0017
0.09	0.108	0.0042	0.9	0.022	0.0015
0.11	0.078	0.0050	1.1	0.010	0.0001
0.14	0.069	0.0036			
0.16	0.056	0.0026			
0.20	0.036	0.0054			
0.32	0.011	0.0005			

Table E.3 Continued

time (day)	exp.23 PCE (mM)	STDEV
0.00	0.248	
0.03	0.156	0.0002
0.07	0.097	0.0014
0.11	0.062	0.0100
0.15	0.051	0.0048
0.19	0.040	0.0001
0.24	0.031	0.0007
0.30	0.023	0.0010
0.36	0.019	0.0002

Table E.4 Nitrate reduction by GR-F(Cu) or GR-F(Pt) (task 8-11)

	exp. 24				exp. 25		
Time (day)	NO_3^- (mM)	NO_2^- (mM)	NH_4^+ (mM)	Time (day)	NO_3^- (mM)	NO_2^- (mM)	NH_4^+ (mM)
0	1		0	0			0
0.0035			0.062	0.0014		0.051	0.023
0.0069			0.155	0.0028			0.040
0.0108			0.302	0.0042			0.092
0.0139			0.353	0.0056	0.241	0.238	0.143
0.0156			0.387	0.0069			0.225
0.0174			0.445	0.0083			0.327
0.0191	0.205		0.490	0.0097	0.082	0.248	0.427
0.0208			0.546	0.0111			0.548
0.0243	0.141		0.627	0.0125			0.621
0.0285			0.728	0.0139			0.738
0.0313			0.799	0.0153			0.823
0.0347	0.048		0.835	0.0167			0.875
0.0386			0.884	0.0181			0.945
0.0417			0.964	0.0194			0.958
0.0486			1.002	0.0243			0.996
0.0563			1.038				

	exp. 26				exp. 27		
Time (day)	NO_3^- (mM)	NO_2^- (mM)	NH_4^+ (mM)	Time (day)	NO_3^- (mM)	NO_2^- (mM)	NH_4^+ (mM)
0	1	0	0	0			0
0.0014			0.009	0.0007			0.009
0.0028			0.020	0.0017			0.055
0.0042			0.021	0.0028			0.079
0.0056	0.395	0.026	0.026	0.0038			0.151
0.0069			0.026	0.0049			0.270
0.0083	0.268	0.194	0.030	0.0059	0.260		0.352
0.0097			0.070	0.0076			0.539
0.0111			0.100	0.0090			0.673
0.0125	0.066	0.391	0.154	0.0104	0.133		0.799
0.0139			0.204	0.0118			0.901
0.0153			0.259	0.0132			0.923
0.0167			0.349	0.0146			0.924
0.0181			0.472	0.0160			0.984
0.0194			0.534	0.0174			0.943
0.0215			0.637				
0.0243			0.746				
0.0278			0.828				
0.0313			0.893				

Table E.4 Continued

	exp. 28			exp. 29	
Time (day)	NO_3^- (mM)	NH_4^+ (mM)	Time (day)	NO_3^- (mM)	NH_4^+ (mM)
0	1	0	0	1	0
0.0014		0.130	0.0014		0.062
0.0028	0.502	0.215	0.0028		0.066
0.0042		0.349	0.0042		0.070
0.0056		0.458	0.0056		0.068
0.0069	0.305	0.598	0.0069		0.090
0.0083		0.699	0.0090		0.092
0.0097		0.799	0.0111		0.203
0.0125		0.948	0.0132	0.418	0.284
0.0139		0.998	0.0146		0.322
0.0153		1.026	0.0167	0.374	0.435
			0.0188		0.524
			0.0208		0.598
			0.0244		0.732
			0.0278		0.786
			0.0313		0.848
			0.0347		0.898
			0.0382		0.915

	exp. 30			exp. 31	
Time (day)	NO_3^- (mM)	NH_4^+ (mM)	Time (day)	NO_3^- (mM)	NH_4^+ (mM)
0	1	0	0	1	0
0.042		0.013	0.003		0.019
0.085		0.023	0.012		0.062
0.126		0.035	0.022		0.142
0.180	0.441	0.043	0.031		0.226
0.228		0.060	0.042		0.317
0.319	0.141	0.071	0.054		0.451
0.392	0.067	0.124	0.063	0.258	0.521
1.000		0.180	0.073		0.597
			0.083		0.656
			0.094		0.726
			0.104	0.151	0.784
			0.115		0.846
			0.125		0.839
			0.135		0.860
			0.146		0.894

Table E.4 Continued

Time (day)	exp. 32 NO_3^- (mM)	NH_4^+ (mM)	Time (day)	exp. 33 NO_3^- (mM)	NH_4^+ (mM)
0	1	0	0	1	0
0.0069		0.112	0.0035		0.043
0.0139		0.316	0.0069		0.174
0.0208		0.424	0.0104		0.270
0.0278	0.166	0.530	0.0139	0.333	0.368
0.0347	0.113	0.663	0.0174		0.474
0.0417		0.756	0.0208	0.200	0.579
0.0486		0.813	0.0243		0.680
0.0556		0.921	0.0278		0.730
0.0625		0.940	0.0313		0.810
0.0694		0.969	0.0347		0.898
0.0764		0.979	0.0382		0.902
0.0833		1.011	0.0486		0.983
			0.0590		0.891
			0.0694		0.935
			0.0764		0.984

Time (day)	exp. 34 NO_3^- (mM)	NH_4^+ (mM)	Time (day)	exp. 35 NO_3^- (mM)	NH_4^+ (mM)
0	1	0	0	0.05	0
0.0042		0.031	0.0017		0.007
0.0090		0.131	0.0035		0.010
0.0139		0.269	0.0052		0.015
0.0174		0.362	0.0069	0.008	0.023
0.0208		0.456	0.0087	0.005	0.031
0.0243	0.141	0.539	0.0104		0.037
0.0278	0.067	0.617	0.0122		0.045
0.0326		0.713	0.0139		0.046
0.0382		0.812	0.0174		0.049
0.0451		0.903	0.0208		0.050
0.0521		0.977			
0.0625		0.991			
0.0736		1.014			

Table E.4 Continued

Time (day)	exp. 36 NO_3^- (mM)	NH_4^+ (mM)	Time (day)	exp. 37 NO_3^- (mM)	NH_4^+ (mM)
0	0.1	0	0	0.5	0
0.0035		0.023	0.0069		0.097
0.0052		0.032	0.0104		0.167
0.0069	0.016	0.048	0.0139	0.089	0.242
0.0087	0.008	0.049	0.0201	0.046	0.372
0.0104		0.061	0.0271		0.438
0.0122		0.072	0.0354		0.501
0.0139		0.075	0.0417	0.007	0.513
0.0156		0.085	0.0451		0.537
0.0174		0.088			
0.0191		0.094			
0.0208		0.096			
0.0226		0.099			

Time (day)	exp. 38 NO_3^- (mM)	NH_4^+ (mM)
0	1.2	0
0.0069		0.198
0.0140		0.347
0.0208		0.536
0.0243		0.622
0.0278	0.195	0.707
0.0313		0.777
0.0347	0.086	0.846
0.0382		0.915
0.0417		0.985
0.0486		1.088
0.0556		1.099
0.0625		1.122

VITA

Jeong Yun Choi was born in Kimje, Korea. He completed his Bachelor of Science degree and Master of Science degree in environmental engineering at Chonbuk National Univiersity in 1997 and 1999. His research activities at Texas A&M University have been focused on remediation of groundwater contaminated by chlorinated compounds and nitrate using reductive processes. His professional interests are focused on remediation of contaminated soil and groundwater using reductive process, chemical treatment of hazardous wastes. His permanent address is 571-5, Yochon-dong, Kimje, Korea.